UNIVERSITÀ DEGLI STUDI DI SALERNO
Dipartimento di Farmacia

Dottorato di ricerca
in Scienze Farmaceutiche
Ciclo XIV — Anno di discussione 2016

Coordinatore: Ch.mo Prof. *Gianluca Sbardella*

New Encapsulation Technologies for The Development of in Situ Gelling Micro-Nano Particulate Systems for The Wound Healing

settore scientifico disciplinare di afferenza: CHIM/09

Dottorando **Tutor**

Dott.ssa *Felicetta De Cicco* **Ch.mo Prof.** *Pasquale Del Gaudio*

CONTENTS

ABSTRACT

The Ph.D project titled “New Encapsulation technologies for the development of in situ gelling micro-nano particulate systems for the wound healing” aimed to develop novel topical formulations by innovative technologies, based on supercritical CO_2 (SC-CO_2) and nanospray drying. The specific goal of the project was the design and development of *in situ* gelling formulation in form of powders or aerogels for wound healing using biodegradable and biocompatible polymers, active in wound healing process, as carrier for the encapsulated drugs. Uniform filling of the wound bed, good transpiration properties and controlled drug release profiles have been used to evaluate the quality of the different devices.

During the first year, prilling/supercritical antisolvent extraction (SAE) tandem technique and supercritical assisted atomization (SAA) were studied.

Prilling/SAE was tuned for the first time for the production of aerogel beads. Alginate based aerogels with narrow size distribution and high fluid uptake values were successfully obtained after an accurate study of the process parameters and solvent exchange conditions needed to use SAE as curing process.

SAA was applied for the production of an *in situ* gelling dry powder formulation, loaded with gentamicin. High mannuronic content alginate and low methoxyl degree pectin were used as carrier. Very high process yields were obtained (up to 71%), and the powder obtained by SAA showed good technological properties and were able to overcome gentamicin hygroscopicity. When in contact with simulated wound fluids powders moved rapidly to gel enabling a prolonged release of the drug (between 6 and 10 days). Furthermore, formulations were able to increase antimicrobial activity of GS on both *S. aureus* and *P. aeruginosa* strain.

The second year was focused on nano-spray drying technique. It was applied for the production of an *in situ* gelling nanoparticulate powder using an

alginate and pectin blend as excipient for gentamicin formulations. Operative parameters were set to produce particles in nanometric size (~350 nm) with very high process yield (92%) and good encapsulation efficiency (83%). Powder formulations were able to gel rapidly when in contact with simulated wound fluids, had good transpiration and adhesive properties and were able to prolong drug release *in vitro* (till 6 days). Antimicrobial activity of GS loaded formualtions on both *S. aureus* and *P. aeruginosa* strain were also prolonged.

In the same year, a hydrogel based on alginate high mannuronic content or chitosan low molecular weight loaded with Ac2-26 Annexin 1 derived peptide was developed to test the ability of the peptide healing promoting activity. Stability of Ac2-26 was increased due to the formation of ionic interactions between peptide and polymers. Ac2-26 hydrogel formulations were tested on wounded mice. *In vivo* experiments pointed out the efficacy of the alginate loaded hydrogel to increase wound closure, about 60% faster compared to control.

During third year, in order to enhance technological properties of the *in situ* nanoparticulate powder produced during the second year, a three components polymer blend (alginate, chitosan and amidated pectin) was used to test nano spray drying technology. Doxycycline was used as antimicrobial drug due to its well-known inhibiting activity against MMP9 that could enhance wound healing process. Formulations produced by nano spray drying presented very high process yields (up to 99%) and encapsulation efficiency (up to 98%) while powder gelation time was also reduced (5 minutes) enabling fast and complete covering of a wound. A prolonged drug release profile was observed due to drug/polymer interaction, as well as antimicrobial activity against *S. aureus* strain was enhanced (till 7 days) compared to pure doxycycline.

Doxycycline was also used as model drug to test the feasibility of prilling/SAE tandem technique for the production of core/shell aerogel particles. Aerogels were obtained by prilling in co-axial configuration, using amidated pectin as

core and alginate high mannuronic content as shell. Particles were able to easily gel when in contact with exhudates due to the wide aerogel exposed surface area, absorbing large amount of fluid. Core and shell were well separated with doxycycline distributed homogeneously only into the pectin core. As a result, aerogels presented high encapsulation efficiency (up to 87%) and prolonged drug release, till 48 hours.

Moreover, durting the Ph.D course, three months were spent at University of Santiago de Compostela, to study the feasibility of supercritical impregnation method coupled with prilling and supercritical drying to manufacture novel wound healing aerogel devices. Ketoprofen and norfloxacin, were used as model drugs due to their solubility in SC-CO_2. As expected, aerogels presented high porosity, very useful to absorb large quantities of exhudates. Impregnation process was successful for ketoprofen whereas norfloxacin loaded aerogels exhibited poor drug content.

1. INTRODUCTION

1.1 Skin wounds and reparation process

The integumentary system is the widest apparatus in the human body, and consists of skin, and appendages that are hair, nails and exocrine glands. It represents 16% of the total body weight, with a surface of 1.5-2 m^2. It has many functions as the protection of the body from the external environment, the thermoregulation, the excretion of small quantities of waste products, the deposition of nutrients and the syntesis of vitamin D. Furthermore, it is the most important sense organ, containing different receptors for pain, temperature, and tact. Adult skin consists of different layers: epidermis, derma and hypoderm.

Epidermis consists of corneal, germination stratus and melanocytes. Derma is constituted by connective tissue, with the sensorial receptors. Hypoderm is a collagen-rich dermal connective tissue providing support and nourishment. Hairs and glands also called appendages are linked to epidermis but project deep into the dermal layer.

Because of skin acts as a protective barrier against the outside world, any damage should be mended rapidly and efficiently, leading to the restoration of the function (1).

The term “wounds” includes all types of skin injuries: open (lacerations, abrasions, burns) and closed (hematomas), superficial (abrasions, lacerations, burns) and deep (diabetic foot, pressure sores), acute and chronic.

A chronic wound is one that fails to heals whithin a reasonable time (usually three months), an acute wound heals more quickly, causing minimal functional loss in the part of the body damaged (2).

To develop an appropriate therapeutic program, able to take into account the general patient’s status, healt and compliance, it is necessary to perform an accurate anamnesis and to evaluate the kind of injury, in order to prevent complications and to preserve functions.

Wound healing is a complex physiological multistage process composed of a sequence of precise events that lead to complete skin reparation. Generally, they are divided in four parts:

1) When the lesion occurs, a local haemorrhage happens a clot is formed to plug the defect, inhibiting further microbial access. The clot consists of platelets embedded in a mesh of crosslinked fibrin fibers derived by thrombin cleavage of fibrinogen, together with smaller amounts of plasma fibronectin, vitronectin, and thrombospondin. Mastocytes begin the inflammatory response.
2) After a few hours, cells from germinal layer migrate along the edges of the wound, to replace the empty space. Neutrophils and monocytes are recruited from the circulating blood in response to molecular changes in the surface of endothelial cells lining capillaries at the wound site. The role of neutrophils is not only to clear the initial rush of contaminating bacteria, but also they are a source of pro-inflammatory cytokines that can activate local fibroblast and keratinocytes (3).
3) After a week, the fibrin clot dissolves by the fibrinolytic enzyme plasmin derived from plasminogen and the number of capillary decreases. Various members of the matrix metalloproteinase (MMP) family, each of which cleaves a specific subset of matrix proteins, are also up-regulated by wound-edge keratinocytes. MMP-9 (gelatinase B) can cut basal lamina collagen (type IV) and anchoring fibril collagen (type VII), and is thought to be responsible for releasing keratinocytes from their tethers to the basal lamina (4). Furthermore, the phagocytic activity is almost over, and fibroblasts produce collagen fibre and amorphous fundamental substance.
4) After a few weeks, the rind is detached and the denuded wound surface has been covered by a monolayer of keratinocytes, and a new stratified epidermis with underlying basal lamina is reestablished from the

margins of the wound inward (5). Coincident with the onset of basal lamina synthesis, MMP expression is shut off, and new hemidesmosomal adhesions to the basal lamina reassemble. The last components of the epidermal attachment machinery to reach maturity are the anchoring fibrils that link basal lamina to underlying connective tissue (6). A light depression is often observed in the site of the lesion, but the fibroblast activity continues, producing fibrous scar tissue.

The type of wound and the healing environment influence the relative contribution of each step.

Many pathological conditions and the possibility of bacterial infection, as well as the exacerbation of inflammatory phase, do not permit to reach the healing condition and the wound remains in a chronic state with many aftermaths on the health.

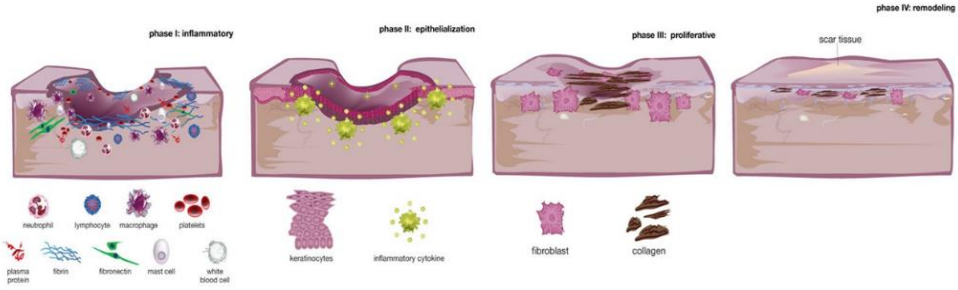

Figure 1: A schematic representation of the healing process phasis.

1.1.1 Factors influencing healing process

A patient with chronic skin wounds, in general, is elderly, with pain and poor quality of life. The patology that caused the lesion is often complex and multifactorial. It is necessary a diagnostic accurate classification and a therapeutic program focused on etiology and on the lesion status, also considering comorbilities and perilesional skin conditions.

Many systemic factors can influence the healing process such as:

1) dismetabolisms as diabetes mellitus
2) circulatory deficiency due to arteriosclerosis and venous stasis
3) ormonal disease, for example glucocorticoids can ihnibit inflammation and collagen synthesis.

Diabetes mellitus is the most important reasons for the onset of chronic wounds.

Although chronic hyperglycemia is an important reason determining diabetes complications, molecular mechanisms are not completely clear yet.

A hypothesis suggests that the increase of intracellular glucose concentration determines the formation of advanced glycosylation end products (AGE).

AGE products form crosslinks between proteins, accelerate arteriosclerosis, alter extracellular matrix structure and composition.

Another hypothesys postulates that hyperglycemia increases the formation of diacylglycerol, inducing activation of protein kinase (PKC).

PKC is able to alter fibronectin genes transcription, collagen type IV, contractile proteins and extracellular matrix proteins in both endothelial cells and neurons. Many diabetes complications are related to these mechanisms (7).

There are other systemic factors that are directly correlated to general health status of the patients, they are different and depend on the etiology of the wound (8).

1) Age of the patient (the healing disorders can depend on a weak immune state, increased chronic, degenerative and disabling pathologies).

The biomedical and socioeconomic burdens posed by wound complications are worsened by the aging global population. As the global population ages, so does the nursing home population, and this will lead to more pressure ulcers. In Europe, similar to that in the US, aging of the population is associated with increase in the number of patients with a chronic wound (9).

2) Nutritional state- obesity.

According to the Center for Disease Control (CDC) and World Health Organization (WHO), in adults a body mass index (BMI) of 25 or more is considered “overweight” and a BMI of 30 or more is considered “obese”. In 2007, more than 1.1 billion adults worldwide were overweight and 312 million of them were obese (10). As the number of larger patients increases, so do the health problems related to obesity, including wound healing.

3) Post surgical complications: thrombosis, thromboembolism.
4) Trauma or shock aftermaths also after operations with extracorporeal circulations.
5) Drugs as corticosteroids.

Different studies, on the use of corticosteroids in the perioperative period, converge on an approximately 30% reduction in wound tensile strength at cortisone doses of 15 to 40 mg/kg/day, equivalent to approximately 200 to 560 mg/day of prednisone in a 70-kg person. Nevertheless, wound healing may be affected by the duration of systemic corticosteroid exposure (11).

Furthermore, local factors can delay directly the tissue reparation process acting with different mechanisms.

For example, perilesional skin maceration due to copious fluid emission, and recurring traumas, happening expecially if the wound is localized in particular position exposed to chafing or presence of necrotic tissue can worsen lesion condition. Inadequate blood supply, as in presence of circulatory deficiencies and pressure on the wound, as in case of bedridden patiens, are other factors, but the most important are the local infections.

Also local factors can influence the healing process such as infections (12). The impact of microorganisms on chronic wounds has been extensively studied and reviewed using different approaches to elicit their possible role in non-healing (13). *Staphylococcus aureus* and coagulase-negative staphylococci have been the predominant organisms isolated from both

prospective, purpose-collected samples and retrospective analysis of clinical investigations. *S. aureus* has been reported in frequencies varying from 43% of infected leg ulcers (14) to 88% of non-infected leg ulcers (15) whereas *Staphylococcus epidermidis* has been reported in 14% of venous ulcer specimens (16) and 20.6% of diabetic foot ulcers. *Pseudomonas aeruginosa* is another frequently identified organism and has been found in 7–33% of ulcers (15, 17, 18). A number of other aerobic species have also been reported, including *Escherichia coli*, (19, 20) *Enterobacter* cloacae (15, 16), *Klebsiella* species (20), *Streptococcus* species (19, 21, 22), *Enterococcus* species (15, 23) and *Proteus* species (24). In addition to aerobes, anaerobic organisms are frequently identified in wounds. The most common isolates found in both the infected and non-infected leg ulcers were *Peptostreptococcus* species and pigmented and non-pigmented *Prevotella/Porphyromonas* species (14).

Many of the problems previously decribed, can determine huge disturbances in the tissue reparation (25) that appears as seroma that are collections of serous exudate that can form infected abscesses, or necrosis of soft parts, also hematomas, expecially in closed wounds or cheloids. In this case granulation tissue can occur, extending beyond the wound borders, without regression.

1.2 Chronic skin wounds

Chronic skin wounds and bedsores represent a relevant problem of health care that involves human, technological, material and economic resources.

Often disguised as a comorbid condition, chronic wounds represent a silent epidemic that affects a large fraction of the world population and poses major and gathering threat to the public health and economy of many countries.

In developed ones, it has been estimated that 1 to 2% of the population will experience a chronic wound during their lifetime (26). In the United States alone, chronic wounds affect 6.5 million patients (27, 28). In the Scandinavian

countries, the associated costs account for 2–4% of the total health care expenses (29).

Bedsores are more frequent in patients with compromised tissue perfusion due to neuromata impairment due to pathologies such diabetes mellitus and in lying in bed patients. Because of these two conditions are often found in old people, the problem increases with the aging of population: the incidence of bedsores in hospitalized people increases from 4-9% to 10-25% in older patients. Life quality is compromised, for the debilitating and painful wounds that not permit to do working activities and to live life normally (30).

Old people with pressure sores spend about 250 euro per month for medical devices, an outgo completely paid by patients. According to the study, 2 million of Italians with ulcers, pressure sores or diabetic foot affect public healt costs for about 1 billion euro per year.

The investigation, carried out on the whole national territory on people with cutaneous ulcers highlited that on 1004 respondents, a representative sample of 2 million of Italian with complicated wounds, suffer mainly of:

- Leg ulcers – 53.3%
- Pressure sores- 24.2%
- Diabetic foot- 23.3%

Between the most relevant problems, pain stands out and in the 42.7% of respondents it is chronic, whereas treatment costs are estimated between 100 and 250 euro per month for 36% of people and exceed 250 euro for 13.2% (31, 32).

Actually, the problem is relevant also because of the long assistance required: for example, ulcers care can involve the 60% of working time of nurses, with high care costs.

The most important chronic wounds are described below.

Pressure sores: they are areas of tissue damage, due to pressure, clutch or sprain. In this group are included ulcers and bedsores that are an important problem for hospitalized patients.

The optimal treatment can be divided into three phases:

1) Remove the pressure, changing the patient position in the bed and using helpful aids.

2) Topic treatment of the wound

3) Treatment of comorbilities that can interfere with the normal healing process as malnutrition or infections.

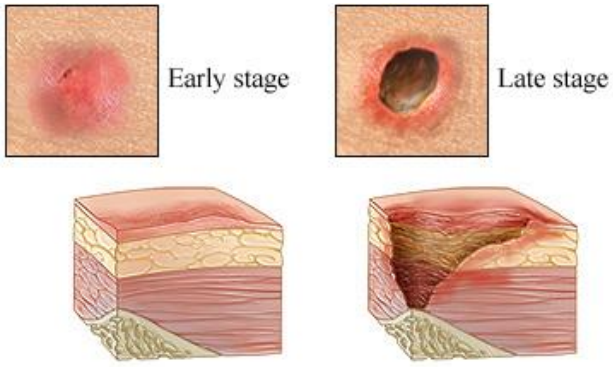

Figure 2: A schematic representation of pressure sores development.

Vascular lesions of lower limbs: they have a venous, arterial or mixed etiology. The localization is often below the knee to the feet and their duration ranges from eight to ten weeks. Chronic ulcers are more frequent in older patients, determining high social costs. Vascular lesions have a frequence of 1.8 to 3.05 per thousand, and the 10 per thousands of adult population had at least once a lower limb wound (33). Optimal treatment is firstly the elastocompressive bandaging with topical drug administration.

Diabetic foot sores: they begin when diabetic neuropathy and arteriopathy of lower limbs compromise foot function and structure. The pathological outline can be the neuropathic foot or the ischemic one, but in old age they often exist contemporarly giving the so called neuroischemic foot (34).

An important complication is microbial infection; this is the most important reason of amputation, infact 50% of amputations regard diabetics.

World Healt organisation estimates that in 2025 more than 300 million people will become diabetic, compared to the 120 million of 1996. About 15% of diabetics will have a foot ulcer that will require medical care (33).

The ideal treatment of diabetic foot sores is:

1) Local treatment of wounds
2) Treatment of infections, if present.
3) Avoiding to charge the interested limb during deambulation
4) Revascularization

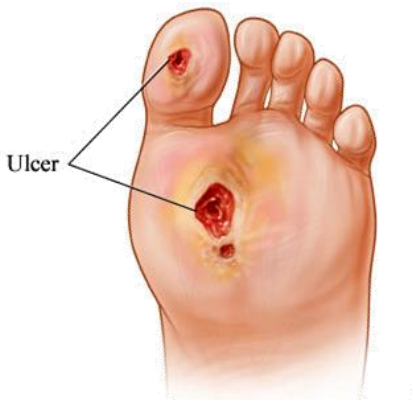

Figure 3: A type of diabetic foot wound

1.2.1 Systemic treatments

Different systemic active molecules are frequently administered to enhance the natural healing process, also as first line treatment, and they are specific for the type of injury identified.

Venous ulcers require, besides compression therapy, oral pentoxyfilline which is effective, but more adverse events (mainly gastrointestinal disturbances) are frequently found in the treated group (35). There is no current evidence on the effectiveness on the routine use of systematic antibiotics. Regard the use of

oral flavonoids there are some experimental data affected by bias, so that results are not completely reliable (36).

Regarding pressure sores, available evidence from four Cochrane systematic reviews showed no effectiveness of enteral or parenteral nutrition (i.e., zinc or protein suppletion) or nutritional supplements (i.e., vitamin C) as treatment modalities for pressure ulcers (37, 38).

Hyperbaric oxygen therapy, granulocyte-colony stimulating factor (G-CSF) administration are advised for diabetic foot sores treatment (39). Adding hyperbaric therapy to usual care appeared to increase the healing of diabetic ulcers after 6 weks, whereas evidence is lacking that G-CSF daily injection might cure diabetic foot infections or improve ulcer healing. Therefore, G-CSF is not recommended in the treatment of relatively mild infections (40).

The use of systemic antibiotic requires many daily doses, due to the short half-life of many antimicrobial agents (such as gentamicin). Many side effects and the development of resistant bacteria are possible, whereas a topical treatment can overcome most of these problems.

1.2.2 Topical treatments

The practice of wound care has improved tremendously and evolved over the years.

The Greek physician Galen (120-201A.D) had noted empirically that wounds heal optimally in a moist environment. However, for almost 2000 years, therapeutic efforts had focussed on drying the wound site with absorptive gauzes serving as mainstay for wound management (41).

Topical treatments present a series of advantages as high drug concentration at the site, reduced drug absorption with consequent reduced systemic side effects.

The importance of a topical application is particularly apparent in ischemic wounds, in which dependable dispatch of a systemic (ie, bloodstream) antimicrobial to the damaged tissue cannot be assured (42).

Wound care includes a series of action to be done to improve general patient's conditions.

After an accurate wash with saline solution to remove debris, the use of antiseptics as clorexidrin or povidone iodine (43) to clean deeply the wound bed and to reduce bacterial contamination by inhibiting the growth of microorganisms is advised if the wound is infected.

Clorexidrin and povidone are better than fuxine, gentian violet, mercury chromium that have a reduced antiseptic activity and do not allow to evaluate the healing progression (44, 45) .

However, antiseptics may increase the intensity and duration of inflammation (46), and they have also been shown to be toxic to human keratinocites and fibroblasts (47) and to retard epithelialization. The deep of wound is very important to know, in order to evaluate the risk/benefit ratio of the antiseptic use.

Topical treatment of infected wounds is very important because the presence of necrotic tissue and the poor blood supply do not allow to reach adequate concentration of antibiotic systemically administred and the growth of bacterial resistent lines is very frequent. In this case, a local wound control is needed by the use of proper device, containing active pharmaceutical ingredients such as antibiotic, silver or growth factor after abundant cleansing.

Following the guide lines advices, wound dressings should remain as long as possible on the wound, because frequent changes can induce a local temperaure decrease, with consequent slowdown of cell replication and then delay in healing process (48). Furthermore, classic devices on market often determine a perilesional skin removal stress, adding other damages.

Changing medication is nedeed:

1) When the absorbent capacity of the device is saturated, and wound fluids are not manageable any more.
2) When it appears fragmented, and then the protection aganist external contamination does't work any more. If this phenomenon is frequent, it's important to evaluate the choice of device, considering a replacement.

The idel device, not existing yet on the market, should properly absorb the excess of exudate, control the bacterial growth, fill the wound bed allowing at the same time the correct traspiration and the control of drug release and of bacterial growth, avoid removal trauma.

Advanced device use is not advised in case of: bleeding, allergy to one of the formulation components, skin cancer, wet gangrene, fistula.

1.3 Types of treatments on the market

Topical devices are very useful to stimulate the healing process and, at the same time, to prevent contamination: sometimes, local treatment should be preceded by other precaution (as changing the patient's position in case of pressure sores) to enhance the medication result.

It is possible to distinguish between the self-consistent formulation when it is possible to put it directly on the wound, while other types require a support or device for administration.

The "ideal" medication should have many characteristics useful to obtain rapid effects as well as to assure patients' compliance. They should absorb the excess of exudates, provide a moist microenvironment in order to guarantee the correct transpiration, they should be sterile/clean, easy to use and impermeable to microorganisms. They also should reduce pain, by avoiding removal trauma.

A great number of devices for local drug administration containing active pharmaceutical ingredients are on the market, but the ideal one is not exising yet.

The choice of the appropriate device should take into account many factors as the kind of injury, the site, the dimension, the presence of infections, the typology and quantity of exudate, and the care goals.

Traditional medication can be distinguished in:

1) Simple
2) Antiseptic
3) Fatty

Simple gauzes are used only to hide lesions and for the protection from external insults. The antiseptic contains active substances that can decrease the bacterial charge on the lesion. The fatty medications contain fatty substances able to reduce adherence, and to maintain hemostasis. The main disadvantages of traditional devices regard the accidental removal of granulation tissue, the patient's difficulties to maintain a correct personal hygiene, the risk of infections, the loss of liquids and the lesion dehydration.

Advanced medication can help the reparative processes, also maintaining a moist microenvironment. The categories of products now on the market include: alginates, polyurethanes foams, hydrogels, hydrocolloids, hydrofibres. They are impermeable to virus, bacteria, determining a thermal stability useful for healing. However, they cannot be used in infected wound because they can worsen the conditions (49).

Only formulations nowadays on the market containing micronized silver can help infections. Silver mechanism of action is related to Ag^{+} ions, which inhibit cellular functions, such as energy production, enzymatic function and cellular replication.

Silver in Ag-antibiotic mixtures are frequently used to inhibit bacterial growth (silver sulphadiazine ointment or cream- “Sofargen”). The problem of this product is related to the poor durability. Infact, many applications per day are required. Other kind of products are “Hyalosilver” composed by ialuronic acid and silver, “Katoxyn” composed by benzoylperoxide and silver.

A different formulation is “Contreet M” that is a polyurethane foam with this active, indicated in venous ulcers or infected sores.

The problem of foams is related to their very high expensiveness that does not allow to extend the treatment for long times, since patients have to support costs completely.

Another product is “Acticoat”, an antimicrobial barrier dressing, consisting of an absorbent rayon/polyester core, containing silver nano-crystals. This product has strong antibacterial activity on the wound bed, acting in 30 minutes (*in vitro*).

However, long-term effects about biodistribution and eventual systemic activity of nanoparticles are unknown, as well as, this product is still too expensive.

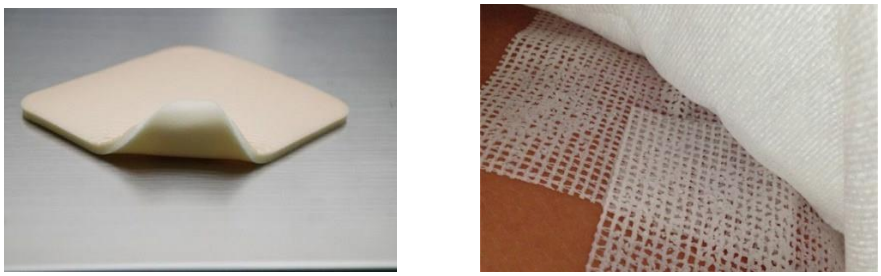

Figure 4: On the left a polyurethane foam, on the right gauzes loaded with antiseptics.

1.4 New formulations

Novel formulations are required to overcome most of the problems of the devices available nowadays on the market. In this context, the present work focuses its attention to the use of novel technologies, proper excipients and

active drugs for the development of new wound healing formulations, administered topically, able to tailor the release of the encapsulated active ingredient.

Micro- nano particulate powders able to gel in situ when in contact with the wound environment, are able to maximize the drug persistence in the site of action and to control the drug release, allowing an easy, reproducible and accurate administration of the loaded dose. Moreover, the use of proper ecceipients could promot wound healing process while stabilizing the loaded drug. Nevertheless, local drug administration avoids most of the problem of the systemic one, such as the antibiotic resistance, regarding the antimicrobials, which influences negatively the patients' compliance (50).

Such new therapeutic platforms are made by micro/nano-particulate systems in form of dry powders or aerogel, based on dextrans which are biocompatible and biodegradable, able to gel in presence of wound exudate, useful to treat chronic wounds, able to maximize the effect of the incapsulated model drug (i.e. antinflammatory, antimicrobial, wound healing promoter). Furthermore, some excipients chosen are able to stimulate the wound healing by theirselves, giving a synergic effect with the encapsulated active molecule. Gelling only on the lesion and not on the perilesional skin, the formulations permit to avoid the adverse effects of conventional medical devices, nowadays on the market, characterized by traumatic removal, giving, at the same time, wound protection from external environment and further infections.

An aerogel is a type of material derived from a gel in which liquid has been substituted by a gas, generally air. They are obtained from hydrogels by a supercritical drying process that preserves the original gel nanostructure due to near zero surface tension of the solvent mixture (51, 52).

Aerogels can be used in different field, for example for catalysis, chemical separation processes and to capture pollutants in waste water (53). Nevertheless, the typical open pore structure and high surface area make them

promising carriers for drug delivery as well as for the so called TERM (Tissue Engineering and Regenerative Medicine) (54). Because of the high mesoporosity of this kind of material, it is possible obtain the cell growth in it, with many biomedical applications. The assessment of the biological performance, attributed to the presence of calcium in the matrix, showed that the aerogels do not present a cytotoxic effect and the cells are able to colonize and grow on their surface.(55).

Regarding their use in pharmaceutics, the peculiar nanoporous aergel structure is able to entrap large quantities of drugs, permitting to obtain formulation with high encapsulation efficiencies. Furthermore, this peculiarity can be useful in for wound healing applications, due to the ability to absorb large quantities of exudates.

1.5 Polymers for pharmaceutical applications

Synthetic and natural-based polymers have found their way into the pharmaceutical and biomedical industries and their applications are growing at a fast pace.

Particular attention has recently been paid to chemistry of biocompatible and biodegradable polymers, because they have an advantage of being readily hydrolyzed into removable and non-toxic products, which can be subsequently eliminated by metabolic pathways. Furthermore, the biomedical polymers have to be synthesized now using friendly for the environment and safe for human health, effective natural initiators, co-initiators and/or catalysts (56).

Other peculiarities are their covering power, elasticity, chemico-physical stability and resistence to mechanical stress.

Materials generally used for the development of controlled release formulations are:

- Cellulose derivatives: semisyntetic polymers obtained by alchilation and esterification reactions of ossidrilic groups of cellulose polymeric

chain. There are different types that differentiate by the substituent linked to cellulose structure. For modified drug release formulations for oral delivery, the most intersting are hydroxipropylmethylcellulose (HPMC), cellulose acetatephtalate (CAP), because of their insolubility at acid pH, but solubility at intestinal pH (6.8).

- Chitosan: natural polysaccaride, constituited by glucosamine and N-acetyl glucosamine units, linked by β (1-4) bonds, extracted from shellfish. This polymer is able to gelify in presence of tripolyphosphate solutions, by an ionotropic mechanism, by an ionic bond between ionized species. It can be used for oral drug release controlled system (57), as well as for wound healing applications, particularly low molecular weight chitosan, due to its intrinsec ability to induce macrophages proliferation by a mechanism described in literature (58).
- Pectin: natural polysaccaride constituted by D-galatturonic acid units linked by α-(1-4) bonds. It gelifies ionotropically in presence of bivalent cations and to resist to gastric hydrolysis. It has been proposed for colonic delivery (59), because specific enzymes of intestinal colon flora, the pectinases, promote drug release from polymer. Furthermore, specific pectins (low methoxyl degree, high amidation degree) are able to gelify very quickly in presence of liquids, as well as of exudates (60).
- Alginate: is a linear copolymer composed by β-D–mannuronic acid and α-L–guluronic acid, extracted from differen species of brown algae such as Phaeophycaceae, able to gelify ionotropically in presence of bivalent cations as calcium, forming a typical harsh structure, defined "egg box", very useful for controlled drug release profiles formulations or for biomedical applications. High mannuronnic alginate induces cytokines production from human monocytes, a useful intrinsec activity in wound healing (61).

- PLGA is a biodegradable polymer belonging to block copolymers class, constituted by poly-lactic and poly-glycolic acids chains. With respect to the nature and to the strength of chains, it is possible to foresee the drug release kinetic. This polymer category is widely used for the formulation of injectable micro-particulate systems.

  PLGA micro-nano particles can be obtained with different methodologies, particularly "solvent evaporation" that is able to produce controlled drug releae systems for different route of administration (62).
- PLA is a polymer of lactic acid. It exists in two enantiomeric forms (L-D), but only L-enantiomer gives the polymeric crystal, with melting temperature at 180°C. PLA is a synthetic, environmentally degradable polymer, used in biomedical applications for more than ten years.

  It is derived from renewable resources such as corn, and it is hydrolytically degradable, with the products formed being bioenvironmentally compatible (63).
- Poly-ε Caprolactone is a biodegradable polyester prepared by ring opening polymerization of ε-caprolactone using stannous octoate as catalyst. It has a melting point of 60°C, and it is frequently used for the manufacture of polyurethanes.

  Polyesters prepared by ring opening polymerization of lactones are intrinsically different from conventional polyesters. Depending on the distance between the ester groups in the chain and their interactions, it is possible to find different inter- or intramolecular arrangements of the chain (64).

1.6 Encapsulation technologies

Different novel encapsulation techniques can be applied to formulate properly many kind of drugs to obtain controlled drug release topic devices, also using one-step processes, leading to the final products ready for use.

Furthermore, the abundance of different methodologies and excipients allows the production of formulation suitable for every route of administration. Micro and nano-encapsulation are fundamental for the manufacture of controlled release systems, to obtain an immediate, delayed or prolonged drug release in a specific body compartment.

1.6.1 Supercritical based technologies

In the last few year, new discoveries in supercritical fluids technology have allowed to increase the processes based on supercritical CO_2 (SC-CO_2). Conventional supercritical technologies are based on different mechanisms, such as CO_2 depressurization and expansion (rapid expansion of supercritical solutions-RESS) or supercritical antisolvent precipitation (supercritical antisolvent-SAS, solution enhanced dispersion-SEDS, or aerosol solvent extraxtion system-ASES).

In addition to conventional SC-CO_2 extraction and separation process, applied particularly in food technology, new techniques such as Supercritical antisolvent extraction (SAE) or Supercritical Assisted Atomization (SAA) are gaining much interest in drug delivery. Both such techniques have been proposed recently in production (SAA) or curing (SAE) of particle system in form of dry powders or aerogel, and in this work they were compared to traditionals, as mini spray drying, and to the innovative nano spray drying. Also supercritical solution impregnation (SSI) was proposed as innovative method to load different drugs in polymer matrix.

Supercritical fluids (SCF) are obtained reaching critical pressure and temperatures of determined substances. SCFs show liquid-like densities with

gas-like transport properties and solvent power that can be continuously adjusted by changes in pressure and temperature (65). Due to the possibility to use them in place of organic solvents, SCFs have many applications in industry. The graph below shows the phase diagram for one-component system.

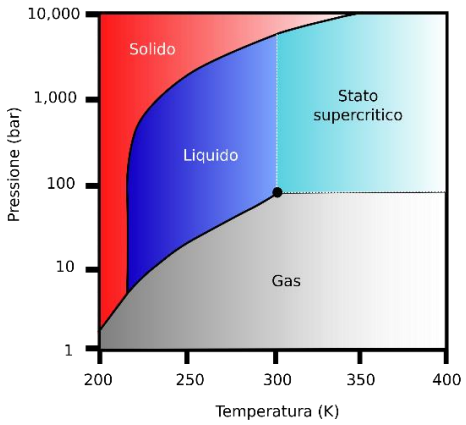

Figure 5: State diagram of carbon dioxide

Above Critical temperature (CT) and Critical pressure (CP), specific for every substance, it's not possible to distinguish liquid and vapour phase, and the system shows intermediate properties between liquid, as density, and gas, as diffusivity and viscosity (66).

The possibility to modulate density varying temperature and pressure at critical point, makes SCFs versatile for different uses such as the extraction of components from natural materials, micronization, chemical reactions, and synthesis of aerogels and aerogel based composites (67).

Sometimes, critical temperature of some substances are too high for pharmaceuticals. The higher the molecular weight, the polarity and the intramolecular bonds, the higher CP and CT (68). Carbon dioxide is the most important fluid in this field, due to its safety, availability, non toxicity and low

cost; nevertheless, it's easy to reach the critical pressure and temperature (CT 31°C; CP 73.8 bar).

The SCFs properties are known since 1897 when Hannay e Hogart (69) reported the first results regarding solid solubilization using high pressure gas. However, the first concrete applications appeared only in 1970s. Their properties such as the possibility to solubilize many substances optimizing the process conditions, make them very versatile. Supercritical processes can be used in place of old technologies, evaluating their many advantages also related to the mild conditions applied (minimization of thermic degradation of labile drugs, non toxic fluid, low costs, easily scalable and green processes).

1.6.1.1 Supercritical Antisolvent Extraction

Supercritical antisolvent extraction (SAE) is an innovative process based on supercritical CO_2, that makes possible the extraction of many components, such as catechins, polyfenols from a natural matrix (coffee beans, seeds, berries) using a co-solvent as ethanol or acetone, with very high yields and without any solvent residues.

SAE was also proposed as curing method (also named "supercritical drying" in this text), by a modification of the apparatus scheme, to remove organic solvents from solid formulations in order to obtain aerogel from alcolgel. The problems of conventional evaporation/extraction are avoided using SC-CO_2 because of its negligible surface tension. Because this fluid has no affinity for water and it is not able to extract it, it is necessary to replace aqueous medium with an organic solvent as ethanol or acetone (70). This procedure, named solvent exchange, requires a few hours before supecritical process, obtaining a complete solvent elimination.

During the process, a supercritical mixture of SC-CO_2 and the cosolvent is formed, permitting to extract liquid completely in a system with negligible

surface tension. These conditions, allow to maintain the nanostructured gel network, avoiding matrix collapse (71).

Alginate gelifies in presence of calcium cations giving ionotropic gelation that makes possible the formation of the so called “egg box” (72). Substituting water with absolute ethanol before supercrtical process (73), it was obtained an alcolgel that could be processed with SC-CO_2.

The first step consists on putting the material to be processed into the vessel of the apparatus with a proper quantity of ethanol, close ermetically all the plant and set temperature at the optimized value. Then it is necessary to wait until temperature is reached, and then CO_2 is pumped into the vessel to reach the desired pressure. At the end of the extraction process, conducted with a continuous flux of CO_2 in the system, the organic solvent is completely separated from the dried polymer matrix.

1.6.1.2 Supercritical Assisted Atomization

Supercritical assisted atomization (SAA) is one of the most efficient micronization technique based on supercritical CO_2, which principle is the formation of solvent plus solid solution that are contacted with supercritical CO_2 to form an expanded liquid of reduced viscosity and surface tension (74). These conditions produce an improved atomization. By the use of this technique it is possible to obtain microparticles in form of dry powder from a solution/dispersion. Schematically, two pumps are utilized, one for the SC-CO_2 and one for the processing solution. SC-CO_2 is pumped into the pressurized chamber reaching the supercritical condition. Stainles steel elements allow the contact between SC-CO_2 and the processing solution. A nozzle divides the pressurized chamber from the one at atmospheric pressure. A filter on the bottom allows the powder deposition. A N_2 heated flux is sent into the chamber.

The expanded liquid formed in the pressurized chamber sprayed through a micro-nozzle. The droplets formed through the nozzle are called primary and they still contain SC-CO_2. When they arrive in the atmospheric pressure chamber, the CO_2 becomes gas again, causing the breaking of the primary droplets in to secondary of controlled dimension. The evaporation of the solvent is also obtained by the pre-heated N_2 flow in the same chamber, and a filter at the bottom of the system allows the powder collection. This technique is versatile and suitable for many conditions. Differently from other SC-CO_2 based techniques in which water is not exploitable, SAA allows the processing of water based solution, and the manufacture of thermolabile pharmaceutical products by little apparatus modifications.

1.6.1.3 Supercritical Solution impregnation

The conventional preparation of drug/polymer composite is to suspend a drug into a polymer solution (75) but there are some problems related to this method such as heterogeneous drug incorporation, undesired drug reaction and low processing efficiency (76).

Supercritical solution impregnation (SSI) is an innovative method to obtain drug loaded formulation of insufficiently soluble in water active molecules (77), by dissolving drugs into SC-CO_2 forming a binary mixture drug/ SC-CO_2 that enhances the mass transfer in the drug loading process (78). After depressurization, the drug is entrapped in matrices, and finally homogeneous drug-loaded polymer matrices would be obtained. This technique is suitable for pharmaceutical, biomedical, cosmetics and food applications, as the final products are solvent free.

This method is reported for the loading of norfloxacin in contact lenses (79) or for the preparation of flurbiprofen in PMMA-EHA-EGDMA for ophthalmic delivery (80) or PLLA films loaded with roxithromycin in bacterial implants (81).

SSI allows to control the drug loading by the modification of some process parameters as well as the depressurization rate (82).

1.6.2 Prilling

Prilling or laminar jet break-up is a mild encapsualtion technique based on the principle of the laminar jet break-up, which is the breaking of a fluid in a laminar flow rate, under the action of a vibration frequence. It allows the production of particles with desired diameter and in narrow size distribution using room temperature and atmospheric pressure.

The longitudinal vibration is obtained by a radio frequence applied on a nozzle of dimension ranging from 200 to 600 μm. When the vibration wavelenght reachs the critical value, called Rayleigh wavelenght, the fluid is broken in droplets that become spherical by the action of surface tension. During their formation, droplets fall in a cationic gelling solution ($CaCl_2$), forming hydrogel with high encapsulation efficiency (83, 84).

This technique allows the formulation of also core/shell particles, by a change in the nozzle configuration. Using two concentric nozzles, it is possible to process, one step, two different polymeric solutions.

Laminar jet break-up has been studied since the end of 1800s by Savart (1833) and Magnus (1855) who showed that a stationary vibration can break precisely a liquid jet coming from a circular tube.

The most important study was the linear stability analysis by Rayleigh (1879); he analyzed the breaking of liquid jet in air studying theoretically its instablity. According to these studies, instability depends on the variability of surface tension during the vibration. The most important application of this technique is in pharmaceuticals due to the favourable operative conditions also for unstable drugs.

Figure 6: The Nisco var. D encapsulator

1.6.3 Spray drying techniques

Spray drying is a consolidate well known process. It is used all over the world in both chemical and food industry, for the production of hundreds of products. Starting from liquid solutions, it is possible to produce stable dry powders, with different applications. Also thermally sensitive material, such as pharmaceutical products, can be processed. Air is the heated drying medium; however, if the liquid is a flammable solvent such as ethanol or the product is oxygen-sensitive, then nitrogen is used.

1.6.3.1 Mini Spray drying

Mini spray drying Buchi B-191 has been used for the lab-scale production of dry powders, for both food and pharmaceutical application and its functioning can be outlined taking into account the conventional spray drying process.
Typically, it can be divided in four fundamental steps:
(a) atomization of feed into a spray, (b) spray–air contact, (c) drying of droplets, and (d) separation of dried product from the drying air (85).
A liquid feed solution is atomized into a spray of fine droplets into the drying chamber where they are in contact with hot gas at proper temperature for the moisture evaporation. As the moisture evaporates from the droplets, the solid

product is formed, and the powder is readily recovered from the drying gas. A cyclone separator is used as powder-collection equipment, in which particle-laden gas enters a cylindrical or conical chamber tangentially at one or more points and leaves through a central opening at the top. Solid particles, by virtue of their inertia, move toward the wall of the separator from which they are led into a receiver. Working essentially as a settling chamber, the cyclone uses centrifugal acceleration to replace gravitational acceleration as the preparation (86, 87). Powder collection by the cyclone is governed by a complex fluid dynamic behavior in the cyclone and the receiver (88). The fluid behavior is affected by cyclone design (89).

Figure 7: Mini spray drier Buchi B 191 and the internal parts of the atomizator.

1.6.3.2 Innovative Nano spray drying

Nano spray drying technology is an evolution of the spray drying and has been used for the production of nanometric particles as novel drug delivery system for different route of administration (90, 91).

Nano spray Buchi B-90 uses a different atomization method, based on a piezoelectric crystal driven actuator, vibrating a thin, perforated, stainless steel membrane in a small spray cap. The perforated membrane has a precise dimension of 4 µm, 5.5 µm or 7 µm mesh sizes that can be used to tune the average droplet size. The liquid feed based on aqueous or organic solvents, is

fed through a peristaltic pump, at the desired flow rate. When an ultrasonic frequence (60 kHz) is applied on the piezoelectric system, the nozzle mesh vibrates upwards and downwards, generating the feed droplets with very narrow size distribution (92). A drying gas, generally air, enters in laminar flow from the top into the drying chamber and is heated up to reach the set inlet temperature. The laminar flow is generated by air passing through a compact porous metal foam; laminar flow allows a gentle heating, making the system ideal for heat-sensitive materials.

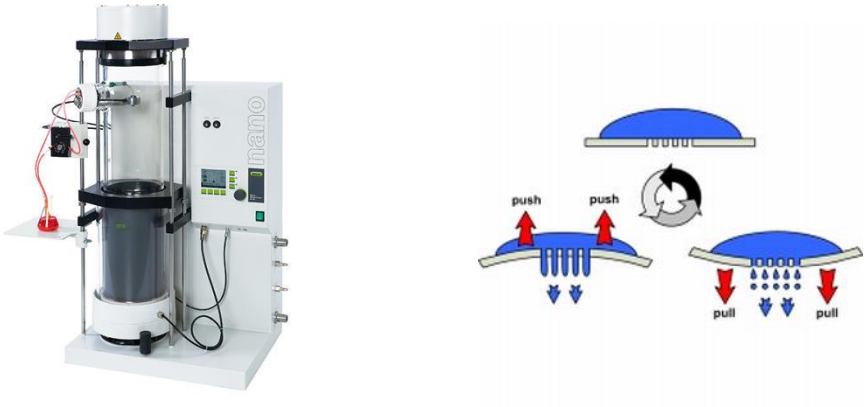

Figure 8: Nano spray drier Buchi B-90 and a schematic representation of the vibrating nozzle membrane.

Particle collection mechanism is indipendent of particle mass and it's obtained by an electrostatic precipitator. The vertical configuration of the spray dryer reduces particle adherence to the glass of the chamber, increasing collection yields. Prior the collection the solid particles are electrostatically charged and deposited at the surface of the collecting electrode consisting of a grounded star electrode (cathode) and cylindrical particle collecting electrode (anode). The presence of a high voltage around the particle collector creates an electrostatic field that accelerates the deposition of negatively charged particle onto the inner wall of particle collecting electrode. This is followed by a discharging process.

Figure 9: The Nano spray drier electrostatic particle collector: On the left clean and on the right with particles attached.

1.7 Aims of the thesis project

The worldwide problem of complicated chronic skin wounds focuses the scientific community interest on the research of innovative and appropriate solutions, potentially able to reduce hospitalization and to replace the expensive treatments nowadays available on the market.

In this context my Ph. D. project proposes the production of novel *in situ* gelling formulations based on natural biopolymers able to control drug release profiles and to overcome many problems related to conventional devices (traumatic removal, poor conformability, occlusiveness, high costs).

High M content sodium alginate, low molecular weight chitosan, and pectins were chosen as biodegradable and biocompatible drug carrier. Alginate and chitosan are known for their intrinsic activity in wound healing as well as for technological characteristics, such adesivity, fluid uptake ability very useful in topic administration. Differences between the pectins chosen in terms of fluid uptake and swelling rate were considered important for the development of a proper novel medical device for wound healing.

Objective of my study was to verify these properties and the processability of such materials with the innovative techniques proposed.

Antibiotics such as gentamicin, doxycycline, norfloxacin were chosen to act as antimicrobial agent in infected wounds and to enhance the healing process by contrasting bacterial spreading. In fact, all the proposed antimicrobials have a wide spectrum of action, are inexpensive and are easily available, and their systemic side effects are well known. Ketoprofen was used as antinflammatory model drug belonging to class II BCS, while the peptidomimetic, Ac2-26 Annessin 1 N-terminal residue, was chosen due to its ability to repair membrane, to organize cytoskeleton and to promote migration, all activities enhancing wound healing, and because it is unstable at normal physiological conditions. The aim was to verify the possibility to encapsulate efficiently

these active ingredients by novel encapsulation technologies as spray drying and SC-CO_2 based techniques, to improve their stability after the encapsulation, to increase their efficiency in wound healing treatments by improving their bioavailability and to obtain novel formulations with tailored drug release profiles.

The project proposed to study the feasibility Nano spray drying and supercritical CO_2 based technologies such as Supercritical Assisted Atomization (SAA), Supercritical Antisolvent Extraction (SAE), Supercritical Impregnation and the tandem technique prilling/SAE.

Important objectives were to optimize process parameters, in order to obtain high yields, reducing processing times and to produce successfully drug loaded devices in form of dry powders and aerogel.

General objectives were to produce formulations easy to handle and administer directly on the wound, with rapid gelation and a proper transpiration and moisture control on the wound site. Moreover, a tailored drug release profile was mandatory. Then, all the studies were carried out in order to understand the formulations' behaviour *in vitro* and *ex-vivo*, particularly using scanning electron microscopy, laser scattering and fluorescence microscopy for morphological characterization; the optimization of drug release profiles using Franz type diffusion cells was conducted in simulated wound fluids as acceptor solutions; the characterizations in terms of adhesiveness and transpiration properties of the formed gel, of flowability of the producted powders, and of gelation rates were carried out with proper experiments.

In vitro tests were selected for the antimicrobial loaded formulations on bacterial strains; *ex-vivo and in vivo* experiments were carried out to understand reparative activity of peptide loaded hydrogels using murine models.

During the last year, three months were spent in Spain at Universidade de Santiago de Compostela, with the aim to study an innovative supercritical process, the superitical impregnation, for the production of norfloxacin and ketoprofen loaded alginate aerogels. Objectives were to optimize process conditions, and characterize the formulations containing norfloxacin and norfloxacin/ketoprofen.

2. MATERIALS AND METHODS

2.1 Chemicals

In this work, many polymeric materials were used as carrier and different molecules as active pharmaceutical ingredients, as reported below:

1) Sodium Alginate, high M residues content, high viscosity from brown algae- (1% viscosity 65 mPa s; mannuronic acid content 70%- Carlo Erba reagents, Milan, Italy)
2) Sodium Alginate, high M residues content, medium viscosity- (mannuronic acid content 70%- Dompè Pharma, L'Aquila, Italy)
3) Chitosan low molecular weight- (Sigma Aldrich, Milan, Italy)
4) Pectin low methoxyl degree from citrus fruit, Fluka- (Sigma Aldrich, Milan, Italy)
5) Pectin high amidation degree- (Herbstreit&Fox Corporate group, Neuenbürg/Württ, Germany)
6) Gentamicin sulphate- (Sigma Aldrich, Milan, Italy)
7) Doxycycline Hiclate- (Unione Commeriale Lombarda, purity ≥ 98%)
8) Norfloxacin- (Carbosynth, Compton- Berkshire, UK)
9) Ketoprofen- (Dompè Pharma, L'Aquila, Italy)
10) Annessin like derived peptide, Ac2-26- (Tocris Bioscience, Bristol, UK)
11) Calcium chloride, (Sigma Aldrich, Milan, Italy)
12) Ethanol 96° and absolute, VWR and Fluka reagents (VWR International, Radnor, Pennsylvania, and Sigma Aldrich, Milan, Italy)
13) KBr FT-IR degree (purity >99%trace metal basis), (Sigma Aldrich, Milan, Italy)
14) CO_2 (purity 99%) Società Ossigeno Napoli (S.O.N., 104 Naples, Italy).
15) Simulated wound fluid (SWF) consisting in 50% foetal calf serum (Sigma Aldrich, Milan, Italy) and 50% maximum recovery diluent

(Sigma Aldrich, Milan, Italy), composed by 0.1% (w/v) peptone, peptic digest of animal tissue, and 0.9% (w/v) sodium chloride).

2.2 Encapsulation technologies systems

2.2.1 Prilling

Prilling instrument used in this work is from Nisco Encapsulator® var. D (Nisco Engineering Inc., Zurigo CH).

The apparatus is composed by:

[1] A control unit regulating frequence, vibration amplitude, feed solution flux, stroboscopic lamp intensity.

[2] A head containing a membrane vibrating system, used at proper frequency (Hz).

[3] A stainless steel nozzle with different diameters ranging between 100µm and 600µm; for this work 400 and 600 µm were chosen.

[4] A 60 ml syringe containig the feed solution (polymer and drug) to be processed.

[5] A piston pump (Model 200 Series, Kd Scientific Inc., Boston, MA, USA) used to regulate the feed solution flux.

[6] A becker containing the gelling solution.

[7] A magnetic stirrer.

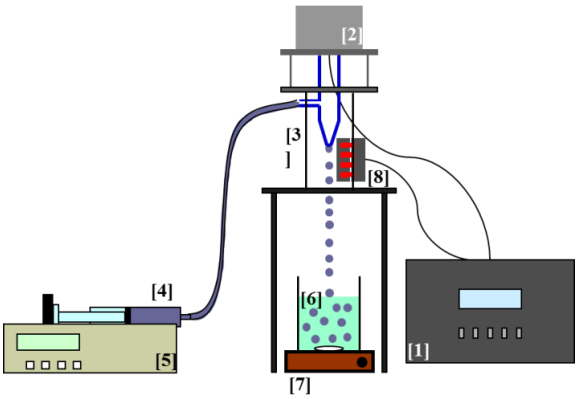

Figure 10: A schematic representation of Prilling apparatus.

2.2.2 Minispray drier

The model of instrument used is Mini-spray drier Buchi-B 191(Buchi Laboratoriums-Tecnik, Flawil, Switzerland). This apparatus includes:

1) A peristaltic pump for the feed delivery to the drying chamber and a spray gas connection to the atomizator.
2) A concentric nozzle for the pneumatic atomization, of 0.5 mm of diameter.
3) A pre-heated drying gas entrance in co-corrent.
4) A drying chamber in which feed droplets are transformed in dried particles.
5) Two collectors, one at the bottom of the drying chamber for liquid droplets, one at the bottom of cyclone for dried product.
6) A cyclone for the separation of the air from the particles to obtain the powder collection.
7) A filter at the end to purify air from particulate before the reintroduction.

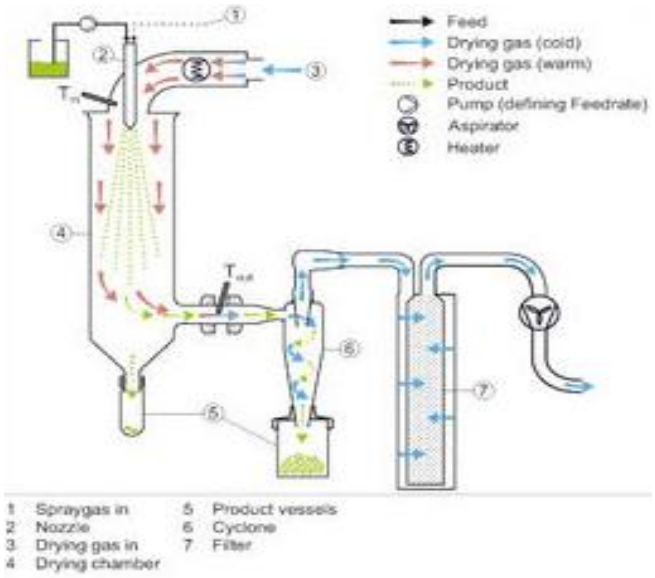

Figure 11: A schematic representation of mini spray drier components.

2.2.3 Nanospray drier

The model of instrument used is Nano spray drier Buchi B-90 (Buchi Laboratoriums-Tecnik, Flawil, Switzerland). This apparatus includes:

1) A pre-heated gas entrance in co-corrent, on the top. A compact porous metal foam produces the laminar flow.
2) A piezoelectric actuator set at 60 kHz that produces feed atomization.
3) A drying glass chamber, in which feed droplets become dry.
4) An electrofilter for particle collection on the bottom of the system.
5) A grounded electrode.

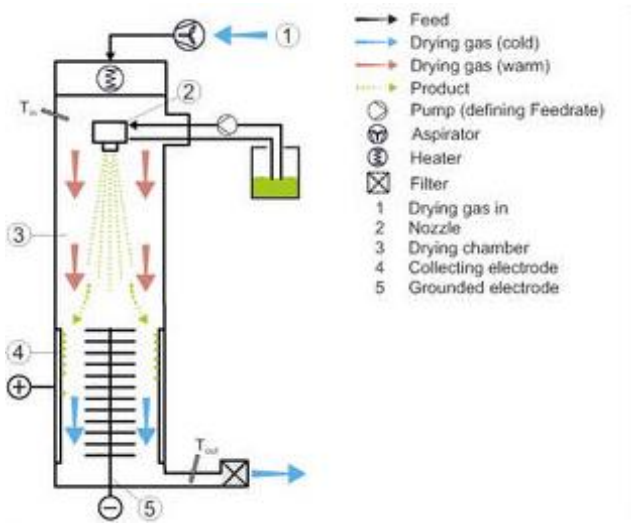

Figure 12: A schematic representation of Nanospray drier components.

2.2.4 SAA apparatus

The implant scheme for supercritical assisted atomization includes different parts:

1) Two peristaltic pump (mod. 305, Gilson, Middleton, MO, USA), one for the feed solution delivery and one for the carbon dioxide which rate is regulated by the gas-liquid ratio.

2) A mixing chamber (saturator- internal volume 25 cm^3), in which stainless steel perforated saddles make possible a large contact between feed solution and SC-CO_2. This is the only implant part at high pressure values (80-100 bar), in which carbon dioxide becomes supercritical. This mixing chamber is linked to the precipitation one by an 80 µm nozzle.
3) Precipitation chamber is heated by electrical resistances and it is at atmospheric pressure. Furthermore, a controlled flow of N_2 was taken from a cylinder, heated in an electric heat exchanger (mod. CBEN 24G6, Watlow, St. Louis, MI, USA) till 85°C and sent to the precipitator to facilitate liquid droplets evaporation.
4) A filter on the bottom permits to collect powder and the gas stream out.

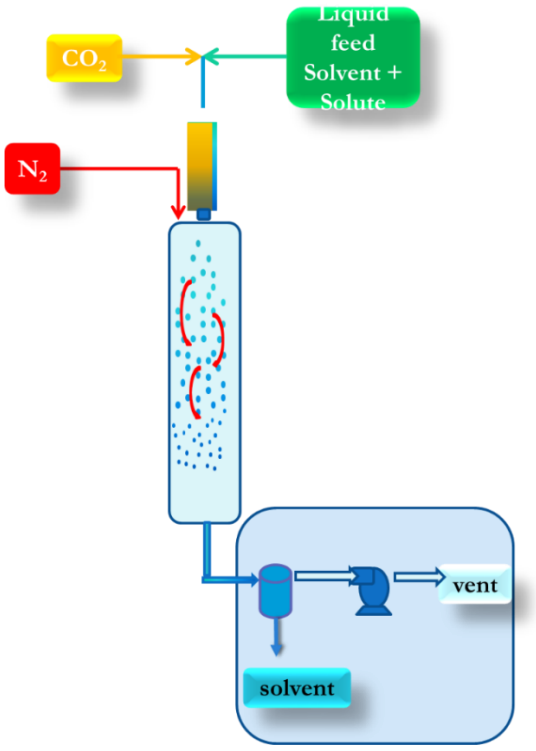

Figure 13: A schematic representation of SAA apparatus.

2.2.5 SAE apparatus

Supercritical drying was conducted using a laboratory implant showed in figure 14.

It can be divided in three sections:

- Pumping;
- Drying;
- Separation.

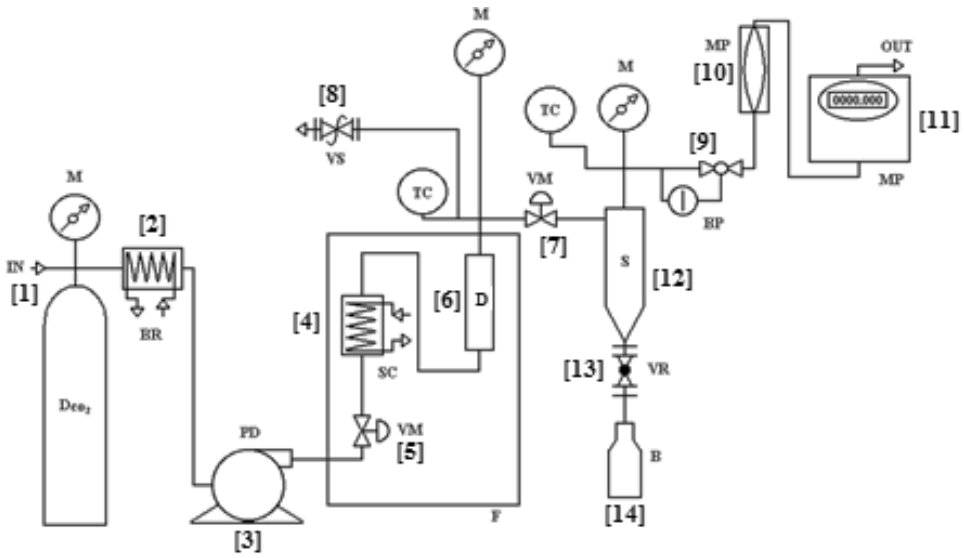

Figure 14: A schematic representation of SAE apparatus.

Pumping section is composed by:

1) Feed line linked to a stock eservoir of 40 liters.

2) A cooling bath;

3) A membrane pump (Milton Roy mod. Milroyal B), modified using a cooling circuit of the pump head and of the CO_2 aspiration line.

Drying section includes:

4) An owen heated by convective air;

5) A micrometric valve allowing the CO_2 entrance into the drying vessel;

6) A drying cilindric stainless steel (AISI 316) vessel;

7) A micrometric valve (Hooke mod.1335G4J) at the dryong vessel exit;

8) A three direction valve (Whithey mod. SS43S4), as a security device;

9) A back pressure valve (Tescom mod. 26-1700), at the end of the separator;

10) A rotameter (ASA mod. N.5-2500, Serval N.115022), for measuring the instant CO_2 flow;

11) A roll counter measuring the total CO_2 quantity flowed (Sim Brunt, mod. B10).

Separation section includes:

12) A conic stainless steel separator (inox AISI 316);

13) An on/off valve (Whithey mod. SS43S4), put on the separator bottom, that allows to withdraw solvent during the process;

14) A glass flask to collect solvent extracted.

Drying implant include salso manometers to measure pressures, termocouple to control operative temperatures. All the controls are localized in a specific electric panel.

2.2.6 Supercritical impregnation apparatus

Supercritical impregnation apparatus scheme is showed below.

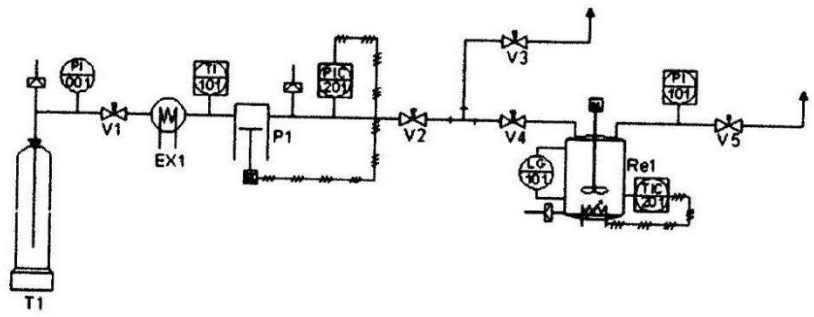

Figure 15: Scheme of Supercritical Impregnation apparatus.

The apparatus is composed by a bottle containing CO_2 (T1) which flux is controlled by valve V1.

Then CO_2 is conducted to peristaltic pumps (P1) cooled by a bath (Ex1).

A series of valve (V2, V3, V4) serves to regulate pressure along the tubes that conduct to the vessel (Re1).

Into the vessel pressure is increased at the desired value and temperature is regulated by termocouples associated to electric resistences.

Valve V5 is at the end of the apparatus to depressurize easily the vessel.

A back pressure valve, controlled by a software, is needed to perform a precise depressuriation program.

2.3 Analytical technologies

2.3.1 FT-IR spectroscopy

Infrared analysis was performed using a FTIR spectrophotometer (FT-IR Nexus, Thermo-Nicolet, West Palm Beach, FL, USA) equipped with a mercury-cadmium-telluride detector. This analysis was used for powders as well as for aerogel beads. The samples were combined with small amount of potassium bromide FT-IR degree (with ratio sample/KBr from 1/20 to 1/60, depending on the flowability of the powder analized) and pressed from 6 to 10 tonnes in a manual press (OMCN s.p.a., Bergamo, Italy). The thin compacts produced were analyzed using 256 scans with a1 cm^{-1}resolution step.

Figure 16: FT-IR Nexus apparatus.

2.3.2 Differential Scanning calorimetry

Beads, dry powders and raw materials thermal characteristics were determined by differential scanning calorimetry (DSC) (Mettler Toledo DSC 822e module controlled by Mettler Star E software, Columbus, Ohio). An appropriate amount of dried beads or powders was crimped in a standard aluminum pan that was pierced and heated from 25°C to 130°C firstly to obtain dehydration and then from 25°C to 350°C at a scanning rate of 10°C/min to perform the analysis. The characteristic peaks were recorded and the specific heat of the melting endotherm was evaluated. DSC was performed in nitrogen atmosphere at a flow rate of 100 mL/min.

Figure 17: DSC 822e Mettler Toledo apparatus.

2.3.3 Scanning Electron Microscopy

The morphology of all formulations, studied by Scanning electron microscopy (SEM), was performed using a Carl Zeiss EVO MA10 microscope with a secondary electron detector (Carl Zeiss SMTLtd., Cambridge, UK) equipped with a LEICA EMSCD005 metallizator producing a deposition of a 200–400 Å thick gold layer. Analysis was conducted at 20 KeV. Powders were dispersed on a carbon tab previously stuck to an aluminium stub (Agar Scientific, Stansted, UK). Samples were coated with gold using a sputter coater (mod. 108˚A, Agar Scientific, Stansted, UK). At least 20 SEM images were taken into account for each run to verify the microparticles uniformity.

Figure 18: Scanning Electron microscope Evo Zeiss MA 10.

2.3.4 Laser Scattering

Particle size distribution was evaluated by static light scattering (LS) equipped with a microliquid module (Coulter LS 13320, Beckman Coulter, Inc., Fullerton, CA, USA). The Coulter LS 13320 software uses Mie theory to produce an optimal analysis of the light energy distribution and to obtain the size distribution of the particles. Analyses were performed after the preparation of the microspheres suspensions using 30 mg of each sample dispersed in dichloromethane by sample sonication. The effectiveness of the microspheres dispersion was verified performing the measurement after different sonication times ranging between 5 and 30 minutes. Moreover, measurements on each sample loaded in the instrument were repeated at different time intervals, that is, every 5 minutes for 30 minutes. Results were expressed as d_{50} and span defined below:

$$Span = \frac{d_{90} - d_{10}}{d_{50}} \quad (1)$$

where d_{90}, d_{50} and d_{10} indicate the volume diameters at the 90th, 50th and 10th percentiles, respectively. In all time intervals, good reproducibility of results was obtained.

Figure 19: Beckman Coulter LS 13320 apparatus.

2.3.5 Adhesion strength mesuarments

Adhesive properties of the formulations were evaluated by means of a tensile stress tester Electroforce 3200 testing instrument (Bose, Eden Praire, MN) using a modified protocol of ASTM D3808 standard. Briefly, each formulation (15 mg of dry powder) was layered on a nitrocellulose membrane filter (0.45 µm pore size, 3.14 cm^2 area) conditioned with SWF. After gel formation due to the contact between the formulation and the fluid, reached in 30 min, the membrane was placed on the movable horizontal sample-holder of the apparatus. The movement of the sample holder at a rate of 1 mm/min caused the compression of the gel against the measuring head of a calibrated load cell. The force time curve was recorded on a personal computer and the force under which gel detached from substrate was calculated by LabChart 8 (AdInstruments, Oxford, UK).

Figure 20: Tensile stress tester Electroforce 3200 Bose, Eden Praire.

2.3.6 Density measurements

A Helium pycnometer (Accupyc 1340, Micromeritics Corporate, Norcross, USA) was used to study the real density of the powders produced with different polymers.

Figure 21: Micromeritics Accupyc 1340, helium pycnometer.

A calibration program was performed, in order to have optimal results.

For analysis, it was firstly necessary to set the regulator pressure of helium at the higher (plus 2 psig) of the purge fill pressure and the cycle pressure. By

opening and close the valves, it was possible to equilibrate helium flux into the measurement chamber.

Then, a powder amount of about 150-200 mg was put into a sample cup previously dried, and the weight recorded. When the sample was loaded, the cup was immedialtely replaced on the holder, in order to prevent particles from accumulating on the greased.

Ten measurements were performed and an average value was calculated.

2.3.7 Pore volume measurements

Brunauer Emmett Teller theory explains the physical adsorption of gas on solid surfaces and it is the basis to measure specific surface area of a material.

Physical adsorption results from relatively weak forces (van der Waals forces) between the adsorbate gas molecules and the adsorbent surface area of the material.

Specific surface area of the alginate aerogels was quantified from low-temperature N_2 adsorption-desorption data (Nova 3000e, Quantachrome, USA). Prior to measurements, samples were dried for 20 h under vacuum (<1 mPa) at 60°C for the outgassing phase. This procedure is useful to remove gases and vapours that may have become physically adsorbed onto the surface after manufacture and during treatment, handling and storage.

The determination was usually carried out at the temperature of liquid nitrogen. The amount of gas adsorbed can be measured by a volumetric or continuous flow procedure. In this work, a static volumetric determination was conducted. As adsorption takes place, the pressure in the confined volume falls until equilibrium is stablished. The amount of gas adsorbed at the equilibrium pressure is given as the difference between the amount of gas admitted and the amount of gas required to fill the space around the adsorbent, the dead space, at the equilibrium pressure.

Figure 22: Nova 3000e, Quantachrome, USA- Brunauer Emmett Teller measurements.

2.3.8 Polymer solutions rheological characterization

Polymer solutions, of the Ac2-26 loaded hydrogel, were subjected to a complete rheological characterization using a rotational rheometer (Bohlin CS Rheometer, Bohlin Instrument Division, Metrics Group Ltd., Cirencester, UK). A cone plate combination (CP 4/40) was used as measuring system. All measurements were carried out at 37 °C, after a rest time of 3 min. Zero shear rate viscosity, η_0, was obtained after application of 50 s^{-1} shear rate for 1 min. Dynamic oscillatory tests were performed in the linear viscoelastic range. The viscoelastic parameters storage modulus (G') and loss modulus (G'') were measured at frequencies ranging between 0.1 and 5 Hz.

Figure 23 Image of Bohlin CS rheometer instrument

2.4 Experimental procedures

2.4.1 Powders, aerogels and hydrogels preparation

2.4.1.1 Gentamicin, alginate and pectin powders

Gentamicin (GS), alginate and pectin powder formulations were prepared with specific protocol described here. Particles obtained by nanospray drying and SAA (vs Mini spray drying) were prepared by processing different aqueous feeds. After a series of pilot experiments, GS and alginate/pectin ratio were set at proper values, and different total concentrations of the colloidal dispersion were chosen (see results and discussion 3.1.1 and 3.2.1.1). Feeds were obtained by slowly adding a GS solution to an aqueous solution of alginate and pectin blend, previously prepared, under gentle stirring. Dextrans blend solution was obtained by dissolving both polymers in distilled water under vigorous stirring while GS solution was obtained by dissolving a carefully weighted amount of the drug in distilled water under gentle stirring.

Nano spray drying process parameters and conditions were set as follows: inlet temperature 90 °C, feed rate 9.5 ml/min; nozzle diameter 4.0, 5.5 or 7.0 mm, air flow 100 l/min, relative spray rate 100%.

Feeds for pneumatic atomization were spray-dried using spray drying laboratory apparatus (mini spray dryer B-191 BuchiLaboratoriums-Tecnik, Flawil, Switzerland) with process parameters and conditions set as follow: inlet temperature 120°C, outlettemperature 66°C, feed rate 5 ml/min; nozzle diameter 0.5 mm, drying air flow 500 l/h, air pressure 6 atmospheres, aspirator 100%. Feeds for supercritical assisted atomization (SAA) were produced using a laboratory apparatus consisting of two high-pressure pumps (mod. 305, Gilson, Middleton, MO, USA) delivering the liquid solution/suspension and liquid CO_2 to a heated bath (Forlabmod. TR12, Carlo Erba, Milan, Italy) and, then, to the saturator. The saturator (internal volume 25 cm^3) containing stainless steel perforated saddles which assure a large contact surface between

liquid solution and CO_2. The SAA process was conducted dissolving super-critical CO_2 (SC-CO_2) in the feed solutions (mass flow ratio between CO_2 and water set at 2.5). The solution obtained in the saturator was sprayed through the injection nozzle into the precipitator (internal volume 3 dm^3) operating at atmospheric pressure. A controlled flow of N_2 was taken from a cylinder, heated in an electric heat exchanger (mod. CBEN 24G6, Watlow, St. Louis, MI, USA) till 85°Cand sent to the precipitator to facilitate liquid droplets evaporation. The saturator and the precipitator were electrically heated using thin band heaters. A stainless steel filter located at the bottom of the precipitator allowed the powder collection and the gaseous stream flow out.

2.4.1.2 Doxycycline, alginate, chitosan and pectin powders

Doxycycline, alginate, chitosan and pectin powder formulations were prepared using the protocol described as follows.

Briefly, a proper amount of alginate was dispersed in distilled water and left under stirring until a homogeneous solution was obtained. In another becker chitosan was dissolved in HCl 0.1M and then a 50 mM solution of tripoliphosphate (TPP) was added in order to obtain a partial complexation of the polymer (93).

Then the chitosan/TPP solution was slowly added in the alginate one, avoiding total precipitation. A partial precipitation happened in every case, and an adjustment of pH until 5.5 was required to clarify the solution and to have the final powder with a pH value correct for skin application (94).

Mini spray drying parameters were 110°C of inlet temperature, 72°C of outlet temperature, 500/600 air flux, 6 bar of air pressure, 100% aspirator and 10% pump, 0.5 mm nozzle.

Nano spray drying parameters were 70°C of inlet temperature, 65°C of head temperature, and 40°C of outlet, 5.5µm nozzle, 100 l/min of air flux and 30 mbar of pressure.

2.4.1.3 Alginate aerogels preparation

Optimization parameters of prilling and SAE for the tandem technique Prilling/SAE are described in paragraph 3.2.2.1.

2.4.1.4 Core/shell aerogels preparation

Core/shell particles were obtained using a specific protocol described here, after the optimization of Prilling/SAE tandem technique.

Microcapsules were produced using prilling apparatus equipped with two syringe pumps and with coaxial nozzle which consists of two concentric nozzles. Alginate annular solution was pumped through a 600 μm nozzle while for the D/pectin core solution was used a 400 μm nozzle. The vibration frequency set to break up the laminar liquid jet was 350 Hz and amplitude of vibration at 100%. The distance between the vibrating nozzle and the gelling bath was fixed at 25 cm. A stroboscopic lamp set at 65% of amplitude was used to observe the falling droplets. Gelling solution consisted of 0.5M $CaCl_2$ ethanolic solutions (100% ethanol 96°), saturated with doxycycline, under gentle stirring in which the droplets were held for 5 minutes and then put into paper filters (Rishi tea, loose leaf tea bags) for the drying process without rinsing. Supercritical optimized conditions were 150 bar, 38°C, 0.6 kg/h CO_2 flow and the experiments last 90 minutes.

2.4.1.5 Alginate aerogels loaded by supercritical impregnation

In the period spent at Universidade de Compostela, the combination of prilling/supercritical drying/supercritical impregnation was studied. Firstly, alginate hydrogels were prepared by prilling using these optimized conditions (8 ml/min of feed flow rate, 350 Hz of frequency, 100% of amplitude and 400 μm the nozzle diameter and 25 cm the distance between the vibrating nozzle and the gelling bath). Supercritical drying was conducted using conditions set at 120 bar, 40°C, 5-7g/min for 3.5 h. Impregnation process was conducted at

180 bar, 40°C in batch mode. Depressurization was conducted using a specific protocol in order to avoid drug amorphization (from 180 bar to 5 bar in 1.5 h with proper time steps: 180-160 bar in 516 seconds, 160-140 in 308 seconds, 140-120 in 256 seconds, 120-100 in 1835 seconds, 100-80 in 586 seconds, 80-65 in 823 seconds, 65-45 in 655 seconds, 45-30 in 221 seconds, 30-15 in 303 seconds and 15-5 in 108 seconds).

2.4.1.6 In situ injectable Ac2-26 hydrogels

Alginate and chitosan hydrogels for the encapsulation of Ac2-26 Annessin 1 like derived peptide were prepared as described below.

Alginate powder was dispersed in distilled water under vigorous stirring (1500 rpm) for 15 min then the solution was left undergentle stirring (100 rpm) for 2 h. Finally, polymer solutions were left motionless for 4 h to remove air bubbles. Chitosan gels were prepared using the same procedure dissolving chitosan powder in 0.1 M acetic acid buffer solution then pH was adjusted to 6.3 using 0.1 M NaOH aqueous solution. Ac2-26 peptide loaded gels were prepared by mixing in an orbital shaker (Vortex Genius 3, IKA-Werke GmbH & Co., Staufen,Germany) a precise volume of either high M alginate or LMW chitosan solution by means of an Hamilton syringe (Hamilton AG,Bonaduz, Switzerland) and a precise volume of a peptide stock solution by means of a Gilson pipet (Pipetman Classic, Gilson, Inc.,Middleton, WI, USA) in order to obtain a final peptide concentration of 100 nM, 500 nM and 1 µM in either alginate solution at 2.5%and 5.0% (w/w) or chitosan solution at 3.5% and 6.5% (w/w).

2.4.2 Drug permeation and fluid uptake ability studies

Drug permeation profiles of formulations were obtained by means of Franz type diffusion cells using, as donor compartment, a simulated wound fluid (SWF) composed by 50% of Fetal Calf Serum and 50% of peptone, 0,1%

peptic digestic fluid and 0,9% NaCl physiological solution (95) or 100 mM phosphate buffer (KH_2PO_4) correcting pH at 7.4 with NaOH 6N

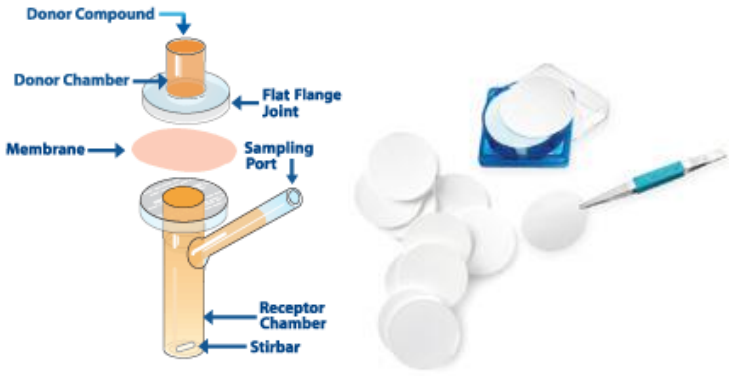

Figure 24: Franz type diffusion cell and Merck Millipore HVLP membranes

The cell was thermostated at 37°C, with 200 rpm of stirring, and the membrane used were of 0.45µm of diameter and HVLP (for biological solution, Merck- Millipore, Darmstadt, Germany) or HAWP (nitrocellulose, Merck- Millipore, Darmstadt, Germany) types. For drug permeation studies, formulation was put on the membrane, previously conditioned, and at defined point of time, the samples were collected by the sampling port in a quantity of 0.2 ml and then analysed using proper methods, adapted on each molecule, as described afterwards.

AC2-26 release assays were performed by means of slide analyzer mini dialysis units, 10 K molecular weight cut off (Thermo Fisher Scientific Inc., Waltham, MA, USA) with an exposed surface area of 0.33 cm^2. The dialysis cup was filled with 200 µl of AC2-26 loaded gel. Experiments were conducted in a cylindrical vial filled with 3 ml of simulated wound fluid (SWF) thermostated at 37°C and magnetically stirred at 200 rpm by a teflon-coated stirring bar placed in the receptor compartment. The receptor solution, 100 µl aliquots, were sampled at specific time points and analysed by LC-MS for the determination of AC2-26 permeated through the dialysis membrane.

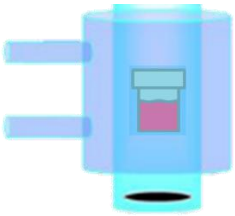

Figure 25: Slide analyzer dyalisis unit

For fluid uptake ability studies, conducted on dry powders and aerogels, Franz cell was used in an open configuration, without the donor chamber, and membrane with sample was weighted at defined point of time, in order to test the quanitity of fluid absorbed by the dry formulation.

Fluid uptake was calculate using the following equation:

$$Fluid\ uptake = \frac{W_w}{W_d} * 100 \qquad (2)$$

where W_w is the weight of the wet formulation, and W_d is the initial weight, when formulation is dry.

2.4.3 HPLC, LC/MS and Uv-vis Spectrophotometry methods for drug content and encapsulation efficiency determination

Drug content (d.c.) was obtained as the ratio between actual drug weight and total formulation weight while encapsulation efficiency (e.e.) was calculated as the ratio of actual to theoretical drug content.

Gentamicin (GS) was analysed with a modified pharmacopoeia method for GS and calibration curves were worked out and proportionality between GS concentration and AUC checked in the range 5–450 µg/ml. The isocratic method had as mobile phase an aqueous solution consisting in 70% Methanol, 25% water and 5% acetic acid glacial. The column was a Macherey-Nagel 150*4,5 mm -100/5Å.

1 mg of powder was dissolved in 3 ml of HPLC water and left under stirring until a homogeneous solution was obtained.

Gentamicin was derivatized in order to become Uv sensible, using an orto-phtaladialdeide solution, with the following protocol: an aliquot of 200 µl of sample was mixed with 2,48 ml of water, 2,75ml of isopropanol, 1 ml of derivatizing solution and 1 ml of mobile phase. The resulting solution, after 15 minutes in a 61°C water bath, was then filtered with 0.45 µm filters for organic solvents and analysed at 340 nm.

Doxycycline was analysed in aqueous medium at Uv-vis spectrophotometer at 342 nm. Briefly, 3 mg of powders were dissolved in 6 ml of distilled water and left under stirring until complete dissolution was reached. The solution obtained was filtered with 0.45 µm Millipore filters and analysed using 1 cm quarz cells.

The procedure for core/shell aerogel doxycycline loded particles was a little different: 2 or 3 beads were put in 2 ml of 100mM PBS and left under vigorous stirring until an homogneous solution was obtained. Then 8 ml of bidistilled water were added and then the solution was sonicated for 5 minutes and finally filtered with 0.45 µm filters.

Ketoprofen and norfloxacin were analysed by Uv-vis spectrophotometry, using wavelenghts of 254 nm and 334 nm respectively, and 274 nm for the mixture of the two drugs. The molecules extraction procedure from aerogel matrix was the following. 2/3 mg of particles were put in 2 ml of 100 mM PBS and left under vigorous stirring until a homogeneous solution was obtained.

Then 3 ml of bidistilled water were added and the solution was centrifuged at 6000 rpm for 10 minutes and then analized. If necessary, a diluition on the sample was performed.

Ac2-26 HPLC-MS method used was the following: after 6 h of incubation, 1 ml of each sample was pre-purified on a Chromabond HR-X SPEcartridge (Macherey-Nagel, Düren, Germany) using water and 70% acetonitrile as washing and elution solution, respectively. LC/MSanalyses were performed on a LTQ XL instrument (Thermo Scientific) equipped by an ESI ion source and

a hybrid quadrupole/lineartrap analyzer and coupled with an Accela 600 HPLC system. Chromatography was performed on an Aeris C18 (2.0 × 150-millimeteri.d., 3µm) reversed-phase column, using a mobile phases A (0.1%formic acid in water, v/v) and B (0.1% formic acid in acetonitrile, v/v), using a linear gradient increase from 25 to 70% B in 30 min. The flow rate was 200 µl/min. Mass spectra were acquired in positive ion mode over the m/z range from 700 to 1600.

2.4.4 Fluid loss experiments

Fluid loss of hydrogel formulations was evaluated over time as the ratio between fluid content of the gel at a specific time point and a carefully weighted amount of gel after preparation. Briefly, 250 µl of formulation was spread over a previously weighted filter paper disc. The membrane was in contact with a donor compartment filled with 100 µl of simulated wound fluid (SWF).

At regular intervals of time, the weight of the gel was measured. Fluid loss percentage was associated to weight loss and calculated by the following equation:

$$Fluid\ (\%) = \frac{W_t}{W_0} * 100 \qquad (3)$$

where W_0 is the initial weight and W_t is the weight at the specific time point.

2.4.5 Antimicrobial tests

Briefly, an overnight culture of *S. aureus* strain A170 was diluted 30 fold with prewarmed Mueller-Hinton Broth (MHB) and incubated at 35°C under constant shaking. The late log phase of growth was normalized to 2.5×10^8 cells/ml and 200 µl were used to inoculate three sterile 96-well plates further treated with the different formulations corresponding to a proper quantity of GS, used as control. At defined time points (6, 12, and 24 days), viable counts were calculated to give CFU/ml (colony forming unit per ml) by plating serial

dilutions on MHA incubated at 35◦C. Kill curves were plotted with time against the number of CFU recovered. Each antimicrobial assay was performed in triplicate in separate days. To assess the ability of formulations to degrade *P. aeruginosa* ATCC-27853 biofilm, bacteria were grown overnight in MHB medium. Cultures were then diluted to approximately 107CFU/mL in fresh MHB medium, and 200 µl was used to inoculate flat-bottom 96-well polystyrene microlitre plates. The biofilms were allowed to develop up to 24 h at 37◦C, afterwards, formulations corresponding to 0.25 or 0.70 mg/ml of GS (for nanospray and minispray/SAA formulation respectively) used as control were added on each well. After incubation for 8 h at 37°C without shaking, the plate wells were washed twice with phosphate-buffered saline (pH 7.2) to remove unattached cells and dried in an inverted position. Finally, the adherent cells were stained for10 min with 200 µl of Gram's crystal violet (CV). Wells were rinsed with water and dried. The amount of biofilm mass was obtained by destaining the wells with 200 µl of 33% acetic acid and then measuring theabsorbance of the CV solution in a microplate spectrophotometer set at 595 nm (Thermo Scientific Multiskan Spectrum Model 1500, Themo Scientific, Milan, Italy).

Disc diffusion test was carried out on MHA according to Clinical and Laboratory Standard Institute (CLSI) guidelines (96), with some modifications. Briefly, a bacterial culture of *S. aureus* (108 cells/ml), was spread by a sterile cotton swabs on MHA agar plate. Similarly, a bacterial culture of *P. aeruginosa* was adjusted to 108 cells/ml was spread on MHA agar plate. The plates were spotted with the different formulations corresponding to a proper quanityt of GS, used as control. After incubation at 35°C for 24 h, the diameter of the zones of clearance produced by each powder were compared.

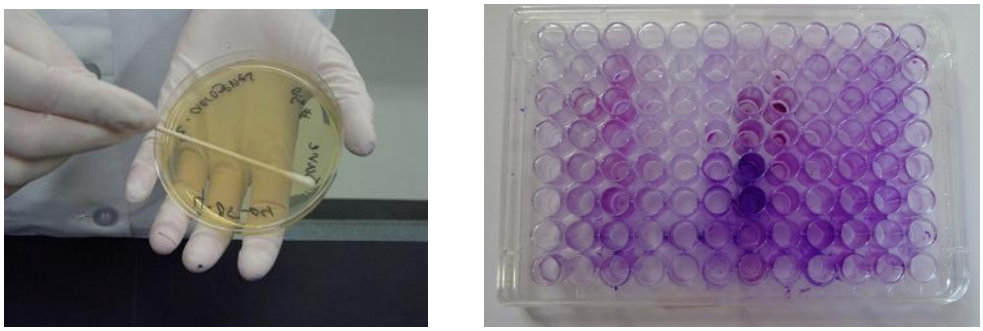

Figure 26: on the left a disc diffusion test preparation, on the right the *P. aeruginosa* biofilm degradation test.

2.4.6 Water vapour transmission rate experiment

Water vapour transmission rate (WVTR) was obtained as described by ASTM standard (ASTM Standard, 2010). Briefly, 25 mm hydrogel disc of each formulation was mounted on the top of a plastic tube containing 20 ml of distilled water. Teflon tape was used to cover the edge of the disc in order to avoid boundary loss. The assembly was kept inside an incubator at 37 °C. Weight loss was recorded at regular time intervals and plotted against time. WVTR was calculated as the ratio between slope of the plot and area of the disc, by the following formula:

$$WVTR = \frac{slope}{A} \quad (4)$$

where A is the test area of the sample in m^2. Water evaporation rate from in situ formed hydrogel was obtained as loss of weight over time by using the same procedure described above and noting the weight of the hydrogel at regular time intervals. Weight loss percentage was calculated by the following equation

$$Weight\ (\%) = \frac{Wt}{W0} * 100 \quad (5)$$

where W_0 is the initial weight and W_t is the weight at the specific time point.

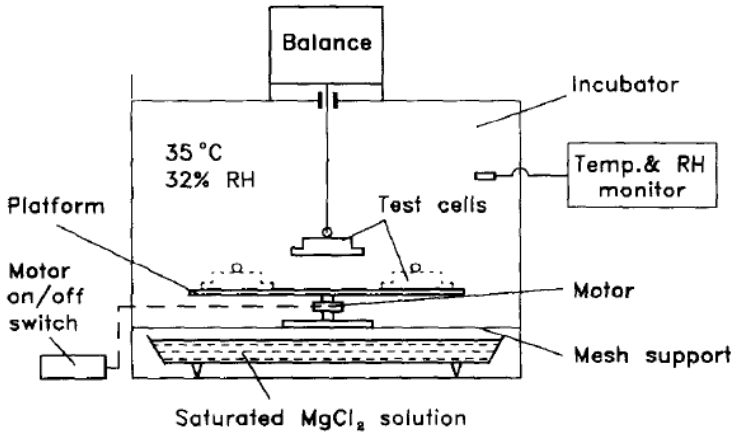

Figure 27: Laboratory apparatus for the measurements of water vapour transmission rate.

2.4.7 Flowability test

Bulk and tap density of all powders was measured by modifying the pharmacopoeia test, as reported in literature (97, 98). Briefly, powders were loaded into a bottom-sealed 1 ml plastic syringe (Terumo Europe, Leuven, Belgium) capped with laboratory film (Parafilm® "M", Pechiney Plastic Packaging, Chicago, IL, USA) and tapped until no change in the volume of the powder was observed. The bulk and tap densities were calculated from the difference between the net weight of the plastic syringe content divided by the volume in the syringe before and after tapping, respectively, obtaining the Hausner Index. The more this value, the lower the flowability. Furthermore, it depended on particle roughness and dimension.

An index of 1.85, measured on a commercial dry powder formulation, was used as comparison in this thesis work.

2.4.8 Molecular dynamic simulations

Molecular dynamics simulations were performed using YASARA 12.7.1650 with the NPT ensemble at 310 K and 1 atm. The YAMBER3 force field was

used. All simulations ran with a 1.25 fs time step for intramolecular forces and a 2.50 fs time step for intermolecular forces. The equilibration period was 20 ns.

2.4.9 In vivo experiments

C57BL/6 mice were obtained from Harlan Laboratories (Indianapolis, IN, USA) and housed 4 per cage prior and 1 per cage during experiments. On the day of surgery, the hair on the back of each mouse was clipped, and the skin was wiped with ethanol. C57BL/6mice, 10 weeks of age, were anesthetized with isoflurane prior to the wound-creating surgery. Full-thickness excision wounds (1 cm × 1 cm) were created by marking the area of the wound in the shaved mid-back with a fine marker and a ruler, lifting the skin with a pair of a forceps and excising the full-thickness skin along the lines with a pair of surgical scissors. Immediately after the surgery on day 0, the wounds were topically treated with 100 µl of either 5.0% alginate gel (placebo) or the same gel containing Ac2-26 peptide. Penicillin (5 mg per mouse) was injected intramuscularly to prevent infections.

Sixty mice were randomly divided into five groups: (1) control group; (2) 5.0% alginate gel; (3) Ac2-26 100 nM/alginate hydrogel group; (4) Ac2-26 500 nM/alginate hydrogel group; (5) Ac2-261 µM/alginate hydrogel group, twelve mice for each group. The control group was treated with 0.5 ml saline solution topically; the blank 5.0% alginate hydrogel group was treated with 0.5 ml of 2.5% alginate hydrogel administered topically; the Ac2-26 loaded 5.0% alginate hydrogel group was treated with 0.5 ml of Ac2-26 loaded 2.5% alginate hydrogel (containing 100 nM, 500 nM or 1 µM of Ac2-26 peptide) administered topically. On 3th, 6th, 9th and 14th day of post-wounding, three mice from each group were sacrificed and the size of wound area was recorded.

3. RESULTS AND DISCUSSION

3.1 SECTION A

Nano spray drying technology

3.1.1 Gentamicin, Alginate and Pectin Nanospray drying formulations

In this study, feeds were processed by the novel nano spray drying technology to produce a nanoparticulate powder based on alginate-pectin blend loaded gentamicin sulphate (GS) able to gel quickly into a wound cavity. Polymeric blend was composed by high mannuronic content alginate, able to stimulate cytokine production by human monocytes very useful in wound healing process (61), and low methoxyl degree pectin that, in combination with reduced particle dimensions, is able to speed-up in situ gel forming rate.

The encapsulation technology has been evaluated regarding its effect on yield, drug encapsulation efficiency, particle micromeritics, morphology and size distribution.

The innovative atomization mechanism, due to a vibrating nozzle membrane activated by a piezoelectric crystal, and the electrostatic collector of Nanospray drier, make possible to obtain very low particle size distribution, and very high yields, despite the use of small quantities of feed solution and the employ of short times.

During my first approach to this innovative technique, I studied how to optimize all the process parameters and the feed solution preparation steps, in order to achieve the best results.

With the aim to obtain an easy in situ gelling and removable formulation for local antibiotic controlled release, properties related to a good wound dressing gel such as gelation rate, swelling, wound fluid uptake and moisture transmission rate were studied.

Particles obtained by nanospray drying were prepared by processing different aqueous feeds. After a series of pilot experiments, GS and alginate/pectin ratio of 1:1:1 and total concentration of the colloidal dispersion of 0.10%, 0.25% or 0.50% w/v were set. Feeds were obtained by slowly adding a GS solution to an aqueous solution of alginate and pectin blend, previously prepared, under

gentle stirring. Dextrans blend solution was obtained by dissolving both polymers in distilled water under vigorous stirring for 1 h, while GS solution was obtained by dissolving a carefully weighted amount of the drug in distilled water under gentle stirring.

All formulations were spray-dried with the Nano Spray Dryer B-90 (Buchi Laboratoriums-Tecnik, Flawil, Switzerland) with process parameters and conditions set as follow: inlet temperature 90 °C, feed rate 9.5 ml/min; nozzle mesh diameter 4.0, 5.5 or 7.0 µm, air flow 100 l/min, relative spray rate 100%.

Table 1: Yield, particle size and span, drug content, encapsulation efficiency and water content of all samples (from GAPNs1 to GAPNs 9).

sample code	Nozzle (µm)	feed (w/v%)	yield (%)	d_{50} (µm) and () span	drug content (%)	water content (%)	e.e.* (%)
GAPNs1	4	0.1	82.4	310 (1.38)	23.9±0.3	4.2 ± 0.3	72.4±0.2
GAPNs2	4	0.25	88.2	347 (1.46)	26.7±0.4	4.1± 0.4	80.9±0.3
GAPNs3	4	0.5	91.9	405 (1.60)	25.4±0.2	4.1 ± 0.4	77.0±0.1
GAPNs4	5.5	0.1	67.5	520 (2.02)	23.6±0.2	4.9 ± 0.5	70.8±0.1
GAPNs5	5.5	0.25	72.9	551 (2.05)	26.6±0.3	5.4 ± 0.4	79.9±0.2
GAPNs6	5.5	0.5	78.9	608 (2.12)	25.5±0.2	6.2 ± 0.4	76.5±0.1
GAPNs7	7	0.1	65.7	852 (1.56)	27.8±0.1	7.5± 0.6	83.5±0.1
GAPNs8	7	0.25	66.7	978 (2.01)	26.2±0.2	7.6± 0.3	78.6±0.2
GAPNs9	7	0.5	72.9	1003 (2.46)	27.3±0.2	7.7± 0.4	82.0±0.1

As showed in the table above, GAPNs series 1-3 are made with 4 µm nozzle, 4-6 with 5.5 and 7-9 with 7 µm.

All formulations were obtained with good production yield ranging from 65 to 91%. The smaller the nozzle, the higher the yield. Using 4 µm nozzle is reduced the loss of product on the glass wall of the nano spray dryer with an increase in the yield.

As expected, particles size as well as particles size distribution (PSD) increased with nozzle spray mesh diameter, producing particles with d_{50}

ranging between 1003 (GAPNs9) and 310 nm (GAPNs1). Moreover, GAPNs1–3 exhibited d_{50} under 410 nm with span between 1.60 and 1.38.

As a result of the optimization of parameters conducted during this work, high yields and very interesting particle dimension ranges, expecially for samples produced by 4 μm mesh nozzle, were obtained.

PSD was also affected by feed concentration, the higher the feed concentration the wider the size distribution. This is explainable by the change in viscosity with the increase in concentration of the feed. Consequently, the droplet dimension increases with viscosity.

Drug content (d.c.) and encapsulation efficiency (e.e.) were evaluated by means of HPLC analysis, using a pharmacopoeia modified method for the quantification of gentamicin (99). High encapsulation efficiency (e.e.) was obtained (between 70 and 83%) without any significant difference between formulations. However, both spray mesh diameter and feed concentration increased formulation water content; this effect may be explained considering the decreasing of surface tension of the droplets coming out from smaller nozzles that allows easier water evaporation (75, 100, 101). After their preparation, powders were chemico-physical and morphological characterized in order to foresee their behavior *in vitro* and *in vivo*.

Different particle morphologies were observed in the various formulations in dependence on both vibrating nozzle diameter and feed concentration. Spherical morphology was predominant, especially when 4 μm vibrating mesh nozzle was used (sphericity coefficient about 0.93); wrinkled or doughnut shaped particles mixed with the spherical ones were observed when either feed concentration or mesh nozzle increased reducing sphericity till 0.83. This phenomenon is probably related to a change in droplet/gas contact in the last phases of drying process (102, 103) due to a reduction of the temperature and gas flow rate along the electrostatic drying chamber of the nano spray drying apparatus.

Moreover, when 7µm mesh nozzle was used (GAPNs9) large collapsed particles were also recognizable (Fig. 28 d) due to droplet coalescence occurring at piezoelectric driven spray head (104). High resolution SEM analyses showed that both micro and nanoparticles were composed by close-packed colloidal particles (raspberry particles) (28f).

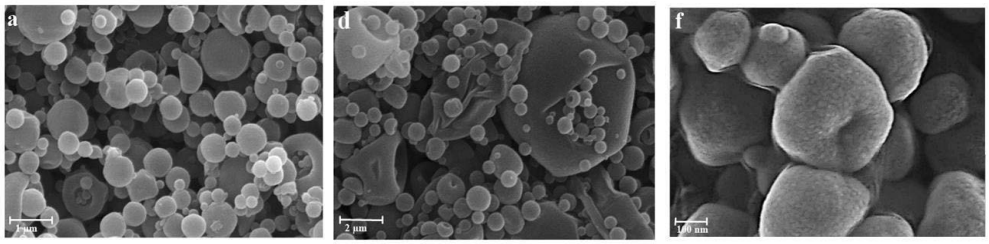

Figure 28: a) GAPNs1 particles produced with 4 µm nozzle. d) GAPNs9 produced with 7 µm nozzle and f) a higher magnification for particles GAPNs9

Colloidal dispersion that originated raspberry nanoparticles is generated during the feed preparation by interaction between amine residues of gentamicin and preferentially the carboxyl groups of M residues of alginate that produce a polyelectrolyte complex that enhance formulation stability (as shown in figure 28 f) and would slow down drug release rate (50, 105). A good flowability in addition to favorable traspiration properties and a good fluid uptake ability are needed to optimize all the formulations (106). Flowability of the powders is, infact, a fundamental parameter that indicates the possibility to sprinkle them on the lesion with uniformity, obtaining a complete and correct covering of the wound. It was correlated to both particle size distribution and shape. The presence of wrinkled large particles in some formulations widened PSD and reduced flowability. In fact, in spite of the increased mean particle size, the enhancement of effective contact surface area between large wrinkled or collapsed particles and the smaller spherical ones (107) lead to lower flowability. Flowability of the powders expressed as ratio between tapped density (ρT) and bulk density (ρB) ranged between 2.42 and 2.68 for 4 µm mesh nozzle whereas particles obtained by 7 µm mesh nozzle

demonstrated a ρT/ρB ranging between 3.33 and 3.89, in accordance with increased feed concentration. In this work, the value of ρT/ρB ratio for a commercial formulation of 1.85 was used for comparison purposes.

Fluid uptake ability of the powders was evaluated as the ratio between the weight of the formulation after in situ gel formation due to contact with simulated wound fluid (SWF) and initial dry state. SWF uptake was very fast; all the formulations moved completely from powder to gel state within 15 min where they reached the maximum swelling followed by an equilibrium phase. Swelling rate was directly correlated to particle size, resulting in the fastest swelling kinetic for GAPNs1 that needed 10 min to move into hydrogel state.

Because of GAPNs series should provide an adequate traspirability on the wound site when gelled, fluid permeability of the different formulations was also evaluated as water vapour trasmission rate (WVTR) after swelling process in order to ensure that gel layers would provide adequate level of moisture at wound bed. WVTR was evaluated by incubating swollen hydrogel in a moisture rich environment (108) at 37°C. In situ formed hydrogel of all formulations exhibited WVTR values ranging between 95 $g/m^2/h$ (GAPNs9) and 90 $g/m^2/h$ (GAPNs1), depending on particle diameter. Hydrogels generated by smaller particles were probably tighter compared to those obtained from particles with larger diameters resulting in a slower water release. However, these values are all in the recommended range (80-105 $g/m^2/h$) to avoid exudate build up as well as excessive wound dehydration then, hydrogel might be able to maintain a proper fluid equilibrium at wound bed (109, 110).

After the complete gel formation, was important to study the fluid loss in order to understand if after use the gel was easily removable. Infact, a massive water loss produces a dried alginate layer, that can cause trauma when removed.

Fluid loss was faster in the first 12 h with formulations loosing around 50% of the fluid whereas, after 2 days, hydrogels still retained over 30% of fluid.

Subsequently there was a tiny water loss from the gel until equilibrium was reached with formulations retaining between 10 and 15% of water after 5 days depending on feed concentration and mesh nozzle diameter; the lower feed concentration and nozzle diameter the lower the retained water. These values show that the quantity of water retained is still good for an easy removal.

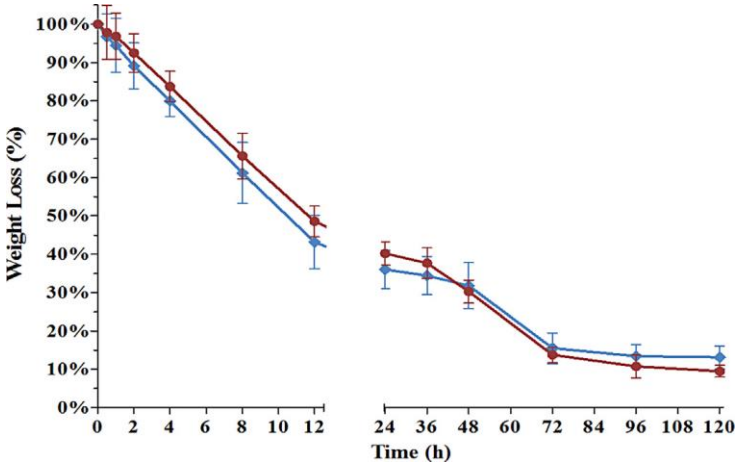

Figure 29: Water loss profile of gel formulations, measured as weight loss during time. Red line: GAPNs1 (0.1%, 4 µm), Blue line: GAPNs9 (0.5%7 µm).

Stability tests were conducted in accelerated conditions (40°C, 75% moisture level) following ICH Q1AR2 guide in order to verify the stability of gentamicin entrapped into the polymeric matrix over time. Results showed that GS content was preserved till 6 months in harsh conditions. In fact, even if raw GS is a deliquescent material when non-encapsulated, only slight increase in water content was detected after 6 months, for all manufactured formulations. It can be suggested that polymeric materials acting as barrier against moisture penetration strongly reduced GS water uptake in accelerated stored conditions.

GS release behaviour from in situ formed gel was monitored using vertical Franz-type diffusion cells with SWF (simulated wound fluid) in the acceptor compartment. Figure 30 showes GS permeation curves of GAPNs micro and nanoparticles in comparison to GS as raw material. Gentamicin permeation

profiles from particles made by nanospray drier were related particle size and feed solution concentration, both affecting hydrogel consistence. In fact, microparticles, produced with 7 mm nozzle mesh exhibited a faster permeation rate, achieving total release of the drug between 2 and 3 days according to the increasing in feed concentration while, 4 µm nozzle mesh nanoparticles, released drug between 4 and 6 days (in SWF). All formulations exhibited a drug burst effect within 4 h from administration that can result very useful to prevent infection spreading at the beginning of a local antibiotic therapy. As expected, burst effect was related to sol-gel process kinetic and gel texture (111). In fact, slower gel formation for microparticles (GAPNs7–9) resulted in the release of 40–50% of the loaded gentamicin whereas nano-particulate powders, GAPNs1–3, released 20–35% of the loaded GS by burst effect. Prolonged release of GS from GAPNs' formulations was achieved by *in situ* gel formation that acted as a barrier to drug release slowing down permeation rate (following a non-fickian diffusion kinetic) in contrast with fast permeation of GS raw material.

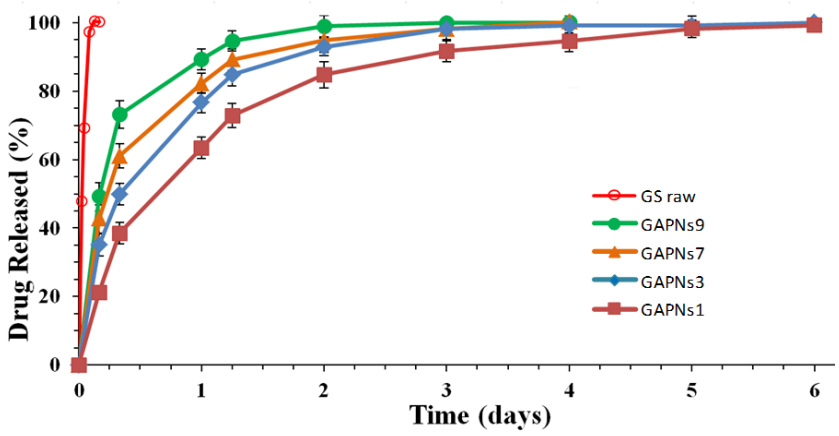

Figure 30: Drug relese profile of GAPNs9 (green), GAPNs7 (orange), GAPNs3 (blue), GAPNs1(carmine), compared to GS raw material (red).

Another important characteristic of the gel is its adhesiveness. The formed gel, infact, should properly adhere into the wound bed with an easy removal after

use, but avoiding, at the same time, gel loss or accidental detachment during the use. The adhesive strength of in situ formed hydrogel was evaluated using a modified protocol of ASTM D3808 standard. Nitrocellulose membrane filter (0.45 mm pore size) conditioned with SWF was used as adhesion substrate. Adhesive strength for the formulations was in the range 5.7–9.5 kPa with maximum adhesiveness exhibited by gel formed by nanoparticulate powders of GAPNs series produced with 4μm nozzle due to the formation of highly entangled gel texture during the powder swelling (112-114). The smaller the particles, the more entangled the gel texture and consequently the higher the adhesiveness. The values showed in the graph of figure 31 were in the proper range to foresee an ideal behaviour in the wound site.

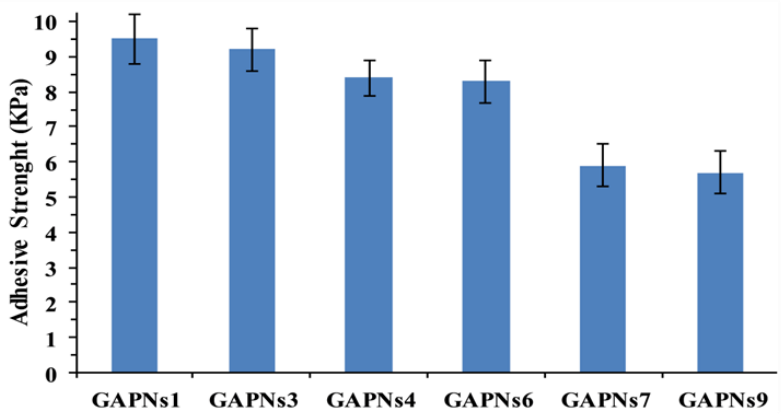

Figure 31: Adhesive strengt graph for the different formulations.

With the aim to evaluate the formulations antimicrobial effect over time, disc diffusion and time-killing assays were conducted against both *S. aureus* and *P. aeruginosa*. A modified disc diffusion test conducted on a Muller-Hinton agar plate spreaded with *S. aereus* demonstrated that the inhibition zone produced by any GAPNs formulation was larger than pure GS at both 24 h and 6 days. The inhibition zone of bacterial growth was larger around the in situ formed gel produced by GAPNs1–3 formulations (13.6 mm) compared to the

homologous formulations GAPNs7–9 (12.8 mm) whereas pure GS produced an inhibition zone of 11.3 mm (figure 29).

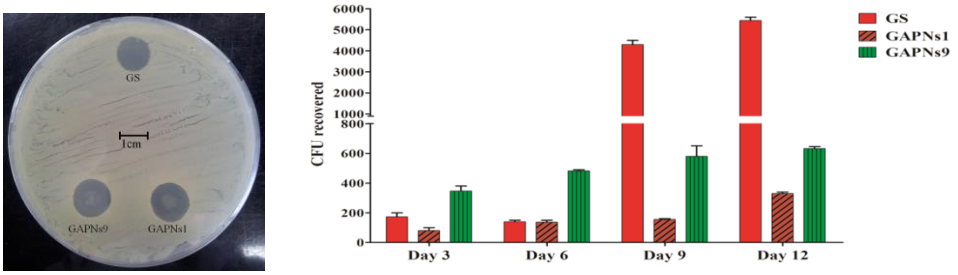

Figure 32: On the left two formulations compared to GS raw material in the disc diffusion test for *P. aeruginosa* and *S. aureus.* On the right time killing assay on *S. aureus* to compare the antimicrobial effect of GAPNs1 (dark red), of GAPNs9 (green) and of GS raw material (red).

Results of a representative time-killing assay against *S. aureus*, measuring the reduction of CFU (colony forming unit) recovered at day 3, 6, 9 and 12, are reported in Figure 32. All formulations showed high bactericidal activity against *S. aureus*, comparable to GS till 6 days. Reduction of CFU till 12 days demonstrated that GAPNs formulation exert a prolonged bactericidal activity, whereas pure GS loosed its activity after 6 days. Formulations killing activity, in accordance with permeation profiles, was related to particle size and gel formation rate. In fact, GAPNs1 (smallest nanoparticles, higher gelling rate) showed a bactericidal activity about 3 fold higher than GAPNs9 till day 9 and it resulted almost doubled at day 12.

In conclusion, nano spray drying technology has been successfully applied to produce stable alginate/pectin based nanoparticulate powders with good gentamicin content. Powders would be able to gelify rapidly into wound bed cavity, absorbing large quantities of wound fluid, due to dextran blend swelling properties. Moreover, in situ formed gels exhibit proper adhesiveness

to allow easy removal from wound bed and WVTR enabling a proper equilibrium of the wound fluids. Release of encapsulated GS from nanocarriers exhibits a burst effect suitable to prevent infection spreading at the beginning of a local antibiotic therapy. Sustained release, following the initial burst of drug, prolonged GS permeation depending on particles size and powder gelling rate, in SWF.

3.1.2 Doxycycline, alginate, chitosan and pectin Nano spray drying formulations

Nanospray with optimized condition was tested for the production of more complex dry powders, constituted by polymers with proper characteristics for wound healing, comparing results with conventional Mini spray drying.

This research study was, infact, focused on the production of an innovative *in situ* gelling dry powder based on different polymers used as adiuvant in the wound healing process and as carrier for doxycycline. The different molecular mechanisms of the polymers alginate and chitosan were considered in order to enhance both wound healing and drug efficacy. In fact, properties of alginate containing high M residues are well known (61), while chitosan low molecular weight enhances the functions of inflammatory cells by a binding on mannose receptors, which mediate the internalization of chitosan particles (58). Pectin high amidation degree was also added to speed up the powder gelification (115), improving the overall formulation performance. The different polymers were individually studied in this application, their behaviour in powder formulation was well known, but it was intersing to study their synergy on wounds. Doxycycline was used as antimicrobial drug model. It is a wide range spectrum tetracycline with high potency, active on both gram negative and gram positive bacteria, also able to inhibit MMP9 with positive effects on wound healing(116, 117).

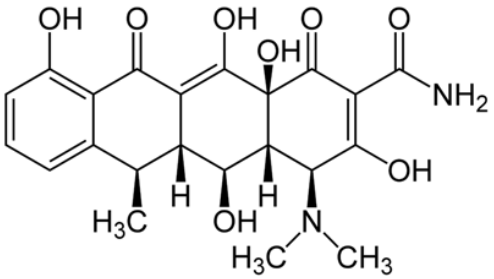

Figure 33: Doxycycline

Dry powders were produced using nano spray drier and mini spray drier used as comparison, both with optimized conditions.

Preliminary studies were conducted to evaluate the proper conditions for feed preparation. In fact, alginate and pectin are soluble in distilled water, whereas chitosan is soluble in aqueous acidic solution where alginate can precipitate. Good results in feeds processability were obtained when chitosan was set as 1:6 compared to other polymers and final solution pH was set at 5.5. Therefore, different formulations were obtained by setting alginate/chitosan ratio at 6:1 (ACD formulations) and doxycycline at 1.43%w/w of the polymers; alginate/pectin/chitosan/doxycycline in the ratio 3:3:1:0.1 (APCD formualations); alginate/pectin ratio 1:1 and doxycycline 1.43% of polymers (APD formulations). Moreover, in order to understand the influence of encapsulation technology on powder technological properties feeds were processed by both mini- and nano-spray drying.

Table 2: Yield, drug content, encapsulation efficiency and drug content after accelerated stability test of all formulations.

SAMPLE CODE	TECHNIQUE	DRUG/POLYMERS RATIO	YIELD (%)	DRUG CONTENT (%)	ENCAPSULATION EFFICIENCY (%)	DENSITY(g/cm^3)	HAUSNER RATIO
ACDN	Nano spray	A:C:D 6:1:0.1	97.65	1.06±0.01	74.58±0.13	1.94 ±0,01	2.44±0.02
APCDN	Nano spray	A:P:C:D 3:3:1:0.1	99.22	0.84±0.01	61.01±0.01	1.74±0,01	1.89±0.02
APDN	Nano spray	A:P:D 3:3:0.1	69.23	1.24±0.00	86.13±0.01	1.62±0,02	2.22±0.01
ACDM	Mini spray	A:C:D 6:1:0.1	45	1.09±0.01	76.60±0.01	1.79±0,02	3.33±0.03
APCDM	Mini spray	A:P:C:D 3:3:1:0.1	40	1.21±0,00	84.44±0.14	1.85±0,03	2.38±0.01
APDM	Mini spray	A:P:D 3:3:0.1	31	1.43±0,01	98.22±0.01	1.64±0,02	2.70±0.02

As shown in table 2, the yield obtained by nanospray drying process was always higher than mini spray drying, due to the differences in process characteristics. This result confirms what observed in the previous work on Gentamicin loaded formulations in which was studied that the electrostatic collector is able to enhance process yield by strongly reducing particle waste on glass walls.

Drug content (d.c.) and encapsulation efficiency (e.e.) studies were conducted using Uv-vis spectroscopy, extracting drug from the polymeric matrix with a specific and validated protocol (paragraph 2.4.2). All formulation showed good encapsulation efficiency, particularly when alginate/pectin blend was used as carrier. Formulations were also tested for stability in accelerated conditions (40°C, 75% moisture). After one month, drug content was almost superimposable to fresh powders, with only a slight decrease (between 4 and 5%), showing that polymers are able to protect doxycycline from degradation (118).

Particle morphology was studied by scanning electron microscopy (SEM), comparing the different formulations and the two different encapsulation techniques.

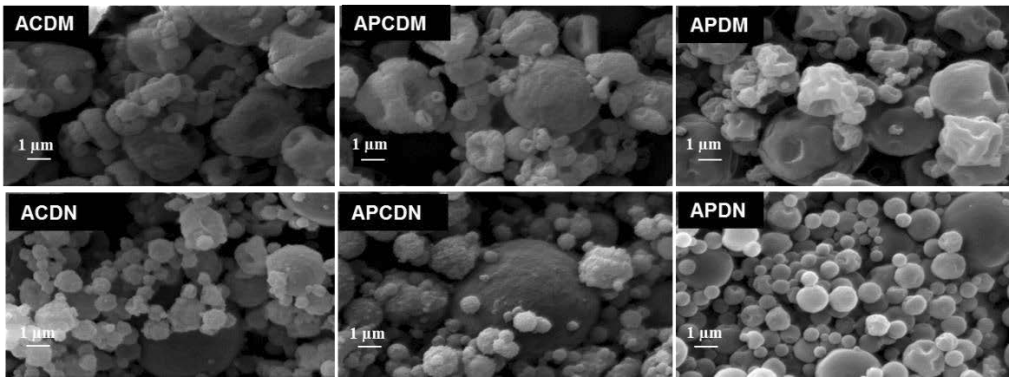

Figure 34: First line on the top: ACDM, APCDM and APDM produced by minispray drying. Second line ACDN, APCDN and APDN produced by nanospray drying.

All mini spray dried formulations presented spherical shape, with the presence of some craters; APCDM and APDM presented rougher surface due to the presence of chitosan. Nano spray dried particles were very similar to mini spray dried ones but smaller in size. Formulations APD (figure 34 f) presented smooth surface and the smallest size.

In order to study powders flowability, an important characteristic for powder easy administration, Hausner ratio was evaluated. As comparison, a similar

formulation present on the market (Cicatrene ®) was tested and, the Hausner value of 1.85, was considered ideal. Table two shows the results of Hausner ratio and density (obtained by helium pycnometer).

Nano spray dried powders showed higher flowability compared to mini spray dried formulations. Moreover, APCDs presented the lowest Hausner index (APCDN) whereas ACDs exhibited the highest values. Flowability is generally correlated to particle size but the SEM extensive analyses showed that particle roughness was able to strongly affect powder floability, in spite of the particle size, due to the increasing effective contact surface area.

Density values were slightly different between formulations produced with the two techniques. Density is related to matrix consistency which is related to the encapsulation technique. Infact, the different atomization mechanisms lead to the formation of a different flow of droplets into the drying chamber (119). This is more evident in formulations made with chitosan, where density values are different between mini- and nano spray dried particles.

An in situ gelling formulation should become rapidly a gel when in contact with wound exhudates and should be able to cover the wound bed homogeneously. To study this kind of behaviour, all formulations were placed in contact with simulated wound fluid and at defined time point the increase in weight was calculated.

Figure 35 shows shows gel formation. The formulation APCD had the faster fluid uptake ability, becoming gel in 5 minutes for nanospray powders (APCDN) and in about 10 minutes for mini spray formulations (APCDM). This result was quite different from that obtained in the previous work in which a low methoxyl degree pectin was used. In fact, the use of pectin with high amidation degree speed-up powders ability to gel, reducing total gelling time from 15 to 5 minutes (95) .

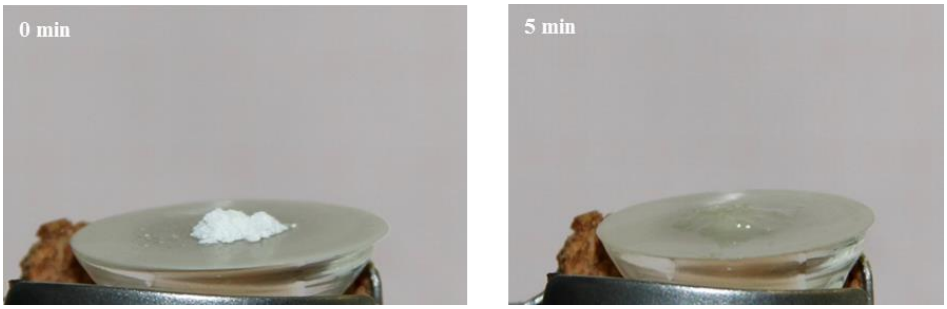

Figure 35: On the left APCDN in dry state. On the right the gelled powder after 5 minutes.

The increase in weight was about 15 times for mini spray powders and above 16 times for nano spray formulations, due to the wider exposed surface area of particles (figures 36 and 37).

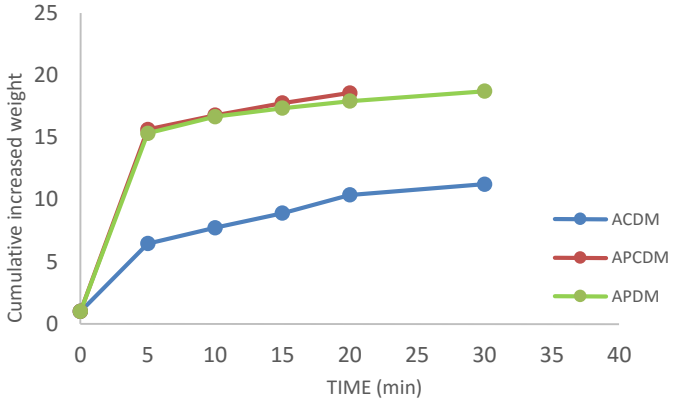

Figure 36: Mini spray drying formulations swelling rate (APDM green, APCDM red, ACDM blue).

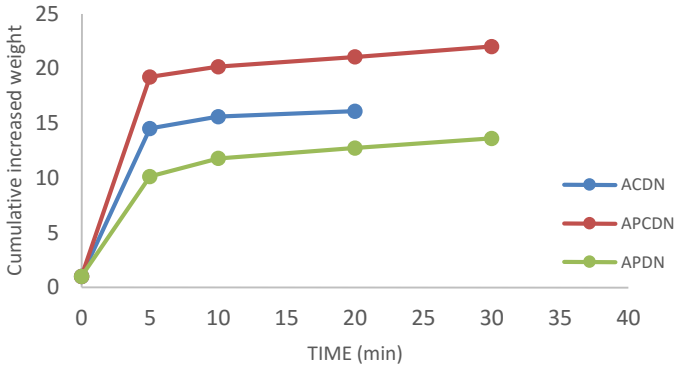

Figure 37: Nano spray drying formulations swelling rate (APDN green, APCDN red, ACDN blue).

In figure 38 and 39 are reported the calorimetric thermograms of polymers as raw material compared to blank formulations (figure 38), and the thermograms of doxycycline loaded formulations compared to pure doxycycline (figure 39).

Alginate showed an exothermic peak at 250 °C whereas chitosan at 300 °C due to polymer degradation. Amidated pectin showed a crystalline endothermic peak at 150°C, a broad peak at 190 °C followed by an exothermic one at 250°C.

Blank formulations showed different thermal profiles. ACs blank formulations, both mini- and nano spray dried, exhibited a new peak at 150°C, not observed in raw materials, probably due to alginate-chitosan ionic interaction and an exothermic related to polymers degradation similar to alginate. APs formulation showed a thermal behaviuor presenting polymers degradation peak at 240 °C, and the melting peak shifted at lower temperature, 145°C, due to the formation of a homogeneous polymer matrix into particles.

APCs blank showed a melting peak shifted at higher value than ACs (170°C), due to the interaction of the three polymers, as well as, it was possible to observe a new degradation peak at 295°C.

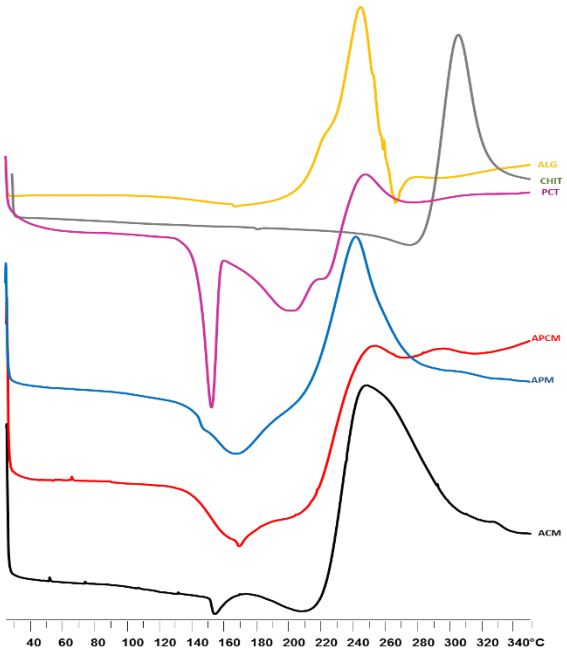

Figure 38: DSC thermograms of pectin (violet), alginate (yellow) and chitosan (green) raw material in comparison with APM (blue), APCM (red) and ACM (black) blank formulations.

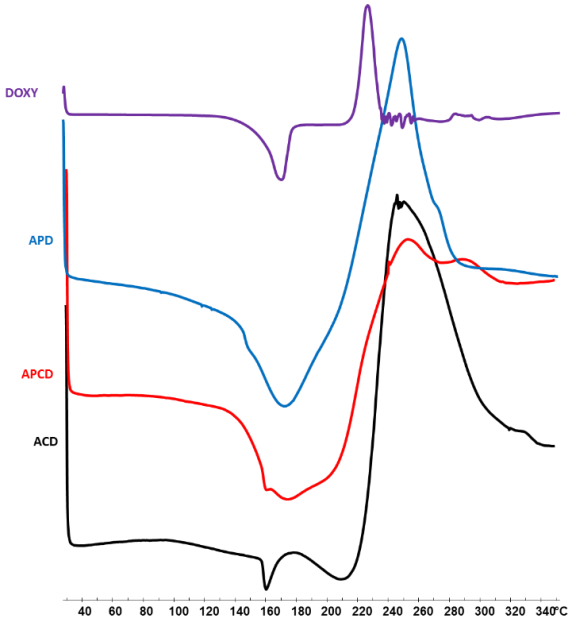

Figure 39: DSC thermograms of ACD (black), APCD (red), APD (blue) doxycycline loaded formulation in comparison with doxycycline raw material (violet).

In figure 39 graphs were compared with doxycycline, which thermogram exhibited the profile of a crystalline material with and endothermic melting peak at 168°C followed by an exothermic peak at 225°C due to drug degradation.

Doxycycline loaded formulations exhibited similar behaviour to the blank homologous but both melting and degradation peaks were shifted at higher temperature. This phenomenon can be explained by the interaction between doxycycline and polymer matrix. Such interaction could be responsible of a prolonged drug release from the formulations. The slight differences in the peaks are probably related to the low ratio between polymers and drug into the formulations

In order to study the drug release, *in vitro* permeation experiments were performed using franz type diffusion cells, using SWF as acceptor fluid.

Results were compared to doxycycline raw material that permeates in a few minutes (about 20). APDN, APCDN and ACDN showed a burst effect in the first hours (3 h) with 50 to 70% of drug released and a prolonged release till 48 h. APDN and ACDN showed almost the same behaviour with 60% released in 4 hours.

APDM, APCDM and ACDM showed a similar behavior, with a lower burst effect (4 h) with a quantity released of 45-50%, reaching the total release of the drug in 50 h.

An initial burst effect within 3 or 4 h from administration that can result very useful to prevent infection spreading at the beginning of a local antibiotic therapy.

The prolonged release showed by formulations, confirmed that drug/polymer interactions, examinated by DSC, made possible the obtainment of tailored release profiles.

Nano spray formulations showed a faster release than mini spray homologous, related to the sol-gel convertion. The smaller the particles (with a lower mean diameter), the higher the burst effect.

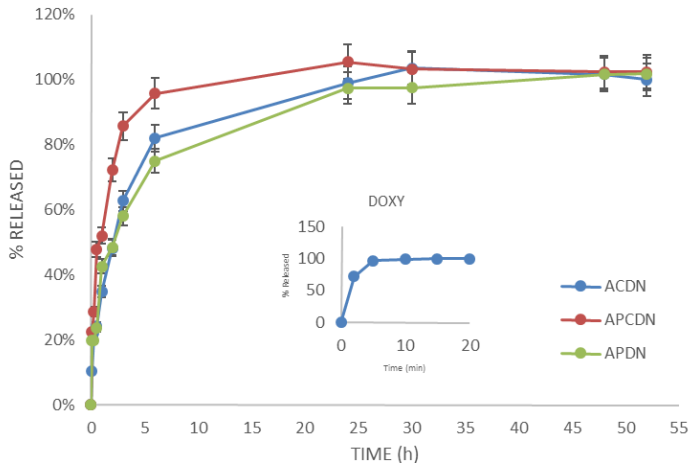

Figure 40: drug release profiles of nano spray dried formulations in comparison with pure doxycycline. ACDN (blue), APCDN (red) and APDN (green).

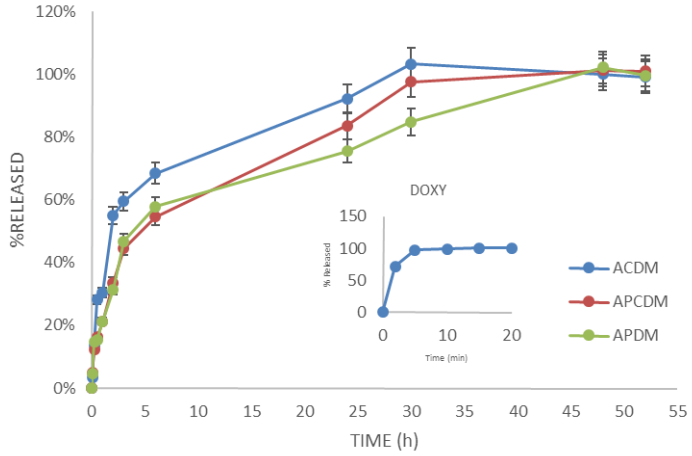

Figure 41 drug release profiles of mini spray dried formulations in comparison with pure doxycycline. ACDM (blue), APCDM (red) and APDM (green).

Antimicrobial *in vitro* studies on *S. aureus* performed using a time killing test, showed that all formulation had a better antimicrobial activity than pure doxycycline and control. At the seventh day, ACDM, APDM and APDN

showed the longer activity, whereas other fomultions had a comparable activity to pure doxycycline. As shown in the figure 42, there is a good correlation between the antimicrobial activity and the permeation profiles. The slower the release, the longer the activity. In fact, APDM and APDN were still active at the seventh day, whereas other formulations presented lower activity at the same time.

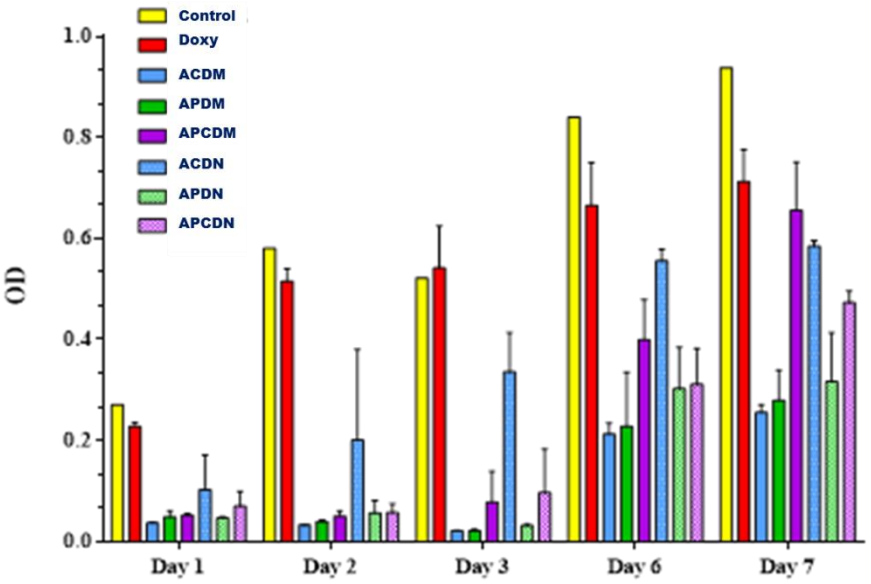

Figure 42: Time killing test on *S. aureus* for all formulations.

In conclusion, in this study highlighted the possibility to use Nano spray drying with optimized conditions successfully, also for the production of more complex dry powders.

The doxycycline based formulations, showed to be able to effectively contrast bacterial growth, in the *in vitro* tests performed. Using proper excipients, such as alginate, chitosan and amidated pectin it is possible to control drug release till 48 hours, and to have rapid gelation of dry powders when in contact with wound exudates.

Nevertheless, powders have good flowability properties, so they could be easily administrated at the wound site.

Further studies are needed to assess doxycycline inhibiting activity on MMP9 with possible better results on wound healing.

3.2 SECTION B

Supercritical based technologies

3.2.1 Supercritical Assisted Atomization (SAA)

3.2.1.1 SAA vs Mini spray drying

SAA is one of the most promising supercritical fluid based technique for application in the field of pharmaceutical products because of the well known advantages of supercritical CO_2 and the high yields gettable.

The contact between feed solution/dispersion and SC-CO_2 determines the formation of an expanded liquid of reduced viscosity and surface tension, with a consequent improved atomization and the formation of particles with specific characteristics.

During this study, SAA was applied for the production of in situ gelling powders loaded with Gentamicin for topical treatment of infected wounds, in which microorganisms have interfered with normal healing process.

Antibacterial agents, infact, should be topically administered in order to reduce wound bioburden and to avoid infection spreading, as well as systemic side effects. A number of wound dressing devices loaded with active pharmaceutical ingredients (APIs) have been manufactured with different polymeric materials. The ideal dressing material should have proper adherence to the wound site and good exudate absorbance. It should be able to maintain appropriate moisture at the wound bed, nonetheless, easy application and removal.

Dextran hydrogels may combine most of these properties; moreover, they are transparent allowing the monitoring of healing process. In this work, alginate and pectin were chosen as biocompatible and biodegradable carrier for drugs. Alginate is extracted from brown algae, and it's a linear co-polymer composed by monomeric units of guluronic acid (G) and mannuronic acid (M). High G content alginates have been demonstrated to be less liquid absorbent and gel forming than high M content alginates, nevertheless they retain a stronger structure and are able to gel in the presence of Na^+ ions highly concentrated in wound fluids (120). Otherwise, M residues has a well known activity as

discussed previously (61), as well as pectin low methoxyl degree, from citrus fruit, a natural polysaccaride consisting in D-galatturonic acid units linked by an α-(1-4) bond, was used to speed up the fluid uptake when in contact with wound exudates.

The conformability problems of conventional alginate dressing, as well as other dextran dressing, produced in form of sheets or membranes (121-123) are overcome by in situ forming hydrogels that could fit the irregular shape of the wound avoiding wrinkles or fluting (109, 123). Also other kinds of formulation available on the market, as spray-on films, have shown partially reduced conformability and high costs, complex manufacturing and, in some cases, bacterial spreading when used over third degree wounds (124-126).

Then a formulation in form of dry powder can overcome these problems, because is able to cover the whole wound bed, avoiding removal trauma, and permitting the drug release control.

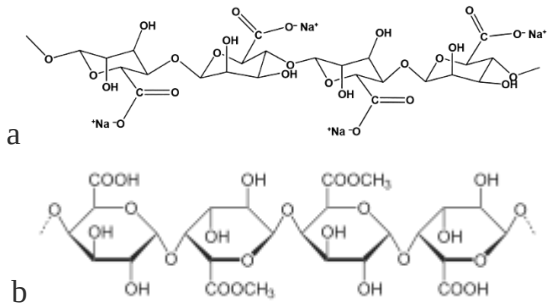

Figure 43: a) Sodium alginate. b) Pectin

The active drug chosen was gentamicin sulfate (GS) that is an aminoglycoside antibiotic worldwide used for the treatment of severe infections caused by both Gram-positive and, especially, Gram-negative bacteria (127). Considering the systemic administration, multiple daily doses are required to achieve a good local antibiotic concentrations due to its pharmacokinetics and biopharmaceutical properties; consequently many side effects such as nefrotoxycity and otoxycity are observed (128, 129). In the last few years,

different GS loaded polymer delivery systems intended for local administration, obtained by different techniques, have been designed to overcome drug systemic disadvantages by maintaining high local antibiotic concentration, to reduce side effects and induced bacterial resistance (130-132).

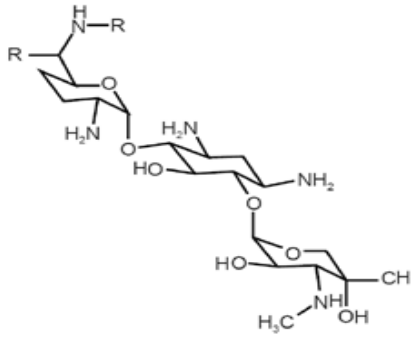

Figure 44: Gentamicin Sulphate.

The alginate-pectin blend loaded with gentamicin of this work was produced in form of dry powder comparing two different technologies: Spray-drying (SD) and Supercritical Assisted Atomization (SAA) based on supercritical carbon dioxide.

Optimized parameters were used for both SD (Mini spray drying Buchi B191): and SAA (paragraph 2.4.1.1).

Both the techniques trasform a liquid solution/suspension in a dry powder with proper characteristic studied in this work. Feed solution of Gentamicin-Alginate-Pectine were produced with 1:1:1 e 1:3:1 ratio and with total component concentration of 0.5 and 1%. Samples GAPS are produced by spray drying (SD) whereas GAP are the SAA particles. GAPS and GAP 1-2 are produced with drug/polymer ratio of 1:1:1 whereas GAPS and GAP 3-4 with a 1:3:1 ratio.

Both the process lead to high yields, from 42 to 68% for SD and from 66 to 74% for SAA.

Table 3: Yield, Particle size and span, drug content., encapsulation efficiency and water content of the formulations.

sample code	GS/Alginate/Pectin ratio (p/p/p)	feed (w/v)	yield (%)	d_{50} (μm) and () span	drug content (%)	water content (%)	e.e.* (%)
GAPS1	1:1:1	0.5%	68.4±2.3	3.88 (1.19)	28.6±0.5	7.6±0.2	85.7±0.3
GAPS2	1:1:1	1.0%	57.6±2.8	4.10 (1.27)	30.3±0.4	7.9±0.3	90.9±0.4
GAPS3	1:3:1	0.5%	42.7±2.1	3.70 (1.29)	17.2±0.3	8.7±0.4	86.1±0.4
GAPS4	1:3:1	1.0%	49.9±2.9	4.07 (1.43)	16.8±0.2	9.1±0.4	84.2±0.5
GAP1	1:1:1	0.5%	74.2±1.2	1.91 (1.07)	35.1±0.4	5.1±0.2	> 100
GAP2	1:1:1	1.0%	68.7±1.1	1.82 (1.19)	39.4±0.6	4.7±0.3	> 100
GAP3	1:3:1	0.5%	70.6±1.2	1.45 (1.15)	21.2±0.2	5.0±0.3	> 100
GAP4	1:3:1	1.0%	66.1±1.1	1.39 (1.13)	29.6±0.1	4.4±0.2	> 100

Scanning electron microscopy (SEM) and laser scattering (LS) allowed to study morphology and dimension of the sample produced. Shape and particle size distribution were influenced by the technology. SAA particles were spherical with narrower size distribution and smaller diameter looking at d_{50} that ranged between 1.39 and 1.91 μm, whereas SD were corrugated with d_{50} ranging between 3.92 and 4.10 μm. It was also noticed that d_{50} increases with GS content and with decrease of polymer concentration.

The particle shape and dimension are also shown in the SEM images in the figure below. SAA particles (figure 45 a-d) are more spherical and uniform than SD. This depends on the different mechanism of particle formation and solvent elimination.

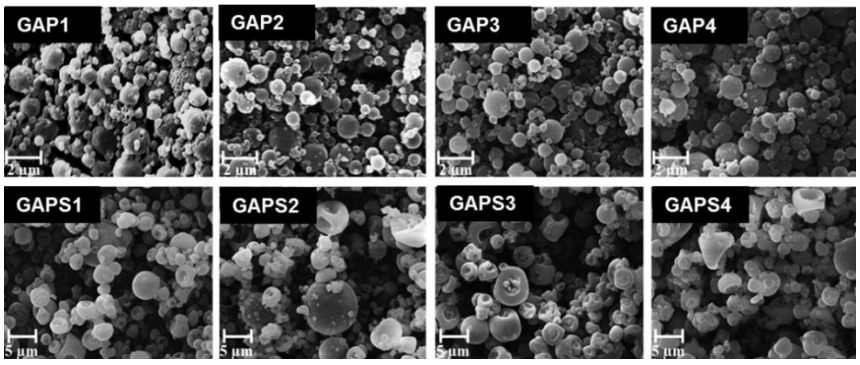

Figure 45: SEM images of GAP (upper line) and GAPS (lower line)

SAA apparatus allows the formation of primary droplets by the spray trough the nozzle. These droplets contain also supercritical CO_2 that into the precipitation chamber at atmospheric pressure becomes gas allowing the fragmentation of primary droplets into secondary ones. These conditions allow to obtain a more uniform particle formation and solvent elimination, than SD.

Drug content (d.c.) and encapsulation efficiency (e.e.) were evaluated by HPLC analysis using a modified pharmacopoeia method (99).

Both techniques produced powders with high e.e.: spray-drying e.e. ranged between 84.2 and 90.9% depending on the feed while encapsulation efficiency obtained by SAA was always slightly higher than 100%. This phenomenon, as previously described (99), is related to the precipitation of small quantities of polymer material into the precipitation chamber due to the so called anti-solvent effect. Thus, the final calculation of drug content is related to a lower total polymer mass, giving an efficiency >100%.

Water content, measured by means of Karl Fisher tritation of spray dried microparticles was higher than SAA's. This can suggest that during decompressive atomization a reduction in surface tension of the feed takes place, due to supercritical CO_2 mixing with feed, allowing faster and more efficient elimination of water from polymer matrix during particle formation (75, 133).

Good powder flowability, high fluid absorbing capacity as well as water permeability at the equilibrium are among the most important properties required for wound dressing preparation to maintain the optimal environment at the wound bed and to enhance healing process (106). The tapped density (ρ_T) e bulk density (ρ_B) ratio was evaluated as Hausner index (HI). These values were also compared to that of a commercial formulation which was established at 1.85. HI for SD particles was between 2.00 - 2.44, whereas SAA powders showed values closer to the commercial formulation, ranging

between 1.97 -2.51, that indicate the good flowability of powders and their easily administration.

As well known, Hausner ratio (ρT/ρB) is strictly correlated to particles size but it is also influenced by their shape and roughness. Consequently, both sphericity coefficient (SC) and surface roughness (SR) for GAP and GAPS microparticles were evaluated.

Because of powders should gel in situ, absorbing the wound exudates, samples fluid uptake ability was evaluated *in vitro* using a specific protocol (paragraph 2.4.2). The increasing in weight of the dry powder and the speed of gel formation was evaluated. GAPS formulation showed a gel/powder ratio ranging between 11.91 and 14.81 whereas GAP ratio was included between 12.27 and 14.19. Complete gelification happened in 30 minutes for GAPS and in 25 minutes for GAP. As expected, fluid uptake was directly related to alginate content. Furthermore, SAA particles show a faster gelification speed due to their higher surface area at the same weight compared to SD particles.

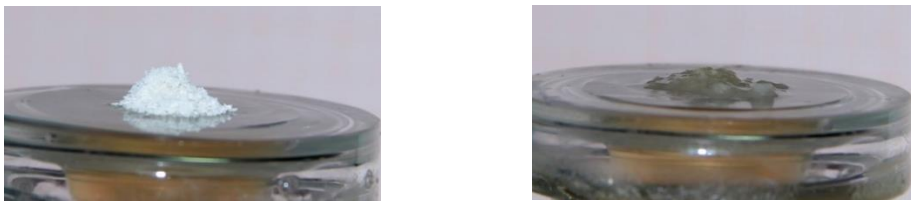

Figure 46: Gelification of a GAP powder in 15 minutes when in contact with simulated wound fluid.

A topical formulation for wound healing should provide an adequate traspirability. Then fluid permeability of the different formulations was also evaluated as water loss after swelling process in order to ensure that gel layers would provide adequate level of moisture at wound bed. The values of this parameter, named water vapour trasmission rate (WVTR), reported in literature, should range between 80 and 105 g/m^2h to avoid wound occlusion or loss of liquids with consequent dehydration.

All GAP formulations presented WVTR values between 93 and 98, then, in the appropriate range to maintain a proper fluid equilibrium. GAPS3-4 showed suitable WVTR (103 and 102) whereas GAPS1-2 WVTR was higher (111 and 110, respectively), but still acceptable. The results from these preliminary studies show that gel obtained by any GAP or GAPS formulation can produce the proper environmental characteristics to promote wound healing.

Storage stability test, conducted in accelerated conditions (40°C, 75% moisture degree) following ICH Q1AR2 guide, highlighted that GS content is stable even in harsh condotions and also the water content doesn't increase significantly in three months (about 5%) as well as thermal behavior doesn't change significantly.

An important goal of this formulation was the optimization of drug release kinetics from swellable and erodible polymers, as a function of the wound treat (i.e. ulcers, pressure sores). Hence, permeation profiles of the encapsulated antibiotic were obtained in vitro by means of franz type diffusion cell, in order to study the GAP and GAPS in vitro behaviour (2.4.2). Results were compared to that of pure GS which permeates in three hours, as expected for a completely water soluble drug of class I BCS.

Regarding GAPS and GAP formulation, their behviour was influenced by drug/polymer ratio and manufacturing process.

Micro-particles produced by spray drying GAPS exhibited the faster permeation rate, achieving total release of the drug into the acceptor compartment between 4 and 6 days according to the increasing in polymer blend concentration, whereas GAP (formulations released the total amount of the encapsulated GS) between 8 to 10 days (in SWF). Moreover, both GAPS and GAP microparticles exhibited a drug burst effect within 7 h related to particles hydration kinetic, resulting in the release of almost 50% of the loaded drug in 6 h for GAP1 and GAPS1 (formulations) while GAPS4, that showed the slowest hydration rate, released in 6 h 35% of the loaded GS.

Such intensive release of gentamicin in the first 6 h of administration, followed by a prolonged release, could be very useful to prevent infection spreading at the beginning of a local antibiotic therapy maintaining high local antibiotic concentration for an extended period of time.

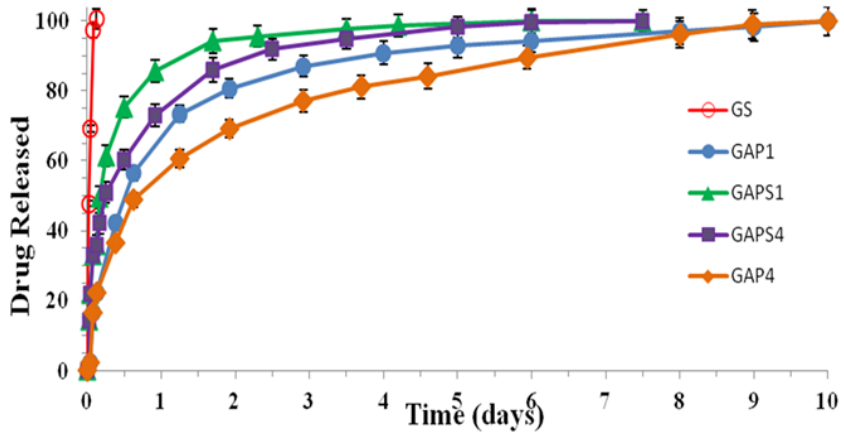

Figure 47: Drug release profile of GAP1, GAPS1 (blue and green) and GAP4, GAPS4 (orange and violet) compared to GS raw material (red line).

Preliminar microbiological assays allowed to evaluate the antimicrobial activity of the formulation aganist *S. aureus* and *P. aeruginosa* that are the most frequently bacteria found in wounds. The time killing test conducted on *S. aureus* measured the reduction of the number of CFU (colony forming unit) recovered at 6, 12 and 24 days. Differently from GS that loses its activity in 6 days, formulations showed activity till 24 days. Moreover, during the first 6 days, all formulations, with the exception of GAP4, showed a bactericidal activity against *S. aureus* comparable to GS. GAP powders had an activity from 12 to 4 folds greater than GS, whereas GAPS had from 6 to 2 folds greater bactericidal activity if compared to pure antibiotic at 12 days. Particularly, GAPS4 and GAP1 and GAP4 were still active after 24 days.

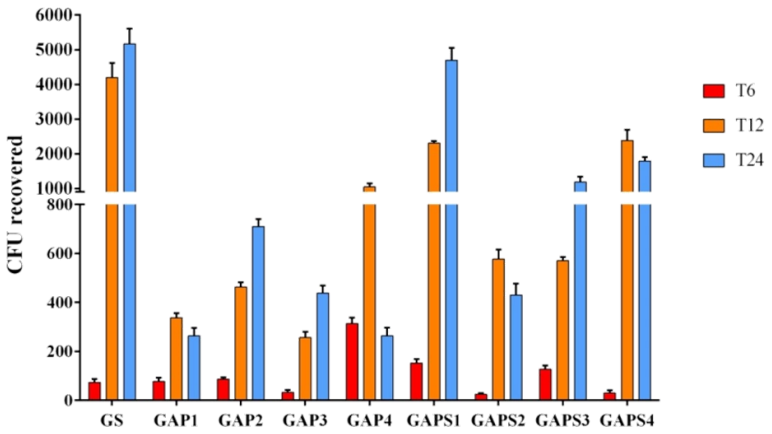

Figure 48: Time killing test on *S. aureus*. Red: day 6, yellow: day 12 and blu: day 24.

Regarding *P. aeruginosa* it's well known its ability of attachment surfaces and subsequent biofilm formation that are important steps in the establishment of chronic infections and persistence in host tissues. GAP and GAPS formulation were tested in order to evaluate their ability on degradation of preformed biofilm. GS destroyed only 10% of biofilm whereas formulations degraded till 90%; furthermore, this ability was strictly correlated to drug/polymer ratio. In fact, formulations with higher drug content, GAP1-2 and GAPS1-2, were able to degrade 90–80%, respectively, whereas GAP3-4 and GAPS3-4 with the lower drug/polymer ratio were able to degrade 50–40% of the preformed biofilm (figure 49).

A disc diffusion test conducted in Petri plates with muller hinton agar spreaded with both *S. aureus* and *P. aeruginosa* showed that the inhibition zone of bacterial growth was larger around thein situ formed gel produced by GAP compared to GAPS homologousformulations. In particular, an inhibition zone diameter ranging from 12.5 to 10.5 mm and from 10.5 and 7.0 mm was recorded for GAP and GAPS series, respectively.

Figure 49: Degradation test on pre-formed biofilm of *P. aeruginosa*.

In conclusion, SAA technique as well as spray drying were able to obtain in situ gelling dry powders with high GS content. Powders are able to gel quickly when in contact with wound simulated exudates, and to maintain the proper wound environment suitable for healing as demonstrated by the WVTR values. Release of encapsulated GS from microparticulate systems follows a non-fickian diffusion kinetics with burst effect suitable to prevent infection spreading at the beginning of a local antibiotic therapy and enabling to prolong drug release till 10 days depending on drug/polymers ratio and manufacturing technology.

Furthermore, GAP and GAPS formulations showed a stronger antimicrobial activity than pure GS on both *S. aureus* and *P. aeruginosa*, allowing a good control on infection spreading till 24 days.

3.2.2 Prilling/Supercritical Antisolvent Extraction (SAE) tandem technique

3.2.2.1 Aerogel preparation by optimization of process parameters

Aerogels are a class of nanoporous materials characterized by open pore structure and high surface area, and considered promising carriers for drug delivery. Dextran-based aerogels are very attractive because of their availability, biocompatibility, biodegradability, and low cost process as well as to their ability to entrap drugs and modulate the release kinetics. Alginate matrix has also been used to deliver drugs or peptides as encapsulated components, protecting the therapeutic agent by environmental stress/degradation (134, 135).

Consequently, they can act as delivery systems generally enhancing the bioavailability of the loaded drug (136).

Furthermore, their nanoporous structure can absorb large quantities of liquids, such as exudates, making them very interesting in wound healing applications.

In this work alginate hydrogel processed by prilling were produced and dried by Supercritical Antisolvent Extraction in order to test the feasibility of the tandem technique prilling/SAE, tuned in this work for the first time, and to optimize the process parameters of both techniques.

Prilling or laminar jet break-up is a mild encapsulation technique useful to obtain polymeric particles with narrow size distribution. Alginate polymeric solution at concentration of 2% w/w were produced by adding a proper polymeric powder amount into distilled water under gentle stirring. The solution formed was processed by prilling at 300 Hz of frequence, 10 ml/min feed rate and with a 600 µm nozzle.

The droplet formed by the laminar jet break-up falled into a $CaCl_2$ 0.5M gelling solution and left into this bath for 5 minutes. The hydrogels formed were then put in a proper organic solvent (ethanol and acetone) for 5 h to obtain a complete and efficient water elimination and then supercritical process was performed. The water in hydrogel, in fact, cannot be direct

removed by SC−CO_2 drying because this fluid shows only a very limited affinity with water; therefore, a solvent exchange step is required.

In this study, different exchange solvents and drying conditions were tested to preserve the original gel internal nanostructure of alginate aerogels. Morphological analysis by means of scanning electron microscopy and calculation of shrinking factors were used to evaluate the differences between the different solvent exchange.

Shrinking factor is calculated by the following equation:

$$Shrinking\ \% = d_h - \frac{d_d}{d_h} * 100 \quad (6)$$

where d_h is the diameter of hydrated particle and d_d the diameter of the dried one.

Particularly ethanol and acetone were selected for this work. The operating pressure and temperature ranges were chosen by considering the vapor−liquid equilibra (VLE) of the two supercritical mixtures selected, namely, ethanol/CO_2 and acetone/CO_2, to work above their mixture critical point (MCP) (137). Indeed, the works on alginate hydrogel drying were performed at pressure and temperature conditions near the pure CO_2 critical point.

Regarding the mixture ethanol/CO_2 using an extraction time of 90 min, hydrogel beads were dried at different operating temperatures of 32, 35, and 38 °C and at different pressures of 100 and 150 bar. It should be noted that CO_2 density is directly connected to its solvent power and increases with pressure, whereas it decreases with increasing temperature. At 100 bar the binary mixture ethanol/CO_2 formed into the beads was too close to its MCP causing a non-uniform extraction. When the SC drying was performed at 150 bar, all alginate beads were spherical and clearly white. A summary of the results obtained at 150 bar and 38 °C, in terms of shrinking factors (SFs), is reported in Table 4.

The lowest SF value (0.6%) was, infact, measured operating at 150 bar and 38 °C which corresponds to a CO_2 density of 794 g/cm3. At CO_2 densities higher than 800 kg/m^3 (operating at 150 bar and at 32 and 35 °C), larger bead shrinkages of 4% and 6% were observed.

Also the lowest solvent residues were found with these conditions, that were considered the optimal.

SC drying for the mixture acetone/CO_2 was performed at the same operating temperatures and pressures as for ethanol. At both operating pressures, the beads produced were spherical and clearly white with a uniform and homogeneous internal nanostructure. Additionally, the SF value was always very low and ranged between 0.6% and 2% with respect to the original bead diameter when operating at 150 bar and between 0.3% and 0.9% when operating at 100 bar. The best results in terms of SF and solvent residue were found at 100 bar and 38°C (table 4).

Table 4: Optimized SAE parameters for both acetone and ethanol as co-solvents. Shrinkage factor and solvent residue in these conditions are reported.

SOLVENT	p (bar)	T (°C)	CO_2density(kg/m^3)	SF (%)	Solvent residue (ppm)
ACETONE	100	38	662.57	0.31	141
ETHANOL	150	38	794.55	0.6	220

Because the MCPs of the ethanol/CO_2 and acetone/CO_2 systems at the selected temperatures are located at very similar pressures (Figure 50), the different processing results do not seem to depend on the distance of the operative points from the corresponding MCP but rather on the different affinities of the two organic solvents with SC-CO_2. This evidence can also be deduced from VLE diagrams (figure 50), in which the area of the two-phase region (at the same temperature) is very different for the two systems. Ehanol/CO_2 exhibits a larger biphasic region than acetone/CO_2, showing that acetone and CO_2 have larger compatibility. Another possible explanation is related to the

composition of the solvent CO_2 in the beads and can be described with a composition path starting from pure solvent to practically pure CO_2 at the end of the drying process, as indicated by the red line in figure 50.

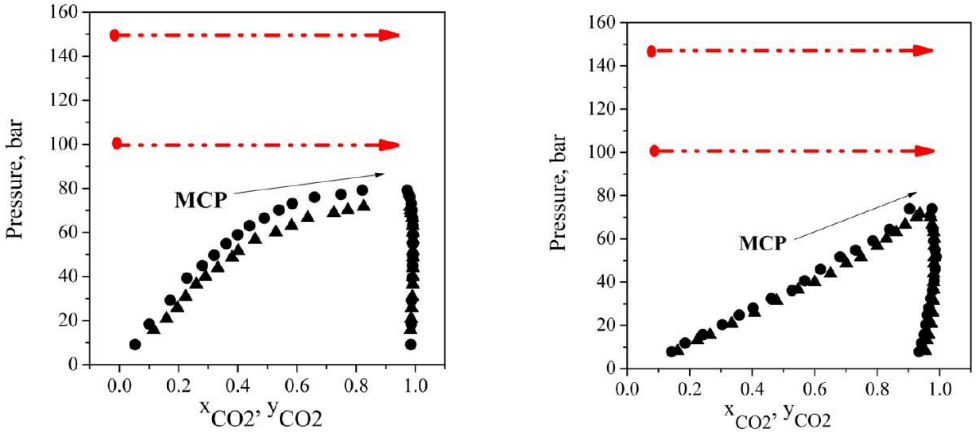

Figure 50: On the left: VLE for the mixture Ethanol/CO_2, on the right VLE Acetone/CO_2.

When the drying process has been performed at lower pressure (100 bar), it is possible that in the case of ethanol/CO_2 the system has maintained a higher surface tension when the expanded liquid region has been crossed (the region of the diagram on the left of the MCP). This event can produce the observed lower efficiency in the case of ethanol drying for the drying process at lower pressure.

However, because of ethanol is a better solvent for pharmaceutical products than acetone, due to its safety, it was preferred to acetone for the following applications.

Aerogel produced by the supercritical extraction of solvents using supercritical carbon dioxide based processes, can be applied in pharmaceuticals due to the mild and green conditions of the process as well as low cost, and to overcome the traditional process limitations.

The process allows a fast and effective solvent elimination, preserving the original gel nanostructure (67, 138) because of the near zero surface tension of

the CO_2 solvent mixture that prevents the structure collapsing during drying. The process is also very fast and yields a complete solvent elimination (71, 139). Indeed, supercritical carbon dioxide (SC-CO_2) shows a large affinity with almost all the organic solvents, and because of its gas-like diffusivity, it has been proposed for the production of several innovative materials such as porous membranes (66, 140), biopolymer microspheres (141, 142), or micro- and nano-particles (143, 144).

Using the optimized conditions studied in this work, nanostructured and completely dry particles were obtained, homogeneous in shape and dimension.

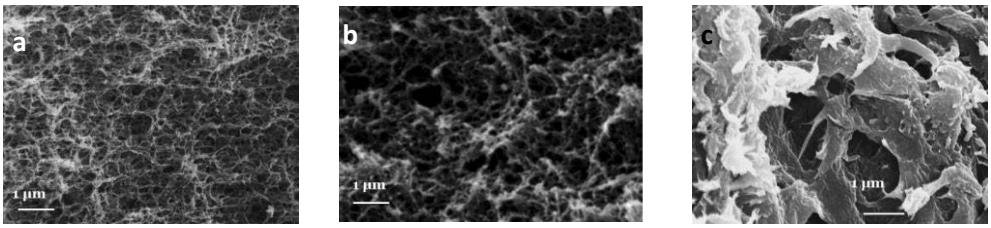

Figure 51: Internal structure of half beads criofractured with liquid N_2. a) alginate beads extracted with ethanol, b) alginate beads extracted with acetone, c) alginate beads dryied using convective methods.

SEM images show a half particle of aerogel obtained after ethanol solvent exchange (51 a) and an aerogel obtained after acetone solvent exchange and of an alginate beads dried by conventional techniques (51 b). As shown in the figure, the nanoporous network of about 200 nm was maintained after the supercritical drying for both the solvent used for the exchange step, whereas a completely collapsed matrix derives from traditional convective drying methods. These characteristic of the matrix are directly correlated to the ability of alginate particles to control the drug release and to obtain a proper release kinetic.

3.2.2.2 Co-axial prilling/SAE

The optimization of process parameters of prilling/SAE tandem technique, performed in the previous study, was useful for its application in an innovative configuration.

Prilling, a mild encapsualtion technique based on the principle of the laminar jet break-up, is proposed in its co-axial configuration as single step technique for the manufacturing of core-shell particles (145).

Two concentric nozzles of different dimension, the inner of 400 µm and the outer of 600 µm, were used to pump contemporarly different polymer solutions obtaining core/shell particles.

In the current study, the development of a novel aerogel formulation in form of polymeric core/shell microcapsules based on alginate and amidated pectin and loaded with doxycycline is reported. Alginate with high mannuronic content, able to stimulate cytokines production by human monocytes, was used as constituent of the shell and as enhancer of the healing process (146). Amidated pectin matrix, loaded with doxycycline, was used as core of the particles and drug diffusion barrier. Both polymers allow the formation of a structured gel able to maintain a balanced transpiration/evaporation equilibrium at the wound site.

Particles were cured using supercritical CO_2 (SC-CO_2) technique to remove solvent from beads allowing the production of aerogels characterized by open pore structure and high surface area. Doxycycline (D) was used as a broad range spectrum of action antibiotic drug, active against both Gram positive and Gram negative bacteria, which both colonize infected wounds. Moreover, this antimicrobial agent acts as a protease MMP inhibitor, particularly MMP-9 (147) and it has shown to be potentially able to inhibit TNF-α converting enzyme (TACE) activity (117), therefore to reduce MMP-2 expression in chronic wounds leading to the enhancement of the healing.

A series of samples were produced (prilling optimized conditions in paragraph 2.4.1.4) to be tested in terms of morphology, density, gelling ability and drug release profiles.

Core/shell droplets produced by prilling were gelled directly in ethanol, producing alcolgel, and were immediately ready for the supercritical drying. Doxycycline saturated gelling solution was useful in order to reduce drug leaking from the alcolgels during the gelation process.

Operative conditions, chosen using the vapour liquid equilibrium diagram for the binary system ethanol/CO_2 (148, 149) were set at 150 bar, 38°C, and a CO_2 flow rate of 0.6 Kg/h, as studied in the previous work. The process last 60 minutes.

Table 5: description of sample composition, aerogel beads diameter, apparent density, sphericity coefficient (SC) and encapsulation efficiency (e.e.)

SAMPLE CODE	PECTIN/CORE SOLUTION (W/W)	DOXYCYCLINE HYCLATE/PCT CORE RATIO	ALGINATE OUTER LAYER SOLUTION (W/W)	Ø AEROGEL BEADS ± SD (mm)	APPARENT DENSITY±SD (g/cm^3)	SC	e.e.(%)
PD1AL1	3.5	0.1	1.50	3.25 ± 0.01	0.31 ± 0.02	0.96	87.5 ± 0.2
PD1AL2		0.2		3.26 ± 0.01	0.32 ± 0.03	0.97	72.3 ± 0.1
PD2AL1		0.1	1.75	3.27 ± 0.01	0.32 ± 0.02	0.98	77.5 ± 0.1
PD2AL2		0.2		3.27 ± 0.01	0.34 ± 0.03	0.98	66.8± 0.1
PAL1	3.5		1.50	3.23 ± 0.02	0.26 ± 0.02	0.97	-
PAL2			1.75	3.26 ± 0.02	0.29 ± 0.03	0.97	

As showed in the table above, the pectin core solution was always set at 3.5%w/w in polymer concentration and D was added in a ratio of 0.1 and 0.2. The alginate outer layer solution was set at 1.5 and 1.75% w/w. The aerogel diameter ranged between 3.25 and 3.27 for beads produced with either the lower or the higher alginate concentration and drug/polymers ratio, whereas blank aerogel beads mean diameter ranged between 3.23 and 3.26 mm.

Complete solvent elimination from the polymeric matrix lead to aerogel beads with spherical shape and slight reduction in size (about 10%) compared to the uncured particles.

Blank aerogels showed low density, between 0.26 and 0.29 g/cm^3, depending on concentration of alginate solution while doxycycline loaded aerogels showed slight increase in apparent density, between 0.31 and 0.34 g/cm^3, depending on concentration of alginate solution and drug-pectin ratio; the higher the both the higher the density. This phenomenon can be explained looking at the differences in three dimensional gel structure of the alginate and pectin into the beads, as highlighted in SEM analyses. In fact, the increase of alginate concentration leads to an increase in cross-linking degree and a subsequent increase in density while the different gelation mechanisms between alginate and pectin into the beads leads to very different polymer matrix nanoporous texture.

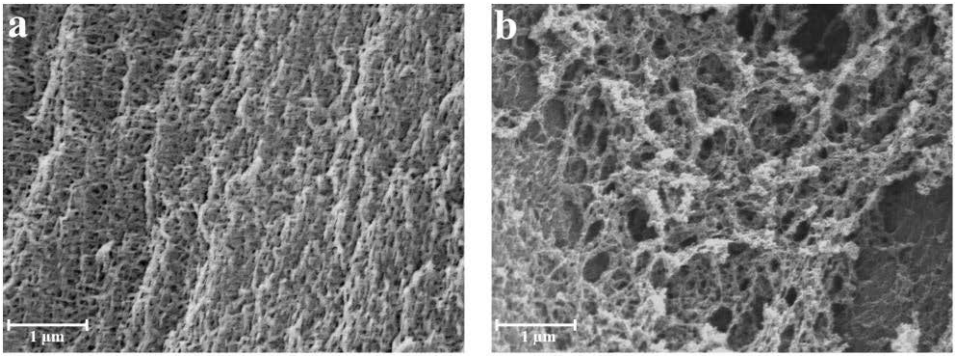

Figure 52: internal structure of half core/shell aerogel obtained by liquid N_2; a) alginate shell, b) pectine core.

Nanoporous structure was not affected by drug loading and no crystals of the drug were observed embedded into the matrix probably due the formation amorphous doxycycline into the beads.

Doxycycline encapsulation efficiency (e.e.) was also correlated to the alginate layer but unexpectedly the ticker the alginate layer the lower the e.e. This is mainly due to the increase in porosity of the alginate outer layer, when higher

concentration are processed, that is not compensated by longer diffusional path during the SC-CO_2 solvent extraction (150).

Moreover, e.e. decreased also with the increase of drug/polymer ratio due to diffusional phenomena strictly related with drug internal concentration.

The figure below is a comparison between SEM analysis and Fluorescence microscopy (FM). SEM photograph evidences the presence of a well formed core/shell bead with an alginate outer layer ranging between 175 and 210µm for 1.5 and 1.75% alginate concentration, respectively (53 b). FM images confirm the good formation of the particle with an evident distribution into the pectin core of the drug that was concentrated only in the internal part of the beads with very tiny spots located into the alginate shell on the border of the pectin core. The presence of such spots was mainly related to the alginate concentration.

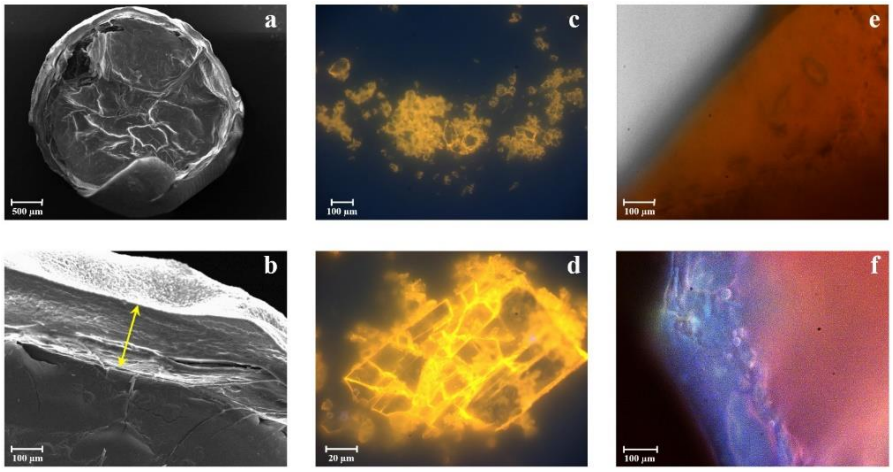

Figure 53: Fluorescence images of core/shell particles, and of doxycycline raw material compared to SEM images. SEM images of a half particle (a), and of alginate shell (b). FM image e shows the doxy loaded core, whereas image f shows the unloaded shell (blue).

This phenomenon can be explained looking at the difference in gelation rate between the core and the shell of the bead. In fact, the faster gelation of

alginate shell, compared to the pectin core, reduces doxycycline diffusion and decreases drug leaking into the shell layer.

Doxycycline has amine groups that could interact with anionic polymer residues of pectin and alginate. Such an interaction could be useful to slow down drug release rate from beads prolonging the drug efficacy. FT-IR studies were conducted in order to verify the presence of such interaction. The characteristic peaks of doxycycline are reported in Figure 54. Strong bands between 3500 and 3000 cm^{-1} represented C-H, N-H and O-H absorption while stretches of C=O and C=C bonds were present between 1700 and 1600 cm^{-1}, 1683 and 1614 cm^{-1}, respectively (151). In the same region alginate exhibited asymmetric stretching band from the carboxylate ion centered at 1640 cm^{-1} and 1420 cm^{-1}, whereas pectin showed stretching vibration of amidated C=O at 1740 cm^{-1} and a band representative of COO^- asymmetric stretching between 1650 and 1600 cm^{-1} (152, 153). PDAL formulations showed most of the characteristic peaks of doxycycline and polymers but also the presence of a new peak centered at 1726 cm^{-1} that can be associated to the interaction between doxycycline and non-amidated acidic residues of pectin.

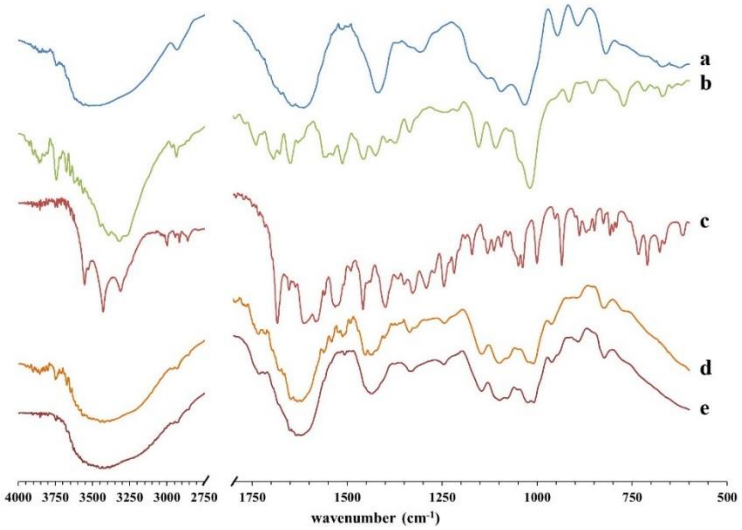

Figure 54: FT-IR spectra of sodium alginate (a), pectin (b), doxycycline raw materials (c), and doxycycline loaded samples PD2AL1 (d) and PD2AL2 (e).

The thermal behaviour of pure doxycycline and blank core-shell beads is reported in Fig. 55. Doxycycline thermogram exhibited, as expected, the profile of a crystalline material with an endothermic melting peak at 168°C followed by an exothermic peak at 225°C due to drug degradation. Blank beads exhibited the melting of both pectin and alginate complex with Ca^{+2} as broad signals at 155 and 178 °C, respectively, while the presence of an exothermic peak at 290°C was related to the polymers decomposition.

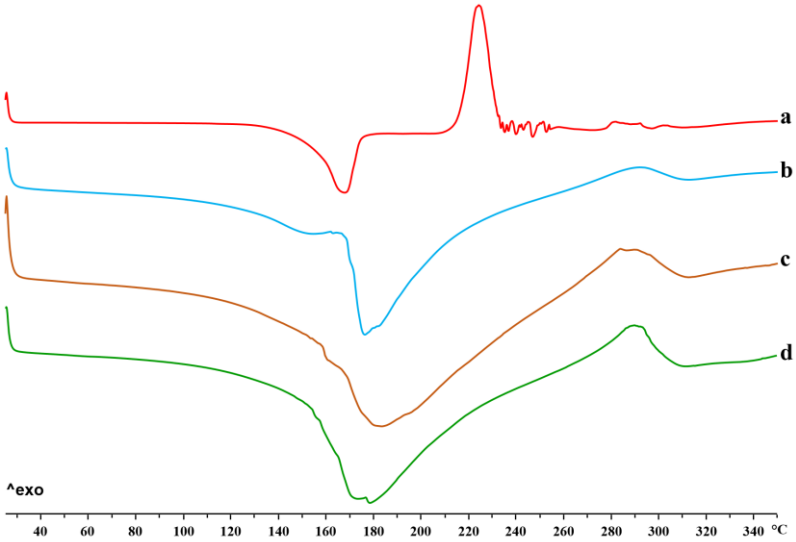

Figure 55: DSC thermograms of doxycycline hyclate (a), and core-shell pectin-alginate beads obtained by coaxial prilling and SC-CO2 drying process: blank beads (b), PD2AL1 (c), PD2AL2 (d).

Doxycycline loaded core-shell beads exhibited similar behaviour to blank beads with shifting of the peaks related to the melting of the polymer matrix that might be explained by the formation of a complex via amine groups of doxycycline and acidic groups of pectin, as shown by FT-IR analysis, too. Homogeneous embedding of the drug into the calcium pectinate core contributes to shift the melting peak to higher temperature. In fact, the higher the content of the drug, the larger the shift.

In order to mimic *in vitro* the ability of the drug loaded aerogels to interact with the exudate at wound bed, simulated wound fluid (SWF) (95) was used to test both wound exudate uptake ability and drug release.

Fluid uptake ability was evaluated as the weight ratio of the aerogel in hydrated and dry state at different time points when formulation was in contact with SWF. As expected, fluid uptake was directly related to polymeric content. In fact, formulations exhibited an increase in weight ranging from 7.5 to 8.1 for PD1ALs and PD2ALs, respectively. Moreover, shrinking of the particles was observed before swelling phase. This phenomenon, due to the partial collapsing of the alginate shell on the pectin core, was more significant and faster for formulations produced with higher alginate content, as shown in Figure 56. Swelling of the particles was related to alginate content, too (154). In fact, doxycycline loaded beads produced with more diluted alginate solutions exhibited a lower increase in size, leading to 50% of the swelling endpoint in about 11 min, and to total swelling of the formulation in about 40 min. Aerogels produced with 1.75% w/w alginate concentration needed about 50 min to move to completed swelled gel, probably due to the presence of more entangled alginate chains into the polymer matrix.

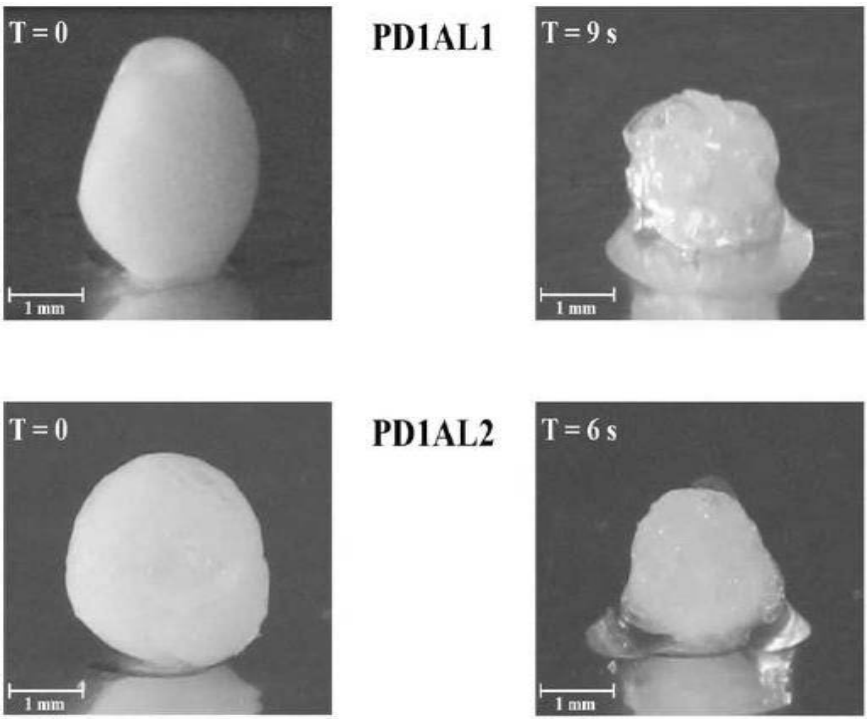

Figure 56: The collapse of alginate shell on the pectin core in the first seconds of contact with fluids.

Figure 57 panel A, reports the permeation profiles of both aerogel formulations in comparison to pure doxycycline as crystalline raw material. As expected for a very soluble drug, total permeation of doxycycline was achieved in around 20 min. On the contrary, drug entrapped into the aerogel formulations exhibited a prolonged permeation, until 48 h, due to the conversion of the beads into hydrogel able to acts as a barrier against drug release. Moreover, drug permeation was dependent on both drug/pectin ratio and alginate concentration. In fact, PD2AL1 exhibited the higher permeation rate releasing almost 55% of the encapsulated drug in about 1 h and achieving total release in about 24 hours while PD1AL2 released less than 35% in 1 h and needed 48 h to release the entire drug dose. The drug burst effect useful at the beginning of an antibiotic therapy can be related to the different amount of doxycycline in alginate shell (higher for PD2AL1 and PD1AL1) that collapse

over the pectin core during the first contact between aerogels and PBS as well as to the formation of a thinner hydrogel. The influence of polymeric shell on drug release rate can be highlighted looking at doxycycline permeation normalized over alginate shell thickness, as reported in Figure 57 panel B. In fact, the amount of doxycycline released by aerogels with thicker shell is 4 times less than for the ones with thinner layer, while, slightly differences in drug release from aerogels produced with the same amount of alginate might be due to the presence of the drug into the alginate shell, as for burst effect The influence of the polymer chains relaxation process on doxycycline release was determined by fitting the experimental data with Peppas-Korsmeyer's equation (using the first 60% of the amount released) (155). All formulations presented non-Fickian transport mechanism involving matrix swelling and erosion. In fact, the diffusion exponent n was found to be between 0.53 and 0.58, depending on alginate concentration. Increasing of alginate concentration lead to a ticker shell around the pectin core able to reduce drug diffusion. Moreover, swelling properties of the core-shell matrix, mainly due to alginate external layer of the formed hydrogel affect drug diffusion, which follows a complex non-Fickian release mechanism, resulting governed by both matrix relaxation and erosion phenomena (156).

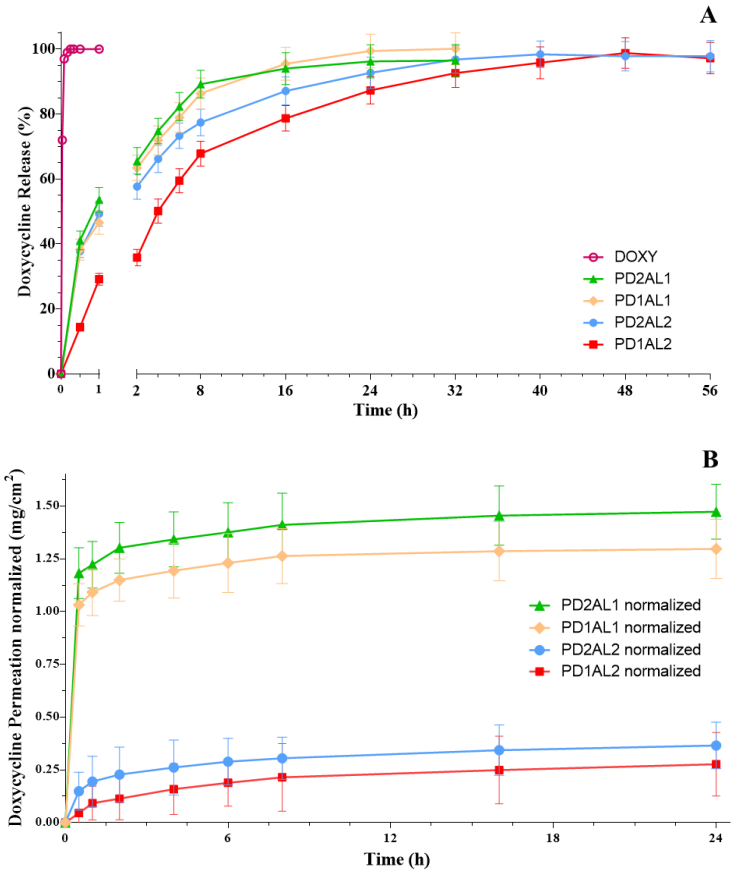

Figure 57: A- Release profiles of PD2AL1 (green), PD1AL1 (yellow), PD2AL2 (blue), PD1AL2 (red) compared to doxycycline raw. B- PD2AL1, PD1AL1, PD2AL2, PD1AL2 permeation rates normalized on the alginate shell thickness.

In conclusion, prilling technique in tandem with a supercritical CO_2 drying allowed to efficiently obtain alginate/pectin core/shell aerogel particles, spherical in shape and with a good encapsulation efficiency (up to 87%). These aerogels consisted of doxycycline entrapped into a pectin core network and coated with alginate as shell of the particles. When in contact with a simulated wound fluid they were able to swell and move into a gel. This ability was directly related to the concentration of alginate in the liquid feeds processed by prilling apparatus, with a lower swelling at the lowest polymer

concentration. However, all formulations moved into gel status between 40 and 50 min. Acting as a barrier to doxycycline permeation, pectin and most important alginate amount in the processed solutions influenced drug release rate. In fact, differently from pure doxycycline that permeates in 20 min, the aerogel formulated with the higher amount of alginate in the outer layer is able to prolong drug release till 48h by delaying diffusion of the drug through the swelled alginate/pectin polymer matrix. Core/shell aerogel particles included in gauze can be used as formulations having great potential application in the treatment of both acute and chronic infected wounds

3.2.3 Prilling/Supercritical drying/Supercritical impregnation

From the results obtained by experiments of Felicetta De Cicco performed during the period spent at Universidade de Santiago de Compostela, -Santiago de Compostela, Spain- under the supervision of professor Carlos A. Garcìa-Gonzalez.

3.2.3.1 Norfloxacin and ketoprofen loaded into alginate aerogels: prilling/supercritical drying/ supercritical impregnation

In this part of the Ph.D course, a combined technique based on prilling/supercritical drying/supercritical impregnation was applied for aerogel beads production. Such technique could be proposed for the development of a dextran based topic formulation loaded with norfloxacin and norfloxacin/ketoprofen.

Prilling was used to produce alginate particles in narrow size distribution, while supercritical drying, applied to polymeric matrix, allows the production of aerogels characterized by open pore structure and high surface area, able to control the drug release as also described in the previous studies done in the first year of course (149).

The expertise on prilling and the supercritical based technologies acquired during my Ph. D. course was very useful to study the feasibility of prilling coupled with supercritical drying and supercritical impregnation.

Supercritical CO_2 (SC-CO_2) was also used for drug impregnation in order to load particles with norfloxacin and ketoprofen to propose as wound healing formulations.

Aerogels, as showed previously, are characterized by open pore structure with high exposed surface area, so they are able to absorb large quantities of liquids, as well as exudates, with possible topical applications for wound healing.

Furthermore, objective was to study the effects of this multi-step process on aerogels, in terms of particle morphology, drug solid state properties and particle apparent density before and after impregnation.

Feed solution of alginate with high mannuronic residues content, able to promote the wound healing, were prepared at different concentrations (1.50-2.25% w/w), and processed by prilling. Optimized prilling conditions were

used to obtain particles with a narrow size distribution (paragraph). Particles were obtained by gelation in both aqueous and ethanolic $CaCl_2$ 0.5M solutions producing hydrogels and alcogels, respectively. This experimental part was conducted at University of Salerno.

At the University of Santiago de Compostela, Department of Pharmacy and Pharmaceutical Technology, the solvent exchange was conducted overnight in absolute ethanol with continuous stirring, and then the SC-CO_2 assisted drying process was conducted under optimized conditions (120 bar, 40°C, 5-7g/min for 3.5 h), collecting ethanol every 15 minutes during the first hours and every 30 minutes for the remaining experiments hours.

Supercritical drying was successfully conducted on both particles gelled in water and ethanol, obtaining aerogels with a nanoporous structure. However, impregnation and analysis were conducted only on aerogels obtained by hydrogels.

Norfloxacin was used as model drug, because of its broad spectrum of action, as well as ketoprofen was chosen as antinflammatory model drug. Both drugs are characterized by a good solubility in SC-CO_2, a fundamental condition for this process (157, 158).

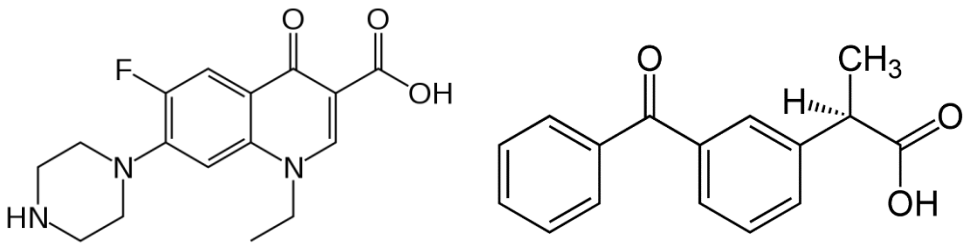

Figure 58: Norfloxacin (on the left) and ketoprofen (on the right).

Supercritical impregnation was conducted in order to load aerogel using optimized conditions, (pressure 180 bar, temperature 40°C, 6 h, batch conditions)(159). Particularly, a specific protocol of depressurization was actuated in order to avoid drug amorphisation.

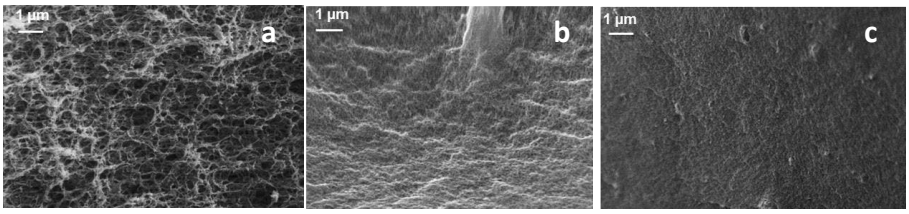

Figure 59: internal structure of criofractured particles with liquid N_2. a) alginate aerogel beads. b) Alginate aerogel beads after impregnation with ketoprofen and norfloxacin, c) alginate beads liohpilized after exchange in ethanol.

Supercritical drying was compared to other drying methods, such as convective method (owen at 40°C) and liophilization. SEM images of half particles criofractured with liquid N_2 were compared. Blank alginate aerogel (figure 59 a) exhibited nanoporous internal structure preserved after the supercritical drying (75). On the contrary, figure 59 b shows the internal structure partially collapsed of an aerogel after impregnation of ketoprofen and norfloxacin. Nevertheless, apparent density is increased due to the partial embedding of the drug into the matrix and to the impregnation process (table 6).

N_2 adsorption/desorption method, based on Brunauer-Emmett-Teller theory, was used to study the effective porosity of the aerogels. Freeze dried hydrogel particles were used as control.

Aerogel porosity, as expected, was higher compared to freeze dried particles, with specific surface area between 172.0219 to 459.7350 m^2/g while specific surface area for lyophilized particles ranged between 122.9677 to 163.1652 m^2/g.

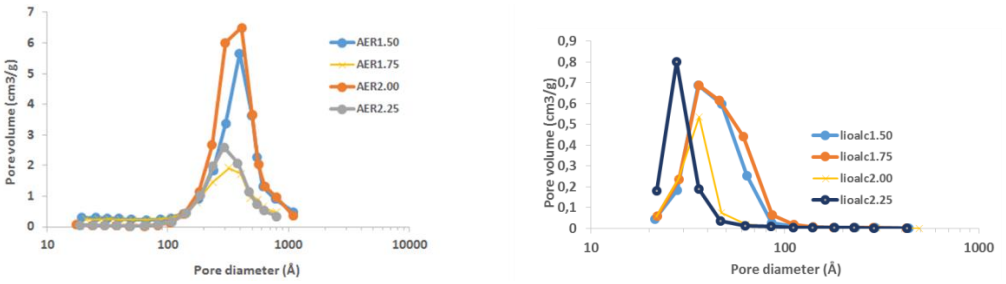

Figure 60 on the left, BJH desorption curves for aerogel at concentration 1.5, 1.75, 2 and 2.25% w/w. On the right, BJH desorption curves for liophilized particles with solvent exchange at polymer concentration of 1.5, 1.75, 2 and 2.25%w/w.

The high porosity of the aerogel particles should allow an increased fluid uptake ability compared to other formulations, that might be very useful for the topical application on wounds. To assess this property, fluid uptake ability experiments were performed. Aerogel particles were placed in contact with SWF using a specific protocol (paragraph 2.4.2). Particles when in contact with the simulated fluid shrinked immediately, then swelling process took place after 10 minutes and lasted till one hour. Swelled aerogels were able to uptake fluid increasing their weight up to 14 times.

The impregnation was firstly conducted only with norfloxacin and then with norfloxacin and ketoprofen using the same conditions. Drug content and encapsulation efficiency were evaluated by means of Uv-vis spectrophotometry.

As showed in the table 6, norfloxacin content was very low, whether the process was conducted for both 6 h and 8 h. Furthermore, the value was still low when the process was conducted impregnating also ketoprofen. However, ketoprofen loading was very high, and a remarkable difference was evident when process was conducted for 6 or for 8 hours.

Table 6: apparent density before and after impregnation process and loading for norfloxacin (N) and norfloxacin/ketoprofen (N/K) for aerogel at 1.5 and 2.25% w/w of alginate concentration. Results are divided for impregnation process conducted for 6 or 8 hours.

FORMULATION code #	Alginate conc. (%)	Impregnation time	apparent density before impr. (g/cm^3)	apparent density after impr. (g/cm^3)	N Loading (%)	N and K loading (%)	
AER15	1.5	6 h	0.08 ± 0.15	0.39 ± 0.18	0.24 ± 0.07	0.28 ± 0.03	3.11 ± 0.10
AER225	2.25		0.13 ± 0.04	0.38 ± 0.05	0.54 ± 0.22	0.74 ± 0.05	3.77 ± 0.12
aer15	1.5	8 h	0.20 ± 0.12	0.40 ± 0.08	0.59 ± 0.05	0.75 ± 0.04	4.65 ± 0.06
aer225	2.25		0.25 ± 0.04	0.52 ± 0.11	0.65 ± 0.11	0.89 ± 0.05	4.73 ± 0.08

In conclusion, this study assessed the feasibility of combination of prilling/supercritical drying/supercritical impregnation. Hydrogels produced by prilling can be easily converted in aerogels, by supercritical process, and aerogels can be impregnated with norfloxacin and with norfloxacin/ketoprofen. However, further studies are needed to increase norfloxacin encapsulation efficiency, optimizing impregnation process.

Aerogels presented high porosity due to their nanoporous structure, as well as the ability to absorb large quantities of fluids.

3.3 SECTION C

In situ injectable peptide loaded hydrogels

3.3.1 In situ injectable hydrogel loaded with Annessin 1 like peptide Ac2-26

The discovery of growth factors (GFs) and their mechanisms of action was a strong stimulus to the design of locally controlled release formulations loaded with different GF molecules (EGF, VEGF, bFGF, GM-CSF, PDGF-BB). Despite the encouraging results from various clinical trials, only PDGF-BB has been approved for its use in diabetic ulcers as a gel formulation (160, 161). However, it showed a modest efficacy and phase IV investigations highlighted significant side effects in patient extensively treated with PDGF (162); therefore, other growth-factors and new formulations must be tested and developed (163).

Annexin A1 (ANXA1, lipocortin-1) is the first characterized member of the annexin superfamily of proteins, able to bind (to annex) to cellular membranes in a Ca^{2+}-dependent way. ANXA1 has been involved in a broad range of molecular and cellular processes, including anti-inflammatory signalling, kinase activities in signal transduction, maintenance of cytoskeleton and extracellular matrix integrity, tissue growth, apoptosis and differentiation (164). ANXA1 N-terminal derived peptide Ac2-26 has been used as an ANXA1 surrogate in view of its ability to replicate the antiinflammatory effects of the parent protein (165). Ac2-26 can activate all three human formyl peptide receptors, promoting calcium fluxes, and cell motility (166).

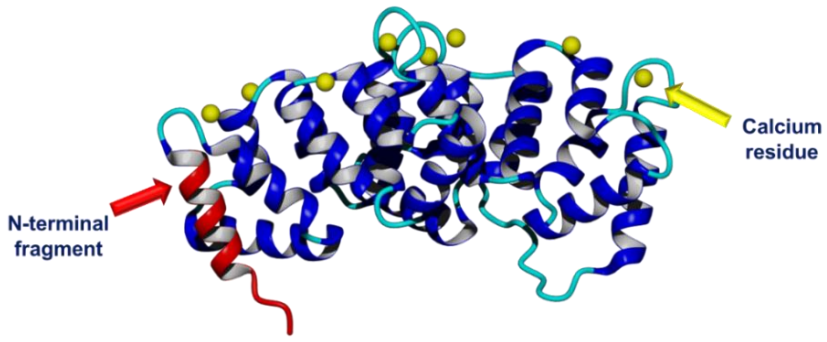

Figure 61: Annessin-1 peptide 3D image. In red, N-terminal peptide Ac2-26.

Such an effect may be part of a reparatory process as demonstrated with intestinal epithelial cells, skeletal muscle myoblasts and WS1human fibroblasts (167-169) where addition of the Ac2-26 peptide engaged FPRs to activate the cytoskeletal machinery amplifying the pathway downstream FPR activation, contributing to actin polymerization and then favouring cell migration and tissue repair.

Naural biopolymer are known for their ability to enhance wound healing process by molecular mechanisms. High M residues content alginate is well known for its ability to induce cytokine production by human monocytes, a process very useful in chronic wound healing (61). Low molecular weight (LMW) chitosan is also able to induce macrophages activation by interaction of the acetylated residues with mannose receptors (58). This action as well as collagenase activity can be enhanced by chitosan oligomers and monomers easy produced by enzymatic degradation of LMW chitosan (170).

Furthermore, this kind of carrier are able to retain high quantities of water, assuring an appropriate moisture at the wound bed (95, 131).

In this preliminar study, in situ injectable alginate or chitosan hydrogel containing different amounts of Ac2-26 were produced (preparation at paragraph2.4.1.6), in order to test the ability on promoting wound healing by the synergic effect of polymers and peptides, also finding the right dosage per each gel. This ability and other properties of this kind of formulation were tested in *vitro* and in *vivo* on a murin model.

The first part of the work included a series of test to evaluate the possibility of using in vivo such hydrogels.

Rheological experiments were performed in order to find the proper polymer concentration range to obtain gels able to remain into the wound bed for an adequate time, without accidental loss, but also assuring easy applicability at the site.

Alginate concentrations were 2.5 or 5% w/w, whereas chitosan concentrations were 3.5 or 6.5%w/w. The table below shows some results for the different samples produced: ACA gels are from alginate, whereas ACC series is related to chitosan based hydrogels. The resulting gels were in the proper range of zero shear viscosity (4100 e 9500 Pa.s) enabling easy administration and retention of Ac2-26 loaded gels into wound cavity. In fact, higher η_0 would not allow clean deposition of gel into the wound bed whereas lower values caused gel leaking from the cavity. Furthermore, a fluid loss mid value was calculated.

Table 7: Alginate and chitosan hydrogels at different concentration of polymer and Ac2-26. Zero shear rate viscosity and fluid loss mid value.

Sample Code	Alginate concentration (%)	Chitosan concentration (%)	Ac2-26 concentration (μM)	Zero shear rate viscosity, η_0 (Pas)	Fluid loss mid value (h)
ACA25-100	2.5	-	0.1	421 ± 4	52
ACA25-500			0.5		
ACA25-1000			1.0		
ACA50-100	5.0	-	0.1	950 ± 6	58
ACA50-500			0.5		
ACA50-1000			1.0		
ACC35-100	-	3.5	0.1	410 ± 5	36
ACC35-500			0.5		
ACC35-1000			1.0		
ACC65-100	-	6.5	0.1	947 ± 4	48
ACC65-500			0.5		
ACC65-1000			1.0		

Alginate and chitosan gels were loaded with Ac2-26 peptide in order to obtain solutions at fixed concentration. On the basis of our previous results on the promigratory effects of the peptide on WS1 human fibroblasts in a *in vitro* wound healing assay (169), Ac2-26 gels prepared at three different concentrations (100 nM, 500 nM and 1μM) were tested in order to assess peptide stability into the polymeric gel matrix over time. Moreover, to evaluate the Ac2-26 tendency to interact with alginate or chitosan, quantitative

LC/MS analyses were performed to measure the amount of recovered peptide following 6 h of incubation into different gels. Specifically, two different concentrations of the peptide (100 nM and 1µM) were loaded into four different gels (2.5% and 5.0% alginate, 3.5% and 6.5% chitosan).

Preliminary results showed that the amount of peptide recovered from alginate gels was of 82 to 96% of the loaded quantity, whereas only 15% of loaded Ac2-26 was recovered from chitosan gels probably due to a chemical interaction between peptide and chitosan aminogroups. In order to understand this behavior, FT-IR analysis were conducted on dehydrated gels.

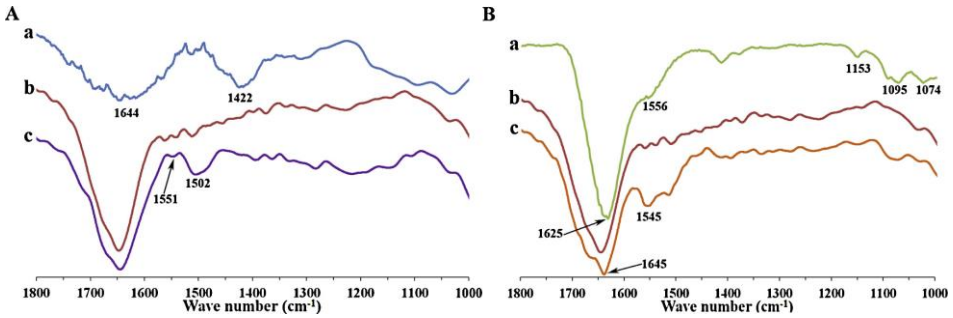

Figure 62: FTIR spectra of alginate and chitosan Ac2-26 loaded hydrogels in comparison with polymer and pure peptide solutions. Panel (A) 5.0% (w/v) high M content alginate solution (a), 0.5 M AC2-26 solution (b) and ACA50-500 hydrogel (c). Panel (B) 6.5% (w/v) LMW chitosan solution (a), 0.5 M AC2-26 solution (b) and ACC65-500 hydrogel (c).

Alginate carboxyl peaks at 1644 and 1422 cm^{-1}corresponding to symmetric and asymmetric COO^- stretching vibration were shifted at 1551 and 1502 cm^{-1}in Ac2-26 loaded alginate gel (Fig 62) probably due to an extensive hydrogen bonding in a crowded environment such as the concentrated alginate solution (171) between Ac2-26 and alginate carboxyl group. The FTIR spectrum of chitosan in Fig 62 B shows the peaks of amide bond at 1625 cm^{-1}, NH_2 bending of the protonated amino peaks at 1556 cm^{-1}due to the presence of N-deacetylated groups and the absorption bands at 1153, 1095 and 1074

cm^{-1}characteristic of the stretching of its skeletal saccharine structure. N-related peaks were shifted in Ac2-26 loaded LMWchitosan gel, amide peak into singlet band at 1645 $cm^{-1}$and amino signal to a broad peak at 1545 cm^{-1}, both not existing into the Ac2-26 peptide spectrum. Changes in the bands of the amide bonds and amino groups can be attributed to an ionic interaction between the amino group of chitosan and the region from Asn 16 and Glu 20 of Ac2-26 peptide that in the ACCs gels bear a negative charge of −2 (172). Such negatively charged portion of the peptide could allow an efficient binding onto the positive chitosan chain that might prevent Ac2-26 loaded chitosan gel to release the peptide under mild pH condition agreement with the recovery data obtained by LC/MS. Moreover, the persisting in ACCs formulation of the peak related to the chitosan amino groups at 1153 cm^{-1}suggests the presence of an interaction between chitosan and Ac2-26 in agreement with the molar ratio between them.

In order to verify the ability of gel to maintain correctly hydrated the wound during therapy, the water loss after air exposition was studied. The amount of gel to be used for the in vivo experiment was put on a support with 200µl of simulated wound fluid, and at defined point of time it was weighted.

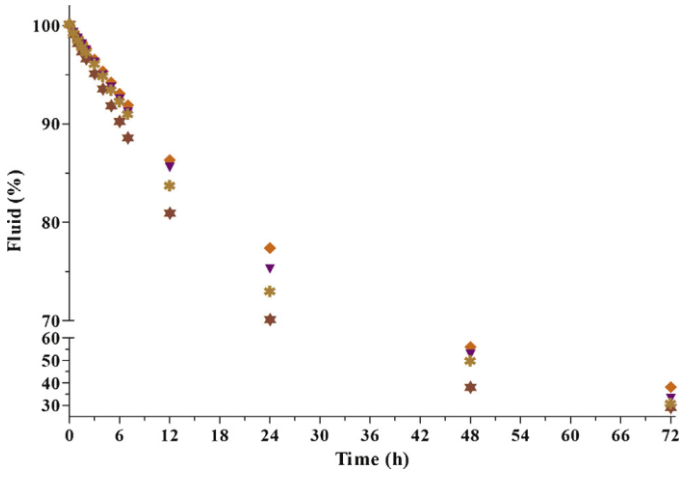

Figure 63: Water loss of 1M AC2-26 loaded hydrogels at different concentrations: high M content alginate 5.0% (♦) and 2.5% (▼), LMW chitosan 6.5% (●) and 3.5% (★).

As shown in the figure 63 all the formulations have an exponential weight loss during the first 24 hours followed by a linear kinetic between 24 and 72 hours. This may explained by the formation of a polymer enriched layer on the surface of the gel able to retard further water desorption (173). However, mid-value of deswelling (fifty percent of fluid loss) was reached in about 42 or 55 h for chitosan and alginate gels, respectively; whereas, dry state was reached between 120 and 132 h depending on polymer concentration. Moreover, fluid loss was also related to polymer concentration. In fact, the higher the concentration the slower the desorption kinetic.

Peptide release kinetic was studied using an *in vitro* test. A dyalisis membrane of 10K with an exposed area of 0.33 cm^2 was used. The system, thermostated at 37°C and stirred at 200 rpm with SWF in the donor compartment was filled with 250 µl of gel. At defined point of time 100 µl samples were collected and LC-MS detected (paragraph 2.4.2). As expected, release profiles were directly correlated to peptide and polymer concentration. Release ranged between 4 to 72 hours and all gels showed a reduction in peptide concentration between 24 to 96 h due to degradation phenomena in SWF at 37°C. This data demonstrate that polymers are able to protect peptide for a long time compared to peptide raw that degradates in a few hours (174).

Moreover, alginate/peptide gels exhibited a burst effect within 2 h related to alginate concentration, resulting in the release of about 90% of the peptide for ACA25 gels while after 2 h ACA50-100 and ACA50-1000 formulations released 69 and 52% of the loaded peptide, respectively.

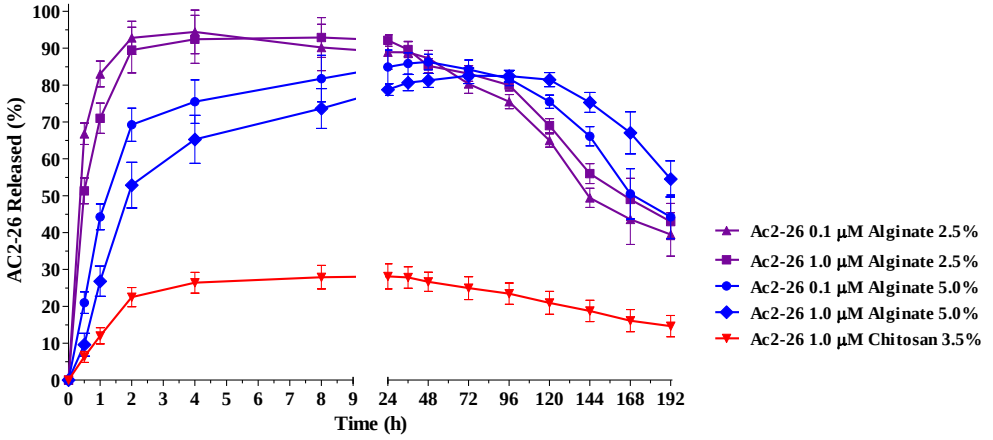

Figure 64: Release profiles of AC2-26 loaded alginate gels at different concentrations: ACA25-100 (▲), ACA25-1000 (■), ACA50-100 (●) and ACA50-1000 (◆) and of AC2-26 loaded chitosan gel at 3.5%: ACC35-1000 (▼). Mean ± SD; (n = 6).

Such intensive release of the active in the first hours of administration, followed by a prolonged release, may be very useful at the beginning of the healing process that could benefit of the strong antiinflammatory and pro-migratory effects related to high concentration of Ac2-26 (175).

In spite of similar viscosity behaviour, diffusion of AC2-26 from chitosan/peptide formulations was very poor with very slow release rate, reaching around 10% in about 72 h even for the most concentrated peptide gel This phenomenon was correlated to the strong interaction between Asn 16 and Glu 20 ofAc2-26 and LMW chitosan, as highlighted by FTIR analyses.

In vivo tests were conducted on C57BL/6 mice (Harlan Laboratories, Indianapolis, IN, USA) according to protocols that followed the Italian and European Community Council for Animal Care (DL. no. 116/92).

On the day of surgery, the hair on the back of eachmouse was clipped, and the skin was wiped with ethanol. C57BL/6mice, 10 weeks of age, were anesthetized with isoflurane prior to the wound-creating surgery.

Figure 65: An example of laboratory mouse.

Full-thickness excision wounds (1 cm × 1 cm) were created by marking the area of the wound in the shaved mid back with a fine marker and a ruler.

These tests were useful to show the effective healing potential of the hydrogels and to confirm the *in vitro* tests results. Only alginate hydrogels were used because chitosan is not able to assure a correct peptide release, as demonstrated by the previous analysis.

A series of mouse were treated only with saline solution as comparison (negative signal). Then mice were treated with alginate, and with alginate loaded with 0.1, 0.5 and 1 μM Ac2-26. At day 0, 3, 6, 9 and 14 some photograph were taken.

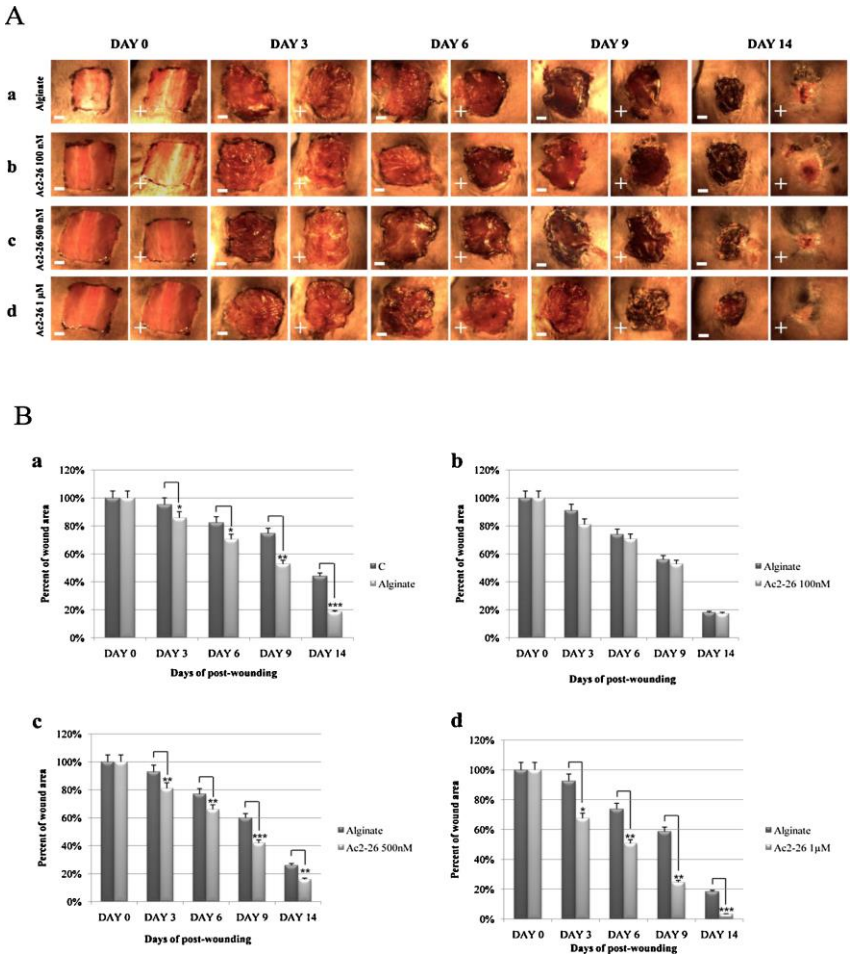

Figure 66: (A) Ac2-26 loaded alginate hydrogel ameliorates skin wound repair in acute skin wound healing. Full-thickness skin wounds (1 cm × 1 cm) in C57BL/6 mice were treated with: (a) 5.0% blank alginate hydrogel or loaded with an optimized concentration of (b) Ac2-26 100 nM, (c) Ac2-26 500 nM, (d) Ac2-26 1 µM (n = 3 mice per peptide, per experiment. Plus signs indicate treated mice, and minus signs indicate control mice. The images of 1 representative experiment are shown. (B) Measurements of blank alginate hydrogel vs Ac2-26 loaded alginate hydrogel in acute wound healing. Percentage of the accelerated wound closure at days 0, 3, 6, 9, and 14 after treatments with ACA50s hydrogel formulations or blank alginate hydrogel vs control ((a)–(d)) (mean ± SD). P ≤ 0.05, compared with control or blank alginate hydrogel.

Standardized digital photographs of the wounds were taken with the same distance between camera and pre-anesthetized mouse, for each animal. The

photographs were examined using planimetry for objective evaluation for degree of wound healing (176). The total pixels that cover the unhealed areas were drawn onto the digital photographs using a pattern overlayin Image J, (Image J software, Wayne Rasband, National Institute of Health, Bethesda, MD, USA). The number of pixels covering an open wound area on a given day was divided by the number of pixels spreading over the initial wound on day 0 to obtain the percentage of closure. Percentage, rather than actual distance (e.g., mm), of wound closure was calculated from the measured wound areas (pixel density). This method allows more accurate measurements of the wounds, considering the fact that certain margin of errors during surgical procedures may exist among different experimental groups or even among the three mice within the same group (177).

As showed by the graph a, in which alginate and the control were compared, alginate is more effective than control at the third day already, obtaining an effective wound closure at the fourtheenth day. Graph b compares alginate without active and alginate plus Ac2-26 at the lowest concentration (0.1µM) and it shows that there is any significative difference between them. Graph c shows that Ac2-26 at the concentration of 0.5µM allows to control the wound closure better than alginate since third day, whereas the maximum concentratio (1µM) allows to obtain a complete wound closure at the 14° day (graph d). This can be explained by the FT-IR results, that show an extensive hydrogen bonding between alginate and peptide in a crowded environment such as the concentrated polymer solution demonstrated by the signal shift for COO^- groups in the loaded formulation. This phenomenon is more evident at low concentration, with a similar behavior between alginate and loaded alginate. When concentration is higher the activity of Ac2-26 is less influenced by alginate, with better results.

In conclusion, this study demonstrated that incorporating the ANXA1 mimetic peptide Ac2-26 in high M content alginate or LMW chitosan it is possible, obtaining an increase in peptide stability as well as a suitable dressing to avoid removal problems and living tissue dehydration over time considering viscosity, gel mid-value deswelling and dry state time point (120–132 h) of the hydrogels. FTIR studies supported by LC-MS results suggest a binding between the negatively charged portion of the peptide and the positive chitosan chain as an extensive hydrogen bonding between Ac2-26 and alginate that stabilizes the peptide when incorporated into the hydrogels. Such interactions are able to slow down peptide release from alginate and prevent its permeation from chitosan. *In vivo* tests, showed an acceleration of wound closure compared with the topical application of unloaded alginate (especially with 0.5 and 1 µM Ac2-26/alginate formulations) allowing 97% of wound closure at day 14th.

4.CONCLUSIONS

This project was focused on the production of innovative polymer based formulation able to promote wound healing.

The innovative technologies proposed were successfully applied for the production of *in situ* gelling formulations, both dry powders and aerogels.

Supercritical assisted atomization, applied for gentamicin, alginate and pectin powder formulations, demonstrated to be able to produce stable powders with uniform morphology and narrow size distribution, proper technological properties, useful for topical applications. Formulations showed to be able to overcome the hygroscopicity of the gentamicin stabilizing drug content and strongly reducing water uptake over time. Moreover, SAA formulations were able to efficiently contrast *S. aureus* and *P. aeruginosa* growth, till 24 days. The optimized process parameters produced reproducible results, particularly very high yields, without waste of energy and time and ebabling the recycling of CO_2.

The tandem technique prilling/SAE was optimized to obtain aerogels with desired size and narrow size distribution. Aerogels presented very high porosity as well as low density due to their nanoporous structure. Absorbance of large quantities of exhudates was promoted by these properties. In fact, aerogels were able to uptake wound fluids till 14 times their weight. A further optimization of tandem technique, using prilling in co-axial configuration, was applied for the production of core/shell aerogels loaded with doxycycline. These formulations showed very short gelation time uptaking large amount of exhudates, drug stability over time and were able to prolong drug release depending on the tuning of the alginate shell thickness.

Supercritical impregnation, tested at the Univerisity of Santiago de Compostela, was successfully applied for the loading of drugs into pre-formed aerogels, with high encapsulation efficiencies. Particles were characterized by high porosity and narrow size distribution. Good encapsulation efficiency was obtained particularly using ketoprofen at the tested impregnation conditions.

Nano spray drying was successfully applied to the formulations of nanopaticulate *in situ* gelling powders (≈ 350 nm diameter) by setting proper operative conditions.

This technique was applied for the production of alginate and pectin blend particles loaded with gentamicin, as well as for the production of a three components polymer blend (alginate, chitosan and amidated pectin) containing doxycycline. This technique allowed to obtain particles with uniform morphology, high yields and high encapsulation efficiencies. All formulations were able to control drug release rate *in vitro*, were able to overcome drug stability problems, even in harsh conditions and demonstrated enhanced antimicrobial activity over time on both *S. aureus* and *P. aeruginosa* strain.

Natural polymers chosen as carrier in this work showed to be very intersting for wound healing applications due to their intrinsic properties, such as biodegradability and biocompatibility, as well as the ability to induce the wound healing process by different mechanisms.

Because of their ability to encapsulate and protect active molecules from external environment, alginate and chitosan were tested also for the delivery of a macromolecule, Ac2-26 Annessin1-like N-terminal peptide, known for its ability to promote wound healing. Despite its instability at standard conditions, Ac2-26 encapsulated in alginate and chitosan hydrogels showed an increased stability at physiological conditions. Moreover, due to the drug/polymers interaction, formulations showed to be able to control drug release profiles up to 72h. Particularly alginate/Ac2-26 loaded formulation showed, *in vivo*, a very intersting activity, promoting complete wound closure on mice at the 14^{th} day of treatment reducing wound closure time up to 60%.

Interesting technological properties, such as good transpiration properties, proper adhesiveness, fluid uptake abilities make all the formulation produced in this work interesting devices able to overcome high costs, poor

conformability problems, occlusiveness and traumatic removal that characterize devices nowadays present on the market.

References

1. Martini FD, Nath JL. ANATOMIA & FISIOLOGIA. EdiSES, Napoli. 1994.
2. Slachta PA. Caring for chronic wounds: A knowledge update. Amer Nurse Today. 2008;3:27-35.
3. Hübner G, Brauchle M, Smola H, Madlener M, Fässler R, Werner S. DIFFERENTIAL REGULATION OF PRO-INFLAMMATORY CYTOKINES DURING WOUND HEALING IN NORMAL AND GLUCOCORTICOID-TREATED MICE. Cytokine. 1996;8(7):548-56.
4. Makela M, Salo T, Uitto V-J, Larjava H. Matrix metalloproteinases (MMP-2 and MMP-9) of the oral cavity: cellular origin and relationship to periodontal status. Journal of dental research. 1994;73(8):1397-406.
5. Tervo T, van Setten G-B, Päällysaho T, Tarkkanen A, Tervo K. Wound healing of the ocular surface. Annals of medicine. 1992;24(1):19-27.
6. Compton C, Gill J, Bradford D, Regauer S, Gallico G, O'connor N. Skin regenerated from cultured epithelial autografts on full-thickness burn wounds from 6 days to 5 years after grafting. A light, electron microscopic and immunohistochemical study. Laboratory investigation; a journal of technical methods and pathology. 1989;60(5):600-12.
7. Braunwald E, Fauci AS, Kasper DL, Hauser SL, Longo DL, Jameson JL. Harrison: medicina interna, 15ª edição: McGraw-Hill; 2002.
8. Arnold M, Barbul A. Nutrition and wound healing. Plastic and reconstructive surgery. 2006;117(7S):42S-58S.
9. Sen CK, Gordillo GM, Roy S, Kirsner R, Lambert L, Hunt TK, et al. Human skin wounds: a major and snowballing threat to public health and the economy. Wound repair and regeneration. 2009;17(6):763-71.
10. Hossain P, Kawar B, El Nahas M. Obesity and diabetes in the developing world—a growing challenge. New England journal of medicine. 2007;356(3):213-5.
11. Wang AS, Armstrong EJ, Armstrong AW. Corticosteroids and wound healing: clinical considerations in the perioperative period. The American journal of surgery. 2013;206(3):410-7.
12. Guo S, DiPietro LA. Factors affecting wound healing. Journal of dental research. 2010;89(3):219-29.
13. Howell-Jones R, Wilson M, Hill KE, Howard A, Price PE, Thomas DW. A review of the microbiology, antibiotic usage and resistance in chronic skin wounds. Journal of antimicrobial chemotherapy. 2005;55(2):143-9.
14. Bowler PG, Davies BJ. The microbiology of infected and noninfected leg ulcers. International journal of dermatology. 1999;38(8):573-8.
15. Hansson C, Hoborn J, Möller A, Swanbeck G. The microbial flora in venous leg ulcers without clinical signs of infection. Repeated culture using a validated standardised microbiological technique. Acta dermato-venereologica. 1995;75(1):24-30.
16. Brook I, Frazier EH. Aerobic and anaerobic microbiology of chronic venous ulcers. International journal of dermatology. 1998;37(6):426-8.

17. Bowler PG. The microbiology of acute and chronic wounds. Wounds. 1999;11:72-8.
18. Chantelau E. Bacterial population of chronic crural ulcers. VASA Zeitschrift für Gefässkrankheiten. 2000;29(2):156.
19. MacDonald YG, Hait H, Lipsky B, Zasloff M, Holroyd K. Microbiological profile of infected diabetic foot ulcers. Diabetic Medicine. 2002;19(12):1032-4.
20. Urbančič-Rovan V, Gubina M. Infection in superficial diabetic foot ulcers. Clinical infectious diseases. 1997;25(Supplement 2):S184-S5.
21. Madsen SM, Westh H, Danielsen L, Rosdahl VT. Bacterial colonization and healing of venous leg ulcers. Apmis. 1996;104(7-8):895-9.
22. Schraibman IG. The significance of beta-haemolytic streptococci in chronic leg ulcers. Annals of the Royal College of Surgeons of England. 1990;72(2):123.
23. Schmidt K, Debus E, Ziegler U, Thiede A. Bacterial population of chronic crural ulcers: is there a difference between the diabetic, the venous, and the arterial ulcer? VASA Zeitschrift für Gefässkrankheiten. 2000;29(1):62-70.
24. Kontiainen S, Rinne E. Bacteria in ulcera crurum. Acta dermato-venereologica. 1987;68(3):240-4.
25. Margolis DJ, Knauss J, Bilker W, Baumgarten M. Medical conditions as risk factors for pressure ulcers in an outpatient setting. Age and ageing. 2003;32(3):259-64.
26. Gottrup F. A specialized wound-healing center concept: importance of a multidisciplinary department structure and surgical treatment facilities in the treatment of chronic wounds. The American journal of surgery. 2004;187(5):S38-S43.
27. Crovetti G, Martinelli G, Issi M, Barone M, Guizzardi M, Campanati B, et al. Platelet gel for healing cutaneous chronic wounds. Transfusion and Apheresis Science. 2004;30(2):145-51.
28. Epstein FH, Singer AJ, Clark RA. Cutaneous wound healing. New England journal of medicine. 1999;341(10):738-46.
29. Gottrup F, Holstein P, Jørgensen B, Lohmann M, Karlsmar T. A new concept of a multidisciplinary wound healing center and a national expert function of wound healing. Archives of Surgery. 2001;136(7):765-72.
30. Callam M, Harper D, Dale J, Ruckley C. Chronic leg ulceration: socio-economic aspects. Scottish medical journal. 1988;33(6):358-60.
31. Bergemann R, Lauterbach KW, Vanscheidt W, Neander K-D, Engst R. Economic evaluation of the treatment of chronic wounds. Pharmacoeconomics. 1999;16(4):367-77.
32. Lepow BD, Downey M, Yurgelon J, Klassen L, Armstrong DG. Bioengineered tissues in wound healing: a progress report. Expert Review of Dermatology. 2011;6(3):255-62.
33. Margolisa DJ, Bilkerb W, Santannab J. Venous leg ulcer: incidence and prevalence in the elderly. Journal of the American Academy of Dermatology. 2002;46(3):381-6.

34. Thomas DR, Rodeheaver GT, Bartolucci AA, Franz RA, Sussman C, Ferrell BA, et al. Pressure Ulcer Scale for Healing: Derivation and Validation of the PUSH Tool: The PUSH Task Force. Advances in Skin & Wound Care. 1997;10(5):96-101.
35. Jull A, Waters J, Arroll B. Pentoxifylline for treating venous leg ulcers. The Cochrane Library. 2002.
36. Scallon C, Bell-Syer S, Aziz Z. Flavonoids for treating venous leg ulcers. Cochrane Database Syst Rev. 2013;5.
37. Langer G, Schloemer G, Knerr A, Kuss O, Behrens J. Nutritional interventions for preventing and treating pressure ulcers. Cochrane Database Syst Rev. 2003;4(4).
38. McInnes E, Dumville JC, Jammali-Blasi A, Bell-Syer S. Support surfaces for treating pressure ulcers. Cochrane Database Syst Rev. 2011;12.
39. Kranke P, Bennett M, Roeckl-Wiedmann I, Debus S. Hyperbaric oxygen therapy for chronic wounds. Cochrane Database Syst Rev. 2004;2(2).
40. Cruciani M, Lipsky BA, Mengoli C, de Lalla F. Granulocyte-colony stimulating factors as adjunctive therapy for diabetic foot infections. Cochrane Database Syst Rev. 2009;3.
41. Sarabahi S. Recent advances in topical wound care. Indian journal of plastic surgery: official publication of the Association of Plastic Surgeons of India. 2012;45(2):379.
42. Saffle J, Schnebly W. Burn wound care. Burn care and rehabilitation–principles and practice Philadelphia: FA Davies. 1994:105-18.
43. Drosou A, Falabella A, Kirsner RS. Antiseptics on wounds: an area of controversy. Wounds. 2003;15(5):149-66.
44. Dorner B, Posthauer M, Thomas D. European Pressure Ulcer Advisory Panel and National Pressure Ulcer Advisory Panel. Role of Nutrition in Pressure Ulcer Healing Clinical Practice Guideline. 2009.
45. Keast DH, Parslow N, Houghton PE, Norton L, Fraser C. Best practice recommendations for the prevention and treatment of pressure ulcers: update 2006. Advances in Skin & Wound Care. 2007;20(8):447-60.
46. Custer J, Edlich RF, Prusak M, Madden J, Panek P, Wangensteen OH. Studies in the management of the contaminated wound: V. An assessment of the effectiveness of pHisoHex and Betadine surgical scrub solutions. The American journal of surgery. 1971;121(5):572-5.
47. Tatnall F, Leigh I, Gibson J. (2) Comparative toxicity of antimicrobial agents on transformed human keratinocytes. British Journal of Dermatology. 1987;117(s32):31-2.
48. Antisepsi M. disinfezione in ambito sanitario e socio-sanitario Guida a cura di Maria Mongardi et al. Agenzia Sanitaria e Sociale della Regione Emilia Romagna Bologna, aprile. 2011.
49. Alfano C, Angelisanti M, Calzoni C, Somma F, Chiummariello S. Trattamento delle ulcere e delle ferite difficili dell'arto inferiore. Ann Ital Chir. 2012;83(2):135-41.
50. De Cicco F, Reverchon E, Adami R, Auriemma G, Russo P, Calabrese EC, et al. In situ forming antibacterial dextran blend hydrogel for wound dressing: SAA technology vs. spray drying. Carbohydrate Polymers. 2014;101:1216-24.

51. García-González CA, Jin M, Gerth J, Alvarez-Lorenzo C, Smirnova I. Polysaccharide-based aerogel microspheres for oral drug delivery. Carbohydrate Polymers. 2015;117:797-806.
52. Placin F, Desvergne J-P, Cansell F. Organic low molecular weight aerogel formed in supercritical fluids. Journal of Materials Chemistry. 2000;10(9):2147-9.
53. Mallepally RR, Bernard I, Marin MA, Ward KR, McHugh MA. Superabsorbent alginate aerogels. The Journal of Supercritical Fluids. 2013;79:202-8.
54. Lutolf M, Hubbell J. Synthetic biomaterials as instructive extracellular microenvironments for morphogenesis in tissue engineering. Nature biotechnology. 2005;23(1):47-55.
55. Martins M, Barros AA, Quraishi S, Gurikov P, Raman S, Smirnova I, et al. Preparation of macroporous alginate-based aerogels for biomedical applications. The Journal of Supercritical Fluids. 2015.
56. Oledzka E, Sobczak M. Polymers in the pharmaceutical applications-natural and bioactive initiators and catalysts in the synthesis of biodegradable and bioresorbable polyesters and polycarbonates: INTECH Open Access Publisher; 2012.
57. Kumar MR, Muzzarelli RA, Muzzarelli C, Sashiwa H, Domb A. Chitosan chemistry and pharmaceutical perspectives. Chemical reviews. 2004;104(12):6017-84.
58. Porporatto C, Bianco ID, Riera CM, Correa SG. Chitosan induces different L-arginine metabolic pathways in resting and inflammatory macrophages. Biochemical and biophysical research communications. 2003;304(2):266-72.
59. Rubinstein A, Radai R, Ezra M, Pathak S, Rokem JS. In vitro evaluation of calcium pectinate: a potential colon-specific drug delivery carrier. Pharmaceutical research. 1993;10(2):258-63.
60. Lootens D, Capel F, Durand D, Nicolai T, Boulenguer P, Langendorff V. Influence of pH, Ca concentration, temperature and amidation on the gelation of low methoxyl pectin. Food Hydrocolloids. 2003;17(3):237-44.
61. Thomas A, Harding K, Moore K. Alginates from wound dressings activate human macrophages to secrete tumour necrosis factor-α. Biomaterials. 2000;21(17):1797-802.
62. Pitt CG, Hendren W. Polyoxymethylene-oxyethylene copolymers in conjuction with biomolecules. Google Patents; 1995.
63. Siparsky GL, Voorhees KJ, Dorgan JR, Schilling K. Water transport in polylactic acid (PLA), PLA/polycaprolactone copolymers, and PLA/polyethylene glycol blends. Journal of Environmental Polymer Degradation. 1997;5(3):125-36.
64. Bittiger H, Marchessault R, Niegisch W. Crystal structure of poly-ε-caprolactone. Acta Crystallographica Section B: Structural Crystallography and Crystal Chemistry. 1970;26(12):1923-7.
65. Brunner IG. Properties of Supercritical and Near-Critical Gases and of Mixtures with Sub-and Supercritical Components. Gas Extraction: Springer; 1994. p. 3-57.

66. Reverchon E, Adami R, Cardea S, Della Porta G. Supercritical fluids processing of polymers for pharmaceutical and medical applications. The Journal of Supercritical Fluids. 2009;47(3):484-92.
67. Reverchon E, Pisanti P, Cardea S. Nanostructured PLLA− Hydroxyapatite Scaffolds Produced by a Supercritical Assisted Technique. Industrial & Engineering Chemistry Research. 2009;48(11):5310-6.
68. Kakumanu VK, Bansal AK. Supercritical fluid technology in pharmaceutical research. Crips. 2003;4(83):8-12.
69. Hannay J, Hogarth J. On the solubility of solids in gases. Proceedings of the royal society of London. 1879;30(200-205):178-88.
70. Reverchon E, Marrone C. Modeling and simulation of the supercritical CO 2 extraction of vegetable oils. The Journal of Supercritical Fluids. 2001;19(2):161-75.
71. Cardea S, Sessa M, Reverchon E. Supercritical CO 2 assisted formation of poly (vinylidenefluoride) aerogels containing amoxicillin, used as controlled release device. The Journal of Supercritical Fluids. 2011;59:149-56.
72. Al-Musa S, Fara DA, Badwan A. Evaluation of parameters involved in preparation and release of drug loaded in crosslinked matrices of alginate. Journal of Controlled Release. 1999;57(3):223-32.
73. Alnaief M, Alzaitoun M, García-González C, Smirnova I. Preparation of biodegradable nanoporous microspherical aerogel based on alginate. Carbohydrate Polymers. 2011;84(3):1011-8.
74. Adami R, Reverchon E. Composite polymer-Fe 3 O 4 microparticles for biomedical applications, produced by supercritical assisted atomization. Powder Technology. 2012;218:102-8.
75. Del Gaudio P, Auriemma G, Mencherini T, Porta GD, Reverchon E, Aquino RP. Design of alginate-based aerogel for nonsteroidal anti-inflammatory drugs controlled delivery systems using prilling and supercritical-assisted drying. Journal of pharmaceutical sciences. 2013;102(1):185-94.
76. Costa VP, Braga ME, Guerra JP, Duarte AR, Duarte CM, Leite EO, et al. Development of therapeutic contact lenses using a supercritical solvent impregnation method. The Journal of Supercritical Fluids. 2010;52(3):306-16.
77. Smirnova I, Suttiruengwong S, Arlt W. Feasibility study of hydrophilic and hydrophobic silica aerogels as drug delivery systems. Journal of Non-Crystalline Solids. 2004;350:54-60.
78. Tang C, Guan Y-X, Yao S-J, Zhu Z-Q. Preparation of ibuprofen-loaded chitosan films for oral mucosal drug delivery using supercritical solution impregnation. International journal of pharmaceutics. 2014;473(1):434-41.
79. González-Chomón C, Braga ME, de Sousa HC, Concheiro A, Alvarez-Lorenzo C. Antifouling foldable acrylic IOLs loaded with norfloxacin by aqueous soaking and by supercritical carbon dioxide technology. European Journal of Pharmaceutics and Biopharmaceutics. 2012;82(2):383-91.
80. Duarte ARC, Simplicio AL, Vega-González A, Subra-Paternault P, Coimbra P, Gil M, et al. Supercritical fluid impregnation of a biocompatible polymer for ophthalmic drug delivery. The Journal of Supercritical Fluids. 2007;42(3):373-7.

81. Yu J-P, Guan Y-X, Yao S-J, Zhu Z-Q. Preparation of roxithromycin-loaded poly (l-lactic acid) films with supercritical solution impregnation. Industrial & Engineering Chemistry Research. 2011;50(24):13813-8.
82. Yokozaki Y, Sakabe J, Ng B, Shimoyama Y. Effect of temperature, pressure and depressurization rate on release profile of salicylic acid from contact lenses prepared by supercritical carbon dioxide impregnation. Chemical Engineering Research and Design. 2015;100:89-94.
83. Brandenberger H, Widmer F. A new multinozzle encapsulation/immobilisation system to produce uniform beads of alginate. Journal of Biotechnology. 1998;63(1):73-80.
84. Sakai T, Hoshino N. PRODUCTION OF UNIFORM DROPLETS BY LONGI-TUDINAL VIBRATION OF AUDIO FREQUENCY. Journal of Chemical Engineering of Japan. 1980;13(4):263-8.
85. Desmond C, Stanton C, Fitzgerald GF, Collins K, Ross RP. Environmental adaptation of probiotic lactobacilli towards improvement of performance during spray drying. International Dairy Journal. 2001;11(10):801-8.
86. Broadhead J, Rouan SE, Hau I, Rhodes C. The Effect of Process and Formulation Variables on the Properties of Spray-dried β-Galactosidase. Journal of pharmacy and pharmacology. 1994;46(6):458-67.
87. Labrude P, Rasolomanana M, Vigneron C, Thirion C, Chaillot B. Protective effect of sucrose on spray drying of oxyhemoglobin. Journal of pharmaceutical sciences. 1989;78(3):223-9.
88. Maury M, Murphy K, Kumar S, Shi L, Lee G. Effects of process variables on the powder yield of spray-dried trehalose on a laboratory spray-dryer. European Journal of Pharmaceutics and Biopharmaceutics. 2005;59(3):565-73.
89. Bloor M, Ingham D. On the efficiency of the industrial cyclone. Trans Inst Chem Eng. 1973;51:173-6.
90. Chan H-K, Kwok PCL. Production methods for nanodrug particles using the bottom-up approach. Advanced drug delivery reviews. 2011;63(6):406-16.
91. Lee SH, Heng D, Ng WK, Chan H-K, Tan RB. Nano spray drying: a novel method for preparing protein nanoparticles for protein therapy. International journal of pharmaceutics. 2011;403(1):192-200.
92. Schafroth N, Arpagaus C, Jadhav UY, Makne S, Douroumis D. Nano and microparticle engineering of water insoluble drugs using a novel spray-drying process. Colloids and Surfaces B: Biointerfaces. 2012;90:8-15.
93. Dung TH, Lee S-R, Han S-D, Kim S-J, Ju Y-M, Kim M-S, et al. Chitosan-TPP nanoparticle as a release system of antisense oligonucleotide in the oral environment. Journal of nanoscience and nanotechnology. 2007;7(11):3695-9.
94. Korting HC, Hübner K, Greiner K, Hamm G, Braun-Falco O. Differences in the skin surface pH and bacterial microflora due to the long-term application of synthetic detergent preparations of pH 5.5 and pH 7.0. Results of a crossover trial in healthy volunteers. Acta dermato-venereologica. 1989;70(5):429-31.

95. De Cicco F, Porta A, Sansone F, Aquino RP, Del Gaudio P. Nanospray technology for an in situ gelling nanoparticulate powder as a wound dressing. International journal of pharmaceutics. 2014;473(1):30-7.
96. Wikler MA, Cockerill FR. Clinical and Laboratory Standards Institute. Performance Standards for Antimicrobial Susceptibility Testing: Eighteenth Informational Supplement Wayne: Clinical and Laboratory Standards Institute. 2008.
97. Gainotti A, Losi E, Colombo P, Santi P, Sonvico F, Baroni D, et al. The effect of residual water on antacid properties of sucralfate gel dried by microwaves. AAPS PharmSciTech. 2006;7(1):E58-E63.
98. Sansone F, Aquino R, Del Gaudio P, Colombo P, Russo P. Physical characteristics and aerosol performance of naringin dry powders for pulmonary delivery prepared by spray-drying. European Journal of Pharmaceutics and Biopharmaceutics. 2009;72(1):206-13.
99. Aquino RP, Auriemma G, Mencherini T, Russo P, Porta A, Adami R, et al. Design and production of gentamicin/dextrans microparticles by supercritical assisted atomisation for the treatment of wound bacterial infections. International journal of pharmaceutics. 2013;440(2):188-94.
100. Schmid K, Arpagaus C, Friess W. Evaluation of the Nano Spray Dryer B-90 for pharmaceutical applications. Pharmaceutical Development and Technology. 2011;16(4):287-94.
101. Tolman RC. The effect of droplet size on surface tension. The journal of chemical physics. 1949;17(3):333-7.
102. Nandiyanto ABD, Okuyama K. Progress in developing spray-drying methods for the production of controlled morphology particles: from the nanometer to submicrometer size ranges. Advanced Powder Technology. 2011;22(1):1-19.
103. Shaw F. Spray drying: a traditional process for advanced applications. American Ceramic Society Bulletin. 1990;69(9):1484-9.
104. Süverkrüp R, Eggerstedt SN, Gruner K, Kuschel M, Sommerfeld M, Lamprecht A. Collisions in fast droplet streams for the production of spherolyophilisates. European Journal of Pharmaceutical Sciences. 2013;49(4):535-41.
105. Iannuccelli V, Montanari M, Bertelli D, Pellati F, Coppi G. Microparticulate polyelectrolyte complexes for gentamicin transport across intestinal epithelia. Drug delivery. 2011;18(1):26-37.
106. Bolton L, Monte K, Pirone L. Moisture and healing: beyond the jargon. Ostomy/wound management. 2000;46(1A Suppl):51S-62S; quiz 3S-4S.
107. Li Q, Rudolph V, Peukert W. London-van der Waals adhesiveness of rough particles. Powder Technology. 2006;161(3):248-55.
108. Kokabi M, Sirousazar M, Hassan ZM. PVA–clay nanocomposite hydrogels for wound dressing. European Polymer Journal. 2007;43(3):773-81.
109. Balakrishnan B, Mohanty M, Umashankar P, Jayakrishnan A. Evaluation of an in situ forming hydrogel wound dressing based on oxidized alginate and gelatin. Biomaterials. 2005;26(32):6335-42.

110. Queen D, Gaylor J, Evans J, Courtney J, Reid W. The preclinical evaluation of the water vapour transmission rate through burn wound dressings. Biomaterials. 1987;8(5):367-71.
111. Cohen S, Lobel E, Trevgoda A, Peled Y. A novel in situ-forming ophthalmic drug delivery system from alginates undergoing gelation in the eye. Journal of Controlled Release. 1997;44(2):201-8.
112. Auriemma G, Del Gaudio P, Barba AA, d'Amore M, Aquino RP. A combined technique based on prilling and microwave assisted treatments for the production of ketoprofen controlled release dosage forms. International journal of pharmaceutics. 2011;415(1):196-205.
113. Sakka S. Sol-gel technology as reflected in journal of sol-gel science and technology. Journal of sol-gel science and technology. 2003;26(1-3):29-33.
114. Zha J, Roggendorf H. Sol–gel science, the physics and chemistry of sol–gel processing, Ed. by CJ Brinker and GW Scherer, Academic Press, Boston 1990, xiv, 908 pp., bound—ISBN 0-12-134970-5. Advanced materials. 1991;3(10):522-.
115. Matia-Merino L, Lau K, Dickinson E. Effects of low-methoxyl amidated pectin and ionic calcium on rheology and microstructure of acid-induced sodium caseinate gels. Food Hydrocolloids. 2004;18(2):271-81.
116. Anumolu SS, DeSantis AS, Menjoge AR, Hahn RA, Beloni JA, Gordon MK, et al. Doxycycline loaded poly (ethylene glycol) hydrogels for healing vesicant-induced ocular wounds. Biomaterials. 2010;31(5):964-74.
117. Simonetti O, Cirioni O, Lucarini G, Orlando F, Ghiselli R, Silvestri C, et al. Tigecycline accelerates staphylococcal-infected burn wound healing through matrix metalloproteinase-9 modulation. Journal of antimicrobial chemotherapy. 2012;67(1):191-201.
118. Injac R, Djordjevic-Milic V, Srdjenovic B. Thermostability testing and degradation profiles of doxycycline in bulk, tablets, and capsules by HPLC. Journal of chromatographic science. 2007;45(9):623-8.
119. Champion JA, Katare YK, Mitragotri S. Particle shape: a new design parameter for micro-and nanoscale drug delivery carriers. Journal of Controlled Release. 2007;121(1):3-9.
120. Meaume S, Vallet D, Nguyen Morere M, Téot L. Evaluation of a silver-releasing hydroalginate dressing in chronic wounds with signs of local infection. Journal of wound care. 2005;14(9):411-9.
121. Berger J, Reist M, Mayer JM, Felt O, Peppas N, Gurny R. Structure and interactions in covalently and ionically crosslinked chitosan hydrogels for biomedical applications. European Journal of Pharmaceutics and Biopharmaceutics. 2004;57(1):19-34.
122. Kickhöfen B, Wokalek H, Scheel D, Ruh H. Chemical and physical properties of a hydrogel wound dressing. Biomaterials. 1986;7(1):67-72.
123. Thu H-E, Zulfakar MH, Ng S-F. Alginate based bilayer hydrocolloid films as potential slow-release modern wound dressing. International journal of pharmaceutics. 2012;434(1):375-83.

124. Hennink W, Van Nostrum CF. Novel crosslinking methods to design hydrogels. Advanced drug delivery reviews. 2012;64:223-36.
125. Peppas N, Bures P, Leobandung W, Ichikawa H. Hydrogels in pharmaceutical formulations. European Journal of Pharmaceutics and Biopharmaceutics. 2000;50(1):27-46.
126. Ratner B, Hoffman A. Thin films, grafts, and coatings. Academic Press, San Diego; 1996. p. 105.
127. Forge A, Schacht J. Aminoglycoside antibiotics. Audiology and Neurotology. 2000;5(1):3-22.
128. Ahmed RM, Hannigan IP, MacDougall HG, Chan RC, Michael Halmagyi G. Gentamicin ototoxicity: a 23-year selected case series of 103 patients. Medical Journal of Australia. 2012;196(11):701.
129. Ali B. Gentamicin nephrotoxicity in humans and animals: some recent research. General Pharmacology: The Vascular System. 1995;26(7):1477-87.
130. Aviv M, Berdicevsky I, Zilberman M. Gentamicin-loaded bioresorbable films for prevention of bacterial infections associated with orthopedic implants. Journal of Biomedical Materials Research Part A. 2007;83(1):10-9.
131. Porta GD, Adami R, Del Gaudio P, Prota L, Aquino R, Reverchon E. Albumin/gentamicin microspheres produced by supercritical assisted atomization: optimization of size, drug loading and release. Journal of pharmaceutical sciences. 2010;99(11):4720-9.
132. Zalavras CG, Patzakis MJ, Holtom P. Local antibiotic therapy in the treatment of open fractures and osteomyelitis. Clinical orthopaedics and related research. 2004;427:86-93.
133. Tripp C, Combes J. Chemical modification of metal oxide surfaces in supercritical CO2: The interaction of supercritical CO2 with the adsorbed water layer and the surface hydroxyl groups of a silica surface. Langmuir. 1998;14(26):7348-52.
134. George M, Abraham T. pH sensitive alginate–guar gum hydrogel for the controlled delivery of protein drugs. International journal of pharmaceutics. 2007;335(1):123-9.
135. Gong R, Li C, Zhu S, Zhang Y, Du Y, Jiang J. A novel pH-sensitive hydrogel based on dual crosslinked alginate/N-α-glutaric acid chitosan for oral delivery of protein. Carbohydrate Polymers. 2011;85(4):869-74.
136. García-González C, Alnaief M, Smirnova I. Polysaccharide-based aerogels—Promising biodegradable carriers for drug delivery systems. Carbohydrate Polymers. 2011;86(4):1425-38.
137. Chiu H-Y, Lee M-J, Lin H-m. Vapor− Liquid Phase Boundaries of Binary Mixtures of Carbon Dioxide with Ethanol and Acetone. Journal of Chemical & Engineering Data. 2008;53(10):2393-402.
138. Daniel C, Alfano D, Venditto V, Cardea S, Reverchon E, Larobina D, et al. Aerogels with a microporous crystalline host phase. Advanced materials. 2005;17(12):1515-8.

139. Caputo G, De Marco I, Reverchon E. Silica aerogel–metal composites produced by supercritical adsorption. The Journal of Supercritical Fluids. 2010;54(2):243-9.
140. Cardea S, Pisanti P, Reverchon E. Generation of chitosan nanoporous structures for tissue engineering applications using a supercritical fluid assisted process. The Journal of Supercritical Fluids. 2010;54(3):290-5.
141. Falco N, Reverchon E, Della Porta G. Continuous supercritical emulsions extraction: Packed tower characterization and application to poly (lactic-co-glycolic acid)+ insulin microspheres production. Industrial & Engineering Chemistry Research. 2012;51(25):8616-23.
142. Porta GD, Falco N, Reverchon E. Continuous supercritical emulsions extraction: a new technology for biopolymer microparticles production. Biotechnology and bioengineering. 2011;108(3):676-86.
143. Campardelli R, Adami R, Della Porta G, Reverchon E. Nanoparticle precipitation by supercritical assisted injection in a liquid antisolvent. Chemical Engineering Journal. 2012;192:246-51.
144. Reverchon E, Caputo G, Correra S, Cesti P. Synthesis of titanium hydroxide nanoparticles in supercritical carbon dioxide on the pilot scale. The Journal of Supercritical Fluids. 2003;26(3):253-61.
145. Del Gaudio P, Auriemma G, Russo P, Mencherini T, Campiglia P, Stigliani M, et al. Novel co-axial prilling technique for the development of core–shell particles as delayed drug delivery systems. European Journal of Pharmaceutics and Biopharmaceutics. 2014;87(3):541-7.
146. Thomas A, Harding KG, Moore K. Alginates from wound dressings activate human macrophages to secrete tumour necrosis factor-α. Biomaterials. 2000;21(17):1797-802.
147. Anumolu SS, DeSantis AS, Menjoge AR, Hahn RA, Beloni JA, Gordon MK, et al. Doxycycline loaded poly(ethylene glycol) hydrogels for healing vesicant-induced ocular wounds. Biomaterials. 2010;31(5):964-74.
148. Chiu H-Y, Lee M-J, Lin H-m. Vapor−Liquid Phase Boundaries of Binary Mixtures of Carbon Dioxide with Ethanol and Acetone. Journal of Chemical & Engineering Data. 2008;53(10):2393-402.
149. Della Porta G, Del Gaudio P, De Cicco F, Aquino RP, Reverchon E. Supercritical Drying of Alginate Beads for the Development of Aerogel Biomaterials: Optimization of Process Parameters and Exchange Solvents. Industrial & Engineering Chemistry Research. 2013;52(34):12003-9.
150. Veronovski A, Tkalec G, Knez Ž, Novak Z. Characterisation of biodegradable pectin aerogels and their potential use as drug carriers. Carbohydrate Polymers. 2014;113:272-8.
151. He Z-x, Wang Z-h, Zhang H-h, Pan X, Su W-r, Liang D, et al. Doxycycline and hydroxypropyl-β-cyclodextrin complex in poloxamer thermal sensitive hydrogel for ophthalmic delivery. Acta Pharmaceutica Sinica B. 2011;1(4):254-60.

152. Del Gaudio P, Russo P, Lauro MR, Colombo P, Aquino RP. Encapsulation of ketoprofen and ketoprofen lysinate by prilling for controlled drug release. AAPS PharmSciTech. 2009;10(4):1178-85.
153. Papageorgiou SK, Kouvelos EP, Favvas EP, Sapalidis AA, Romanos GE, Katsaros FK. Metal–carboxylate interactions in metal–alginate complexes studied with FTIR spectroscopy. Carbohydrate research. 2010;345(4):469-73.
154. Lee KY, Rowley JA, Eiselt P, Moy EM, Bouhadir KH, Mooney DJ. Controlling mechanical and swelling properties of alginate hydrogels independently by cross-linker type and cross-linking density. Macromolecules. 2000;33(11):4291-4.
155. Ritger PL, Peppas NA. A simple equation for description of solute release II. Fickian and anomalous release from swellable devices. Journal of Controlled Release. 1987;5(1):37-42.
156. Del Gaudio P, De Cicco F, Sansone F, Aquino RP, Adami R, Ricci M, et al. Alginate beads as a carrier for omeprazole/SBA-15 inclusion compound: A step towards the development of personalized paediatric dosage forms. Carbohydrate Polymers. 2015;133:464-72.
157. Chim R, Marceneiro S, Braga ME, Dias AM, de Sousa HC. Solubility of norfloxacin and ofloxacin in supercritical carbon dioxide. Fluid Phase Equilibria. 2012;331:6-11.
158. Sabegh MA, Rajaei H, Esmaeilzadeh F, Lashkarbolooki M. Solubility of ketoprofen in supercritical carbon dioxide. The Journal of Supercritical Fluids. 2012;72:191-7.
159. García-González CA, Alnaief M, Smirnova I. Polysaccharide-based aerogels—Promising biodegradable carriers for drug delivery systems. Carbohydrate Polymers. 2011;86(4):1425-38.
160. Hirshberg J, Coleman J, Marchant B, Rees RS. TGF-β3 in the treatment of pressure ulcers: a preliminary report. Advances in Skin & Wound Care. 2001;14(2):91-5.
161. LeGrand EK. Preclinical promise of becaplermin (rhPDGF-BB) in wound healing. The American journal of surgery. 1998;176(2):48S-54S.
162. Margolis DJ, Crombleholme T, Herlyn M. Clinical Protocol: Phase I trial to evaluate the safety of H5. 020CMV. PDGF-B for the treatment of a diabetic insensate foot ulcer. Wound repair and regeneration. 2000;8(6):480-93.
163. Chéret J, Lebonvallet N, Carré JL, Misery L, Gall-Ianotto L. Role of neuropeptides, neurotrophins, and neurohormones in skin wound healing. Wound repair and regeneration. 2013;21(6):772-88.
164. Gerke V, Moss SE. Annexins: from structure to function. Physiological reviews. 2002;82(2):331-71.
165. Perretti M, Dalli J. Exploiting the Annexin A1 pathway for the development of novel anti-inflammatory therapeutics. British journal of pharmacology. 2009;158(4):936-46.
166. Katanaev V. Signal transduction in neutrophil chemotaxis. Biochemistry (Moscow). 2001;66(4):351-68.

167. Babbin BA, Lee WY, Parkos CA, Winfree LM, Akyildiz A, Perretti M, et al. Annexin I regulates SKCO-15 cell invasion by signaling through formyl peptide receptors. Journal of Biological Chemistry. 2006;281(28):19588-99.
168. Bizzarro V, Belvedere R, Dal Piaz F, Parente L, Petrella A. Annexin A1 induces skeletal muscle cell migration acting through formyl peptide receptors. 2012.
169. Bizzarro V, Fontanella B, Carratu A, Belvedere R, Marfella R, Parente L, et al. Annexin A1 N-terminal derived peptide Ac2-26 stimulates fibroblast migration in high glucose conditions. 2012.
170. Minagawa T, Okamura Y, Shigemasa Y, Minami S, Okamoto Y. Effects of molecular weight and deacetylation degree of chitin/chitosan on wound healing. Carbohydrate Polymers. 2007;67(4):640-4.
171. Piotto S, Di Biasi L, Concilio S, Castiglione A, Cattaneo G. GRIMD: distributed computing for chemists and biologists. Bioinformation. 2014;10(1):43.
172. Scrima M, Di Marino S, Grimaldi M, Campana F, Vitiello G, Piotto SP, et al. Structural features of the C8 antiviral peptide in a membrane-mimicking environment. Biochimica et Biophysica Acta (BBA)-Biomembranes. 2014;1838(3):1010-8.
173. Şen M, Güven O. Dynamic deswelling studies of poly (N-vinyl-2-pyrrolidone/itaconic acid) hydrogels swollen in water and terbinafine hydrochloride solutions. European Polymer Journal. 2002;38(4):751-7.
174. Perretti M, Chiang N, La M, Fierro IM, Marullo S, Getting SJ, et al. Endogenous lipid-and peptide-derived anti-inflammatory pathways generated with glucocorticoid and aspirin treatment activate the lipoxin A4 receptor. Nature medicine. 2002;8(11):1296-302.
175. Teixeira RAP, Mimura KKO, Araujo LP, Greco KV, Oliani SM. The essential role of annexin A1 mimetic peptide in the skin allograft survival. Journal of tissue engineering and regenerative medicine. 2013.
176. Woodley DT, Remington J, Huang Y, Hou Y, Li W, Keene DR, et al. Intravenously injected human fibroblasts home to skin wounds, deliver type VII collagen, and promote wound healing. Molecular Therapy. 2007;15(3):628-35.
177. Cheng C-F, Sahu D, Tsen F, Zhao Z, Fan J, Kim R, et al. A fragment of secreted Hsp90α carries properties that enable it to accelerate effectively both acute and diabetic wound healing in mice. The Journal of clinical investigation. 2012;122(2):779.

APPENDIX 1

LIST OF PUBLICATIONS

Papers

- Giovanna Della Porta, Pasquale Del Gaudio, **Felicetta De Cicco**, Rita P. Aquino and Ernesto Reverchon, Supercritical drying of alginate beads for the development of aerogel biomaterials: optimization of process parameters and exchange solvents. Industrial and Engineering Chemistry Research V. No 52, 31 July 2013, pp 12003-12009.

- **Felicetta De Cicco**, Ernesto Reverchon, Renata Adami, Giulia Auriemma, Paola Russo, Elena C. Calabrese, Amalia Porta, Rita P. Aquino, Pasquale Del Gaudio, *In situ* forming antibacterial dextran blend hydrogel, for wound dressing: SAA technology vs Spray drying, Carbohydrate Polymers, V. No 101,30 January 2014, pages 1216-1224.

- **Felicetta De Cicco**, Amalia Porta, Francesca Sansone, Rita P. Aquino, Pasquale Del Gaudio *, Nanospray technology for an in situ gelling nanoparticulate powder as a wound dressing, International Journal of Pharmaceutics, V. No 473, 2014, pages 30-37.

- Pasquale Del Gaudio, **Felicetta De Cicco**, Rita P Aquino, Patrizia Picerno, Paola Russo, Fabrizio Dal Piaz, Valentina Bizzarro, Raffaella Belvedere, Luca Parente, Antonello Petrella, Evaluation of in situ injectable hydrogels as controlled release device for ANXA1 derived peptide in wound healing, Carbohydrate polymers V. No 115, 2015 pages 629-635.

- Pasquale Del Gaudio, **Felicetta De Cicco**, Francesca Sansone, Rita Patrizia Aquino, Renata Adami, Maurizio Ricci, Stefano Giovagnoli,

Alginate beads as a carrier for Omeprazole/SBA-15 inclusion compound: a step towards the development of personalized paediatric dosage forms, Carbohydrate polymers, V. No 133, 2015, pages 464-472.

Presentation at conferences

- **F. De Cicco**, G. Auriemma, G. Della Porta, E. Reverchon, Paola Russo, R.P. Aquino, P. Del Gaudio, Design of Alginate-Based Aerogel for Nonsteroidal Anti-Inflammatory Drugs Controlled Delivery Systems Using Prilling and Supercritical-Assisted Drying. 7° AItUN Meeting, New frontiers in living cell encapsulation, 8-9 March 2013, University of Perugia.
- **Felicetta De Cicco**, Mariagrazia Torello, Rita Patrizia Aquino, Pasquale Del Gaudio, Dextrans nanoparticulate powder for in situ gel forming wound dressing, Bionam 2013- 1° international workshop on nanobiomaterials,18 October 2013, University of Salerno.
- Pasquale Del Gaudio, **Felicetta De Cicco**, Paola Russo, Rita Patrizia Aquino, PLGA micro-nanoparticulate systems obtained by laminar jet break-up and solvent evaporation technologies, Bionam 2013- 1° international workshop on nanobiomaterials,18 October 2013, University of Salerno
- **F. De Cicco**, G. Auriemma, Paola Russo, R.P. Aquino, P. Del Gaudio, Design of NSAIDs pulsatile delivery systems based on prilling co-axial technique, 3rd Conference on "Innovation in Drug delivery: Advances in local drug delivery", 22-25 September 2013, Pisa.

- **Felicetta De Cicco**, Ernesto Reverchon, Renata Adami, Amalia Porta, Paola Russo, Rita P. Aquino, Pasquale Del Gaudio. In situ forming antibacterial dextran blend hydrogel, for wound dressing: SAA technology vs Spray drying, oral presentation, Doctoral school- "summer school- Materials for pharmaceutical applications: chemic-physical and technological characterization", XIII Ed., Arcavacata di Rende 8-12 September 2013.

- **F. De Cicco**, S. Giovagnoli, M. Ricci, R. P. Aquino, P. Del Gaudio, Omeprazole/Sba-15 Mesoporous Silicate Compound Embedded In Alginate Beads: A Novel Versatile Gastro-Resistant Paediatric Formulation. AItUN Annual Meeting, Medicine's for children's safe: challenges and opportunities, 6 -7 March 2014, University of Pavia.

- **De Cicco F**, Scutiero L, Reverchon E, Aquino R P, Della Porta G, Del Gaudio P, Formulazione Di Aerogel Di Alginato Attraverso Il Drying Supercritico, Pharmacy and Medicine days, 22-23 May 2014, University of Salerno.

- Del Gaudio P, **De Cicco F**, Torello MG, Salvati A, Porta A, Adami R, Reverchon E, Aquino R P, Microsfere Di Albumina/Pectina A Rilascio Prolungato Di Gentamicina: Applicazione Della Tecnologia Saa, Pharmacy and Medicine days, 22-23 May 2014, University of Salerno.

- **Felicetta De Cicco**, Valentina Bizzarro, Raffaella Belvedere Antonello Petrella, Fabrizio dal Piaz, Rita P. Aquino, Pasquale Del Gaudio, Dextran hydrogel containing ANXA1 N-terminal derived peptide Ac2-26 as wound dressing, XXV Società Chimica Italiana annual conference, Arcavacata di Rende 7-12 september 2014.

- **Felicetta De Cicco**, Patrizia Picerno, Paola Russo, Valentina Bizzarro, Raffaella Belvedere, Luca Parente, Antonello Petrella, Fabrizio Dal

Piaz, Rita P. Aquino, Pasquale Del Gaudio, Formulazione Di Idrogel A Base Di Destrani Contenenti Il Peptide Annesina Like Anxa1, Per Il Trattamento Di Lesioni Tissutali, Doctoral school- "summer school per la formazione avanzata in discipline tecnologico-farmaceutiche", XIV Ed., Arcavacata di Rende 22-26 September 2014.

- **Felicetta De Cicco**, Amalia Porta, Francesca Sansone, Rita P. Aquino, Pasquale Del Gaudio, Nanospray Drying: Una Tecnologia Innovativa Per La Preparazione Di Polveri Gelificanti in Situ Nel Trattamento Topico Di Lesioni Tissutali, Doctoral school- "summer school- Release and delivery strategies for drug in CNS", XIV Ed., Arcavacata di Rende 22-26 September 2014.

- **Felicetta De Cicco**, Amalia Porta, Francesca Sansone, Rita P. Aquino, Pasquale Del Gaudio, In Situ Gelling Nanoparticulate Powder By Nanospray Technology For Wound Dressing, Controlled Release Society-Italy Chapter, Annual Meeting, Nanomedicine: pharmacokinetic challenges, targeting strategies and clinical outcomes, Florence 6-8 November 2014.

- P. Del Gaudio, **F. De Cicco**, S. Giovagnoli, M. Ricci, R.P. Aquino, A novel versatile gastro-resistant paediatric formulation based on Omeprazole/SBA-15 loaded in alginate beads by prilling, Reims 13-14 April 2015.

- Pasquale Del Gaudio, **Felicetta De Cicco**, Laura Scutiero, Rita P. Aquino, Particulate drug delivery systems of poorly bioavailable drugs by supercritical fluid technologies. Società Chimica Italiana annual conference at University of Salerno, 7-8 September 2015.

- Andrea Cerciello, **Felicetta De Cicco**, Mariachiara Pellegrino, Rita P. Aquino, Pasquale Del Gaudio, Paola Russo, Prilling as a versatile

technique for the development of controlled delivery systems containing anti-inflammatory drugs. International Symposium on Microencapsulation, Northeastern University, Boston (MA), 1-3-October 2015.

- **Felicetta De Cicco**, Andrea Cerciello, Paola Russo, Rita P. Aquino, Pasquale Del Gaudio, Combination of co-axial prilling and supercritical drying for the formulation of doxycycline particles for wound healing. International Symposium on Microencapsulation, Northeastern University, Boston (MA), 1-3 October 2015.

- **Felicetta De Cicco**, Angel Concheiro, Carmen Alvarez-Lorenzo, Carlos A. Garcìa-Gonzalez, Rita P. Aquino, Pasquale Del Gaudio, Green processing of antimicrobial aerogel formulations for wound healing applications, CISDEM 2015, University of Santiago de Compostela, Spain, 5-6 November 2015.

Acknowledgments

Ph. D course in Pharmaceutical sciences was my first working experience. I improved my skills also thanks to many people.

Firstly, I would like to thank prof. Rita P. Aquino, prof. Pasquale Del Gaudio and prof. Ernesto Reverchon for their scientific guidance and because they made possible this experience, following me during these years. Furthermore, they had been knowing me since my degree, so it was possible to create a cordial relationship with them.

People of my research group gave me, individually, their contribute to my personal growth.

I would like to thank all of them for giving me moment of fun and for giving me trust.

Thank you Giulia, Andrea, Michele, Tiziana, Francesca and Teresa for the enjoyable time spent togheter, for your contribute and our familiar moments.

Thank you also Patrizia, Paola and all the people who contribute, during these years, to make nice the time spent at University.

In the last year of the course, I spent three months in Spain at Universidade de Santiago de Compostela. It was a very nice period, I was lucky to stay in that city!

There, I knew my supervisor prof. Carlos A. Garcìa Gonzalez, a warm and helpful person, who gave me many useful teachings. Furthermore, all of spanish people were so kind and hospitable, I'm grateful to Rosalia, Lidia, Jorge, Isa, Clara, Alejandro and Fernando.

Special thank to all my students. I was very lucky, because all of them were nice and clever and contributed to my professional and personal growth. I will never forget you.

Felicia